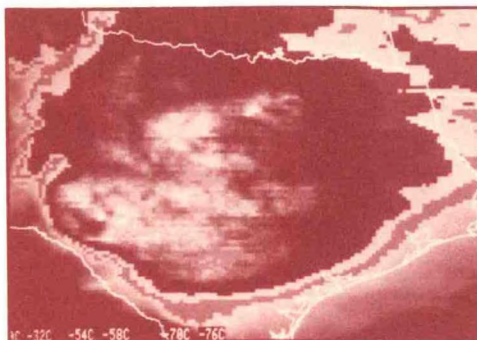


QC
968
.N3
1989

National Severe Storms Laboratory

Annual Report FY 1989



U.S. Department of Commerce

**National Oceanic and Atmospheric Administration
Environmental Research Laboratories**



Left: Tornado near Hodges, Texas, on 13 May 1989. (Photograph © 1989, C.A. Doswell III.)

Top Right: Large Mesoscale Convective Complex (MCC) over Texas on 17 May 1989 at 0800 UTC.

Bottom Right: Mobile Laboratory at Craig, Colorado, on 15 January 1989 during winter downslope wind study.

QC
968
.N3
1989

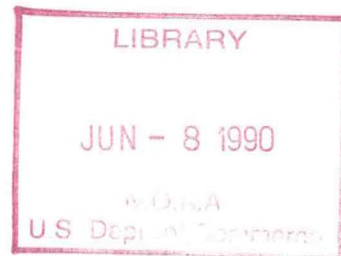
National Severe Storms Laboratory

Annual Report FY 1989

December 1989
Norman, Oklahoma



U.S. Department of Commerce
National Oceanic and Atmospheric Administration
Environmental Research Laboratories



1870

1870

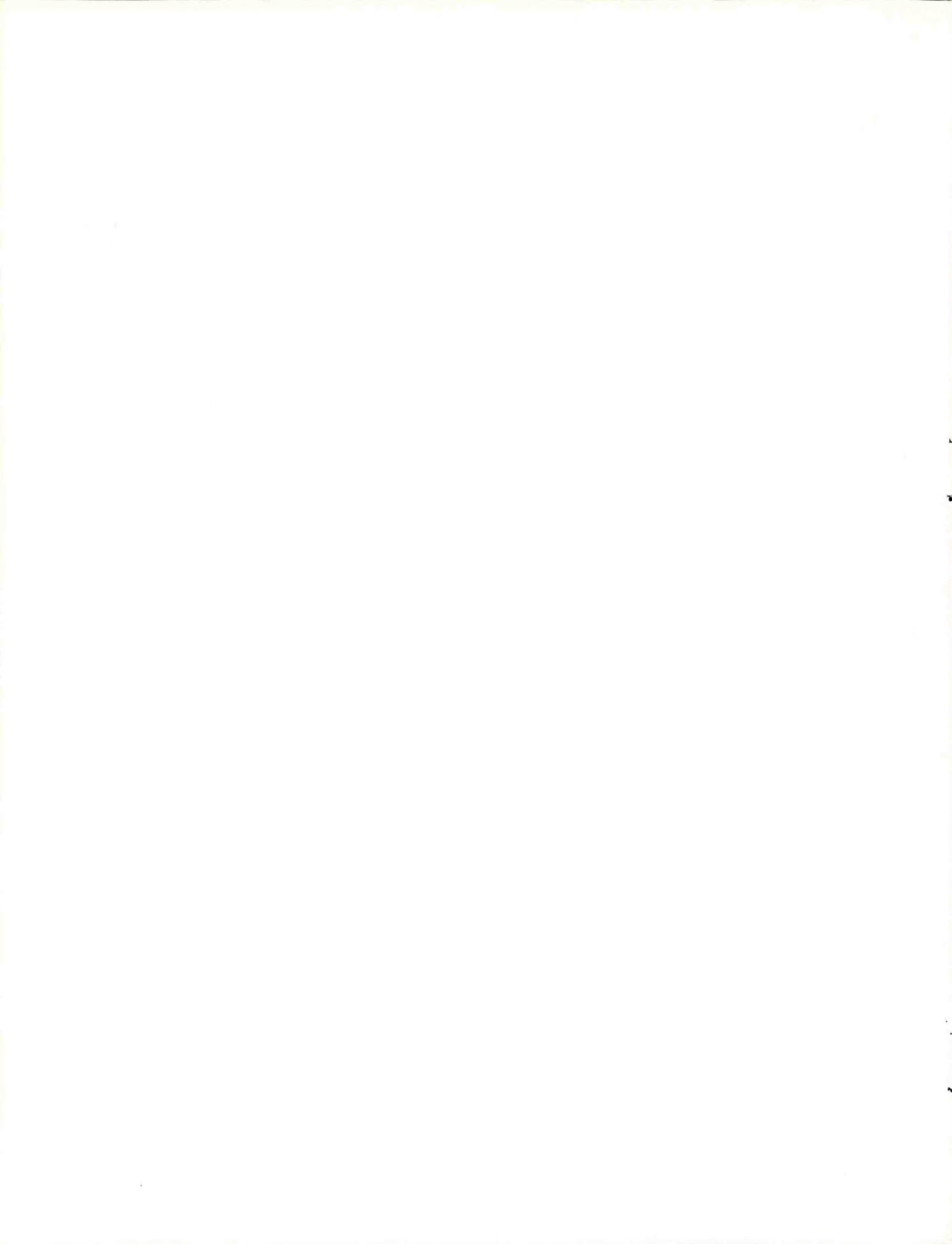
CONTENTS

<i>The NSSL Mission</i>	v
<i>Foreword</i>	vii
<i>Field Observations and Facilities</i>	1
<i>Large-Scale Studies</i>	10
<i>Mesoscale Studies</i>	17
<i>Storm-Scale Studies</i>	34
<i>Modeling</i>	40
<i>Applications and Forecasting</i>	46
<i>NSSL Staff FY 1989</i>	56
<i>FY 1989 Publication List</i>	57
<i>Major Seminars at NSSL</i>	64
<i>Meetings Hosted by NSSL</i>	66
<i>Visitors to NSSL</i>	67



THE NSSL MISSION

The National Severe Storms Laboratory conducts a broad program of research to develop basic understanding of severe weather phenomena, including the large and mesoscale environments that evolve and interact to produce intense storms. The focus is upon observational and theoretical studies of hazardous, middle latitude weather phenomena such as tornadoes, hailstorms, lightning, windstorms, floods, and blizzards. Sophisticated numerical models are often employed as research tools. The Laboratory's research projects provide sound scientific foundations upon which improvements to NOAA's weather and climate forecasting services may be built. NSSL participates in field programs and special projects, usually in coordination with other ERL components, the National Weather Service, and other agencies, intended to demonstrate or improve capabilities to detect, forecast, and warn of hazardous weather events.



FOREWORD

The National Severe Storms Laboratory (NSSL) develops means for improving weather forecasting through studies of storm processes, numerical and conceptual modeling of storm phenomena, and applications of new remote-sensing technologies in the severe weather environment. The work at NSSL, probably the most substantial precursor of the major national initiative NEXRAD, continues to support that program, and a major effort in the Laboratory is directed toward operational implementation of an effective national weather radar network for the 1990s and beyond.

The Mesoscale Research Division (MRD) of NSSL, situated in Boulder, Colorado, gives heavy emphasis to studies of mesoscale convective systems (MCSs) based on data gathered during field programs. Integration of observations from the P-3 aircraft, satellite, ground-based radars, and lightning strike networks contributes substantially to the MRD research effort.

Through numerous relationships with other government agencies and universities, NSSL constitutes a resource for severe-storm data examined by researchers around the country and overseas. NSSL directly participates in many research projects outside Oklahoma; for example, during FY 1989 NSSL staff participated in the Terminal Doppler Weather Radar field project at Kansas City's MidContinent Airport, and gathered mobile CLASS soundings during

winter storms in Colorado and Kansas. The Laboratory utilized the NOAA P-3 research aircraft to gather data in and near convective storm systems simultaneously with the new NEXRAD prototype radar, which is sited immediately south of the Laboratory in Norman.

During coming years increased emphasis will be given to the expansion of research to include larger scales of meteorological phenomena, and to the incorporation of modern research workstations, wind profilers, and digital satellite data into both case study analyses and the development of conceptual and numerical models. The Laboratory is a principal participant in the National Science Foundation's Science and Technology Center, CAPS (Center for Analysis and Prediction of Storms), which came into existence at the University of Oklahoma during the past year. The Center's work focuses on development of new-generation numerical forecast models capable of explicit prediction of individual severe storms and storm systems. The blending of data from diverse and asynchronous observing systems (e.g., Doppler radar, wind profilers, and satellites) must be accomplished if work is to progress rapidly in the application of data from these new sensors. A plan of action to bring edge-of-the-art capabilities for computing, data synthesis, and analysis to the Laboratory has been developed and implementation is well under way.

FIELD OBSERVATIONS AND FACILITIES

COPS-89

In May and June 1989, one of the NOAA P-3 aircraft was used in the field project COPS (Cooperative Oklahoma P-3 Studies). The project had a three-fold focus: mesoscale convective systems (MCSs), the dryline, and evaluation of new observational strategies. Principal investigators of the project included staff from the National Severe Storms Laboratory (NSSL) of the National Oceanic and Atmospheric Administration (NOAA) from both Norman, Oklahoma, and Boulder, Colorado, as well as scientists from Colorado State University (CSU) and the University of Oklahoma. Approximately 18 flight hours were used between 24 May and 8 June during four research missions based at Will Rogers Airport in Oklahoma City. In addition to data collected by the P-3 aircraft, data were also collected by the NSSL Cimarron Doppler radar, the new Next Generation Weather Radar (NEXRAD) prototype Doppler radar that was undergoing tests in Norman, and the NSSL1 mobile laboratory.

Three of the flight missions collected data within MCSs that occurred during the night in central Oklahoma. Airborne Doppler radar data will be used in conjunction with ground-based Doppler radar data from Cimarron and NEXRAD to define the kinematic structure of the systems. Balloon-borne electric field mill observations collected by NSSL's mobile laboratory will be combined with kinematic analyses to address questions of the mechanisms responsible for the electrification of MCSs and the generation of cloud-to-ground lightning. Dynamic retrieval of pressure and buoyancy forces derived from the Doppler analyses and airborne microphysical data will be used to evaluate the impact of heating and cooling rates on the evolution of the pressure forces.

Another feature of the region that was examined was the dryline. The dryline is a

persistent, low-level convergence zone between the dry southwesterly flow—coming from the desert regions of New Mexico—and the moist southeasterly flow from the Gulf of Mexico. This region is a preferred region for the generation of severe convective storms. Little is currently known about the dynamics of drylines and how they differ from cold fronts. The P-3 flew low-level passes through a dryline (no convection) in extreme western Oklahoma while the mobile laboratory was sending up serial soundings using the Mobile Cross-chain LORAN (Long-Range Aid to Navigation) Atmospheric Sounding System (M-CLASS). These data sets (Fig. 1) will be used to document the dryline structure and help initiate and verify nonhydrostatic numerical model simulations of dryline structure.

The third goal of COPS was to test new instrumentation and data gathering strategies before a much larger project in the spring of 1991. New instrumentation that was tested include the balloon-borne electric field meter launched by the mobile laboratory, and the LORAN dropwindsonde system developed by the National Center for Atmospheric Research (NCAR) for the Experiment on Rapidly-Intensifying Cyclones over the Atlantic (ERICA) project and used in COPS for the first time to deploy sondes over land. New data-gathering strategies were used to derive horizontal air motions using the P-3's airborne Doppler radar from a single straight-line flight track, combined with the P-3's radar observations and Doppler radar data from the NEXRAD radar. The Fore/Aft Scanning Technique (FAST) was tested for the P-3's tail radar antenna to allow the collection of pseudo-dual-beam Doppler data. In this method, the antenna was slewed to look forward, then aft of the flight track ($\pm 25^\circ$) during alternate vertical scans. Dual-Doppler winds are computed by combining data from the two looking angles. Analyses of these results will be compared to wind fields computed from the data collected by the NEXRAD and Cimarron

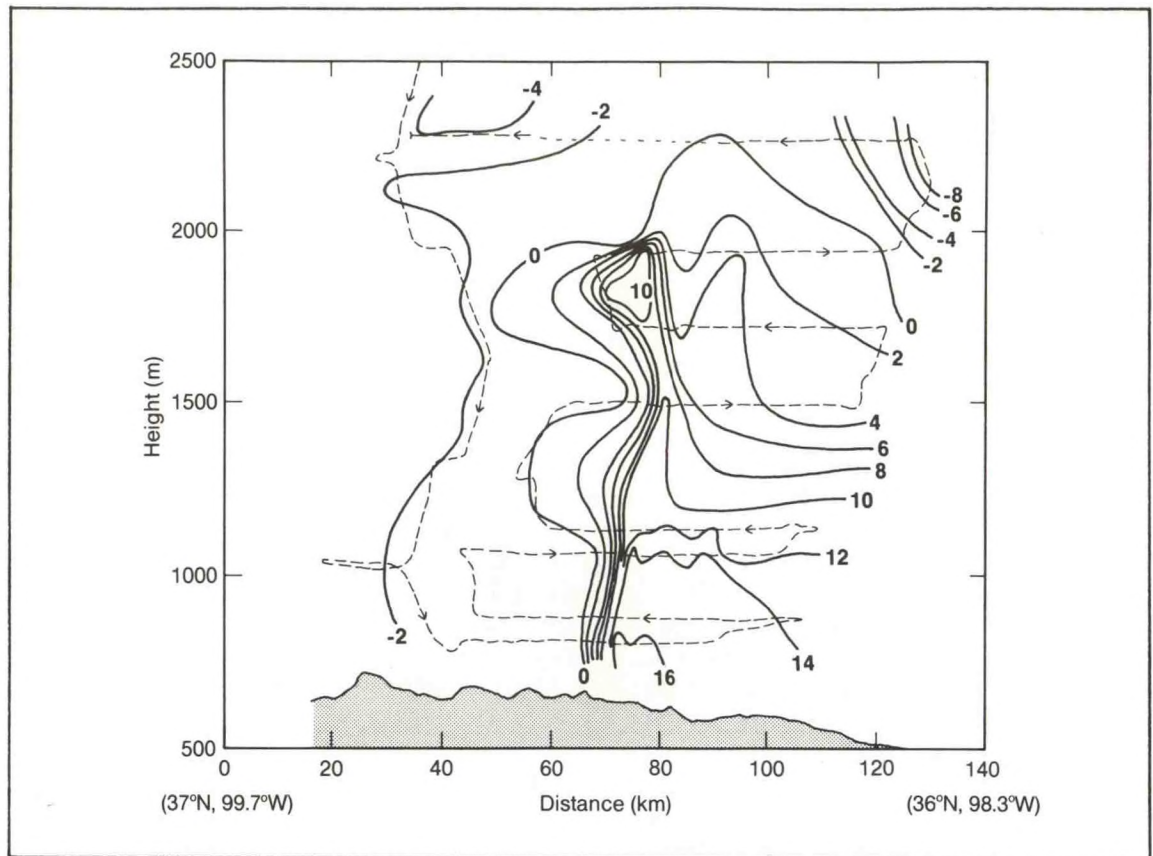


Figure 1. Vertical cross section of dew point temperature ($^{\circ}\text{C}$) in dryline, as measured by the NOAA P-3 aircraft during the 24 May COPS-89 flight. Distance is indicated on abscissa over northwest Oklahoma by aircraft traverses between 2040 and 2238 UTC.

Doppler radars. Figure 2 shows an example from the data collected near a weak north-south-oriented convective band; a pronounced rear inflow is seen at middle levels. If this technique works well, the P-3's Doppler radar will be much more useful in situations where an L-shaped flight pattern cannot be flown. The new dropsonde system was also extensively tested in both clear air and precipitation. Comparisons of balloon-borne LORAN sondes launched by the mobile laboratory and standard National Weather Service (NWS) rawinsonde releases revealed the high quality of the dropsondes in clear air. Near highly electrically active convection, however, data revealed an interference problem that occasionally will interrupt reception of the sonde signal. This interference is due to either corona buildup on

the sonde, or a static buildup on the aircraft that blocks the reception. Communication systems and coordination procedures were also tested to enable the P-3, mobile laboratory, and ground-based radars to collect data in a synchronized manner.

TDWR

The Federal Aviation Administration (FAA) is in the development stage of a Terminal Doppler Weather Radar (TDWR) system that will be deployed near the largest airports in the nation. TDWR will automatically detect wind-shear phenomena in the terminal area and forecast the arrival of wind-shear events up to 20 minutes in

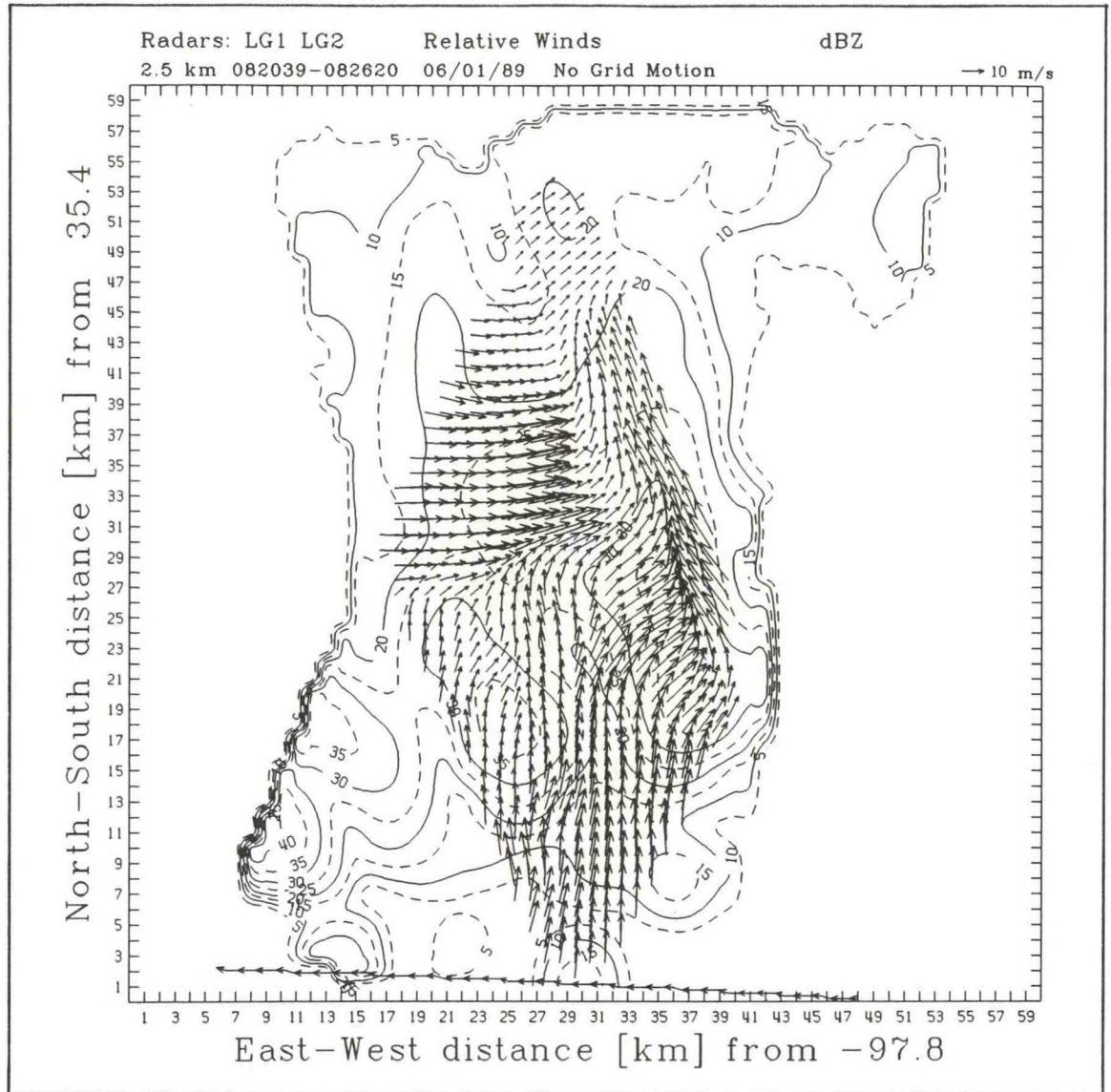


Figure 2. Horizontal plot at 2.5 km of winds and reflectivity derived from FAST on 1 June 1989. Track of P-3 is the solid line with arrows near bottom of figure. Wind vectors are relative to the earth (no system motion).

advance. During the past year, NSSL scientists continued to develop and enhance algorithms to detect hazardous weather phenomena for use with the TDWR system. They also participated in the FAA/TDWR test and evaluation in the vicinity of Kansas City during the spring and summer of 1989. The gust front detection and windshift prediction algorithm, Tornadic Vortex Signature (TVS) algorithm, and the velocity

dealiasing algorithm, all developed at NSSL, ran in real time during a 5-month period from May to September on the Massachusetts Institute of Technology (MIT)/Lincoln Laboratory Doppler radar. During a 2-month period in the summer, output from the gust front and windshift algorithm was displayed in the air traffic control tower for use by controllers for planning and for wind-shear hazard warning.

Overall, air traffic controllers had very favorable comments on the utility of the gust front detection and windshift prediction algorithm products.

North Dakota Thunderstorm Project

NSSL is playing an active role in the North Dakota Thunderstorm Project. The primary objective of the project is to understand better the microphysical and kinematic processes within High Plains convective storms in order to conduct more effective hail suppression operations. Within the project are a number of secondary objectives that are being addressed using the same data sources. The data collection phase of the project took place in south-central North Dakota during June and July 1989. The data analysis phase is under way. NSSL has been involved in all phases of the project, including planning of the field experiment, data collection, and data analysis and interpretation. Research studies of storms

that occurred on 27 June and 11 July 1989 are being conducted in collaboration with meteorologists from the Wave Propagation Laboratory (WPL) of NOAA/ERL, NCAR, and the South Dakota School of Mines and Technology.

Cimarron Radar Upgrade

The Cimarron Doppler radar continued to be upgraded (Fig. 3) to improve the data acquisition speed and polarization measurement performance, under funding from the FAA. The new programmable signal processor was obtained, and the host computer systems were purchased for both Cimarron and Norman. The host computers are VME-bus based systems built by FORCE. All interface cards, such as the timing generator, antenna controller, and the display and archive system, use VME-bus hardware. The microwave link between Cimarron and Norman was installed and is awaiting licensing. In addition, the backup power generator for Cimarron was installed.

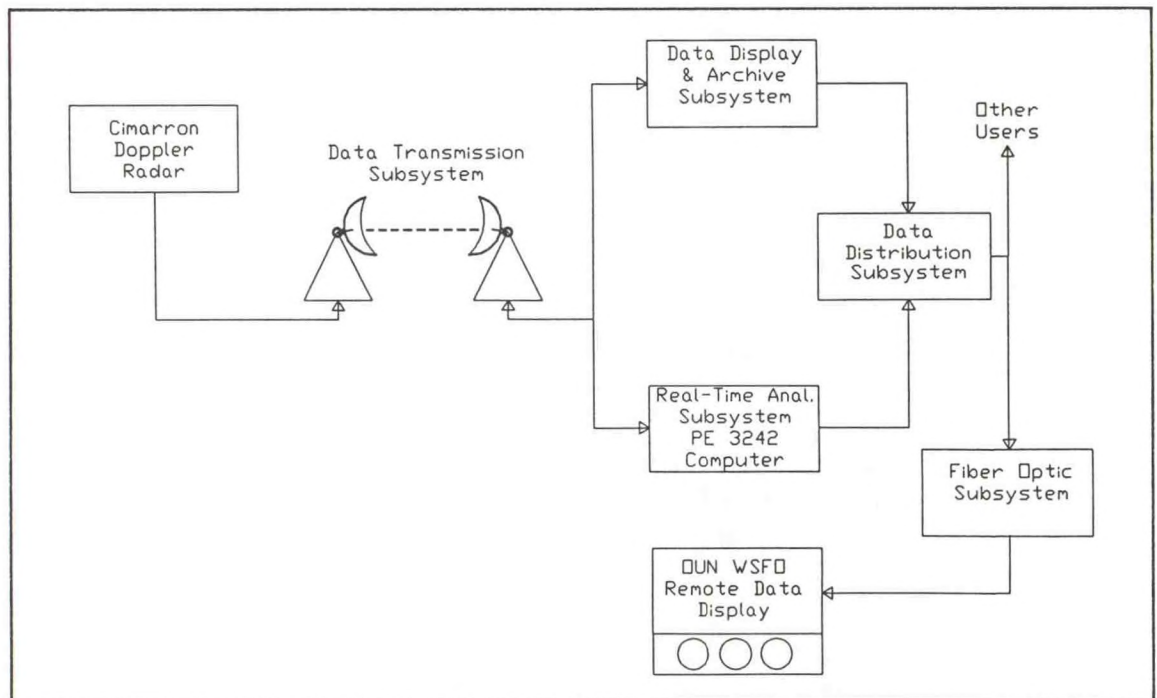


Figure 3. The upgraded NSSL Cimarron Doppler radar facility.

Contractor software for the signal processor has delayed this project by two months. NSSL will continue with this upgrade, as well as starting to add full remote operation capabilities to the system. The Norman processor will be interfaced to the Concurrent 3280 through the VME-bus for algorithm processing and real-time evaluations.

Mobile Laboratories

A collaborative effort among NSSL's Storm Electricity and Cloud Physics Group, Scientific Support Division, and Meteorological Research Group has resulted in research flights using NSSL mobile laboratory and ballooning capabilities. During the last three years, this M-CLASS facility has made the following flights:

- 1987: Flights for the DOPpler-LIGHTning Program (DOPLIGHT) during the spring.
 - 45 flights for the first test version of M-CLASS (20 flights for forecasting, 25 flights in and near thunderstorms).

- 1988: NSSL M-CLASS tests.
 - 10 flights for forecasting, including the Oklahoma Thunderstorm Outlook.
 - 51 flights for low-level jet experiment and comparison with Doppler Velocity Azimuth Display (VAD) and NWS soundings.
 - 18 flights for landfall of Hurricane Gilbert.

- 1989: Uses in multiple seasons.
 - 42 flights in winter storms and downslope high winds.
 - 38 flights for COPS-89 (28 storm, 4 dryline, and 6 forecasting).
 - 50 flights for downburst studies for FAA at Kansas City.

In January 1989, mobile laboratory NSSL1 traveled to Craig, Colorado (cover), to participate in downslope wind studies, then traveled to Kansas to launch M-CLASS soundings in support of a winter-storm study. NSSL1, NSSL2, and NSSL3 were used in their configurations existing in spring and

summer 1989 in support of the NEXRAD Initial Operational Test and Evaluation-Part 2 (IOTE2), and NSSL1 was used in support of COPS-89 during May. In July and August 1989, NSSL1 traveled to Kansas City to participate in the TDWR program. In September, NSSL1 was in Arizona for a feasibility study of using M-CLASS in support of several proposed programs in that area (Fig. 4). Testing continued on the use of M-CLASS in the thunderstorm environment, but an unexpected problem (being addressed by NCAR) with the new modified LORAN receiver and the Vaisala sonde hampered this effort.



Figure 4. M-CLASS system at Salt River Canyon, Arizona, in September 1989 during evaluation prior to the SWAMP project in 1990.

Improvements made to NSSL1 include a new on-board computer; a UNIX operating system to support the electric-field meter, optical and charge device, packet radio, and surface meteorological instruments; a new analog strip-chart recorder; and replacement of the wind speed, wind direction, and humidity sensors. NSSL is continuing to upgrade NSSL2 and ready it for another M-CLASS system; by the end of FY 1989, NSSL2 had been equipped with roll bars, helium carriers, roof air conditioner and heater, power generator, equipments racks, and radio equipment. A collaborative effort with NCAR will provide the Laboratory with three additional M-CLASS systems, resulting in three mobile and one fixed-based system at the end of the development phase.

M-CLASS provides a means of obtaining research-quality sounding data and is an important tool for atmospheric research. For clear-air and prestorm soundings, M-CLASS is exceptionally reliable and has contributed to successful forecasts of severe weather. The tests of M-CLASS for making in-situ measurements in thunderstorms are encouraging, but additional modifications to the sondes will be required to increase the usable data in highly electrified storm environments. To assess previous sonde modifications and develop new ones, the effects of corona discharge from the sondes will be tested in a high-voltage facility in late 1989. Most important to the future of all sounding systems using LORAN (balloon and drop) in the central United States, consistently high-quality soundings of wind in both clear and storm environments require and await the mid-continent LORAN chain.

Balloon-Borne Probe Development

The initial design, construction, and flight testing phases were completed for a modern digital instrument for in-situ measurements of the electric field in storms. This collaborative effort between NSSL's Scientific Support Division, the Storm Electricity and Cloud Physics Group, and the

University of Mississippi has led to a lighter weight, more sensitive, and highly reliable electric field meter (EFM). The EFM is carried aloft beneath balloons that also carry a LORAN tracking radiosonde. This allows determination of standard meteorological sounding parameters, the electric field, and instrument position. About 20 instruments are being built for continued testing and research flights in 1990. Additional sensitivity and dynamic ranges are being tested with a slight enhancement to the new circuit. The final design decisions will be made before production of several tens of instruments for data acquisition in 1991 and beyond.

A related development under NSF sponsorship is the design of a balloon-borne instrument for measuring particle charge and size. Measuring the charge carried on precipitation particles within various cloud types is required in order to develop realistic models to test various electrical charging mechanisms. Without these measurements, there is no way to evaluate how well a model depicts reality. A direct sensor of particle size was developed using a simple optical technique, while keeping the historically used double induction ring system to determine charge and velocity, which allows an estimate of the size of charged particles. This will allow us to relate new measurements directly with earlier ones in the literature, and to assess whether they were technique-biased, as would be the case if only a small percentage of the precipitation were charged. Successful prototype flights were made, and research flights are anticipated in 1990.

VHF Lightning Mapping System

In late May and early June 1989, one station of NSSL's Very High Frequency (VHF) mapping system was operated to evaluate whether the system might be used for lightning detection over mesoscale distances. The station was installed on a slope that was expected to give maximum range over azimuths from approximately 220°

to 290°. VHF data were to be compared with storms detected by radar and the ground-strike locating system to determine the approximate range of storms that were detected by the VHF system. It appears that storms could be detected out to approximately 150 km near the northern extremity of the sector. Unfortunately, suitable storms did not occur at longer ranges within the sector during the test period. The environmental radio noise level was found to increase significantly at night in the frequency band of the system (30-80 MHz), so that some noise reduction by suitable filters or by careful choice of operating frequency bands would be desirable if the system were operated in a mesoscale mode. Some quick trials with different operating bands during the last week of operation suggested that the noise level could be reduced by at least 8 dB by modifying the frequency band.

National Lightning Strike Network

NSSL scientists continued to work with the Office of the Federal Coordinator for Meteorology (OFCM) on plans to provide data from cloud-to-ground lightning strike mapping networks to operational components of NOAA. Data from NSSL's network continue to be incorporated in the Demonstration National Lightning Strike Detection Network that is planned to end in March 1991. The NSSL network was the primary source of lightning strike data for an Automated Surface Observing System (ASOS) demonstration project in Topeka during the spring and summer of 1989. NSSL also played a central role in developing standards for national networks that will be used by the federal government after the present demonstration period ends. The OFCM expects to complete and publish these standards during FY 1990.

An evaluation of positive cloud-to-ground lightning detection by NSSL's direction-finder network compared detections from the network with those from an ELF receiver and visual observations. The comparison for

positive and negative ground flashes suggests that false detection is negligible in the NSSL system for positive ground flashes with range-normalized amplitudes of at least 50 units (arbitrary units used by the commercial locating system), and no more than 15% of the positive ground flashes with smaller amplitudes are false detections. This evaluation forms the basis for using the data in research and is incorporated into recommendations for the standards for a national lightning detection network.

Lightning Location Analysis Methods

Work continued on implementing a mathematically consistent method for determining site-specific errors in direction-finder networks used for cloud-to-ground lightning location. Tests with large data sets from Colorado, Florida, Oklahoma, and Kansas networks (Fig. 5), as well as from strictly controlled simulations, have revealed how complicated and mathematically convoluted is the problem of site-error determination. Adaptations of the method and implementation strategies were devised, and a fuller understanding of site-error determination and flash position optimization was gained. In the coming year, the site-error algorithm will be applied to data from past years, and suggestions for improved configuration of detection networks will be developed.

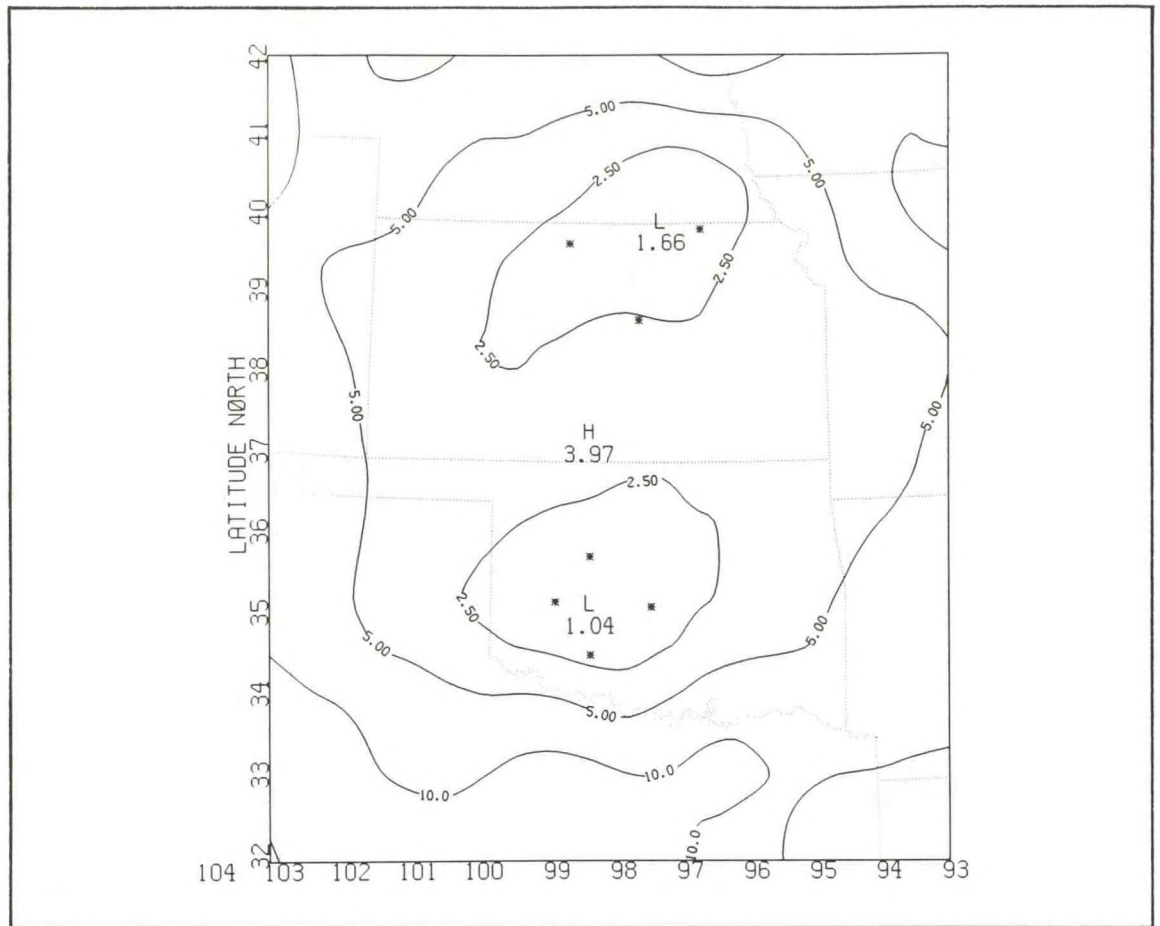


Figure 5. Displacement error (in kilometers) of flash position caused by random inaccuracies (one degree standard deviation) in observed flash azimuth after a seven-direction-finder optimization computation of 400 simulated flashes for Oklahoma-Kansas network.

Data Management

NSSL continues to improve its data management capabilities. Most of the 7-track tapes have been converted to 9-track format, and the last of the 7-track drives will be removed early in 1990. An inventory of NSSL's tape archives has begun, and this inventory is being placed into an easily accessible media library (Fig. 6). This library will allow on-line searches of the content of the tape and allow for easy access

and use of the media within the NSSL computing environment. Currently, the emphasis is on the Doppler radar data tapes; progress is also being made on the ground-strike lightning and M-CLASS databases. Other data bases are being prepared for use in the Management Information System. Plans are to create a comprehensive electronic catalog of all data available at NSSL and provide easily accessible, quality-controlled data to facilitate research efforts of the laboratory.

NSSL MEDIA LIBRARY

MEDIA INFORMATION =====	PHYSICAL INFORMATION =====
Media:	Format:
Label: ██████████	Type:
Volume:	ANSI label:
Owner's name:	Density:
Originating machine:	Parity: 0
Data set:	Write: Y
Status:	

For help, press HELP (PF2)
Press TAB for next field
Press BS for previous field

Figure 6. Data entry screen for NSSL media library.

LARGE-SCALE STUDIES

GUFMEX

The field phase of the Gulf of Mexico Experiment (GUFMEX) was executed between 20 February and 2 April 1988. It was aimed at obtaining information on two interrelated phenomena in the cool season: airmass modification over the Loop Current, and return flow characteristics of modified polar air returning to the southern shores of the United States and to the eastern coast of Mexico. NSSL is the focal point of the research effort, but many other governmental organizations and universities also are participating. A key aspect of the program was the involvement of both the Mexican Weather Service and the NWS Southern Region.

The historical record of Gulf of Mexico return-flow events in the cool season of February to March was examined from 1977 to 1986. The frequencies of cold-air plunges into the Gulf were categorized according to the type of penetrating airmass (maritime or continental polar). The characteristic times between offshore and onshore flow in these synoptic events (flow reversal) were also tabulated. The air follows several characteristic paths in returning to the continent, and data were tabulated from surface stations along these paths. It is hoped that conceptual models of return flow episodes such as Fig. 7 can be generated to aid forecasters in the challenging problem of predicting the wide range of weather associated with these return flows.

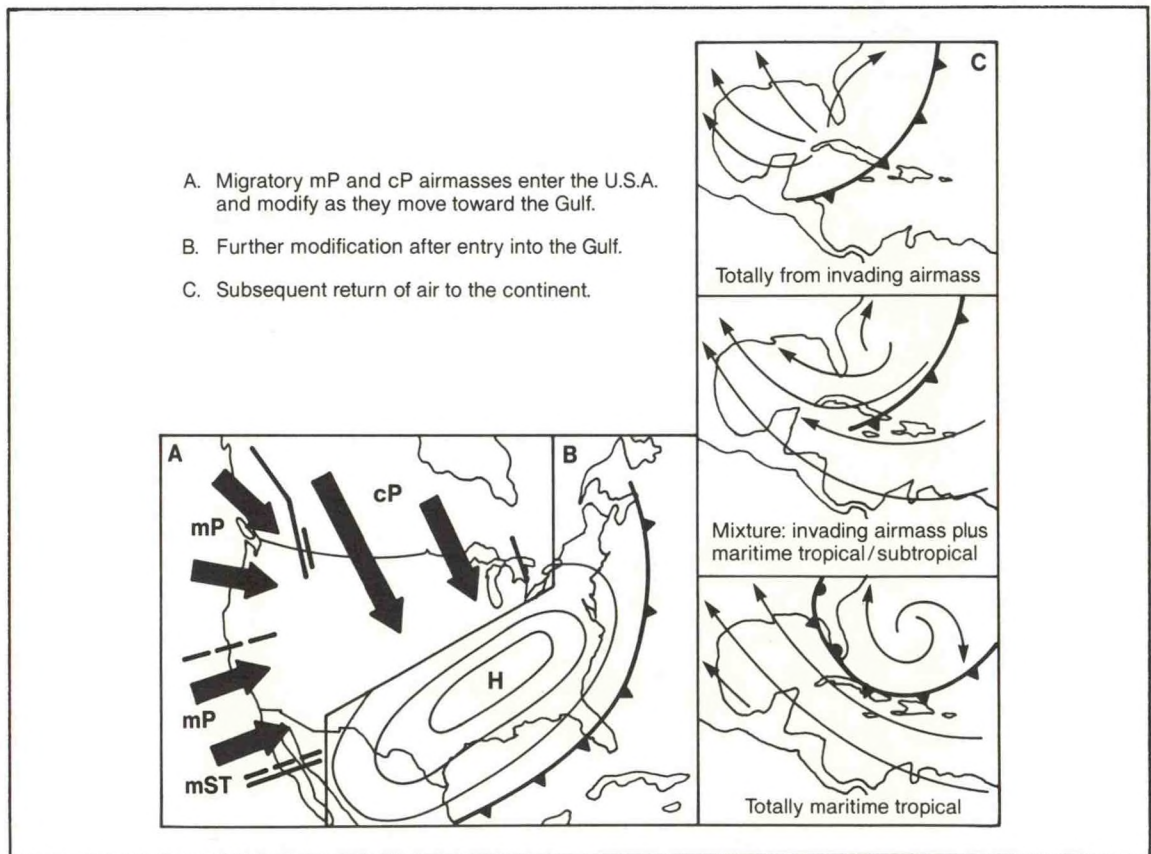


Figure 7. The sequence of events that occur with the phenomenon of return flow in the Gulf of Mexico during the cool season.

The following studies are being actively pursued at organizations other than NSSL:

- The National Environmental Satellite, Data, and Information Service (NESDIS) facility at the University of Wisconsin, a key participant in GUFMEX since its inception, is interested in validating the satellite retrievals over the Gulf of Mexico. Their studies also include analysis of the structure of moisture return shown by precipitable-water data from the Defense Meteorological Satellite Program (DMSP) satellite during the 1988 field phase (Fig. 8), data assimilation of GUFMEX data, trajectory studies, and Vertical Atmospheric Sounder (VAS) retrievals of temperature and moisture over the Gulf.

- The NWS National Severe Storms Forecast Center (NSSF) in Kansas City, Missouri, studied the performance of the Limited Fine Mesh (LFM), Nested Grid Model (NGM), and Medium Range Forecast (MRF) models at the NWS National Meteorological Center for cool-season return-flow episodes. These studies were valuable for the field phase because they identified the biases in the various models when applied to such events.

- The NWS Southern Region offices at San Antonio, Texas, and Slidell, Louisiana, established real-time analyses of return-flow episodes as viewed by forecasters in the Region. A log book is being kept at the two stations, and a program is under way at San Antonio to identify research on return flow that can be carried out by operational forecasters. Another study is under way in the Region to analyze the upper-air situation with the 10-11 March 1988 case.

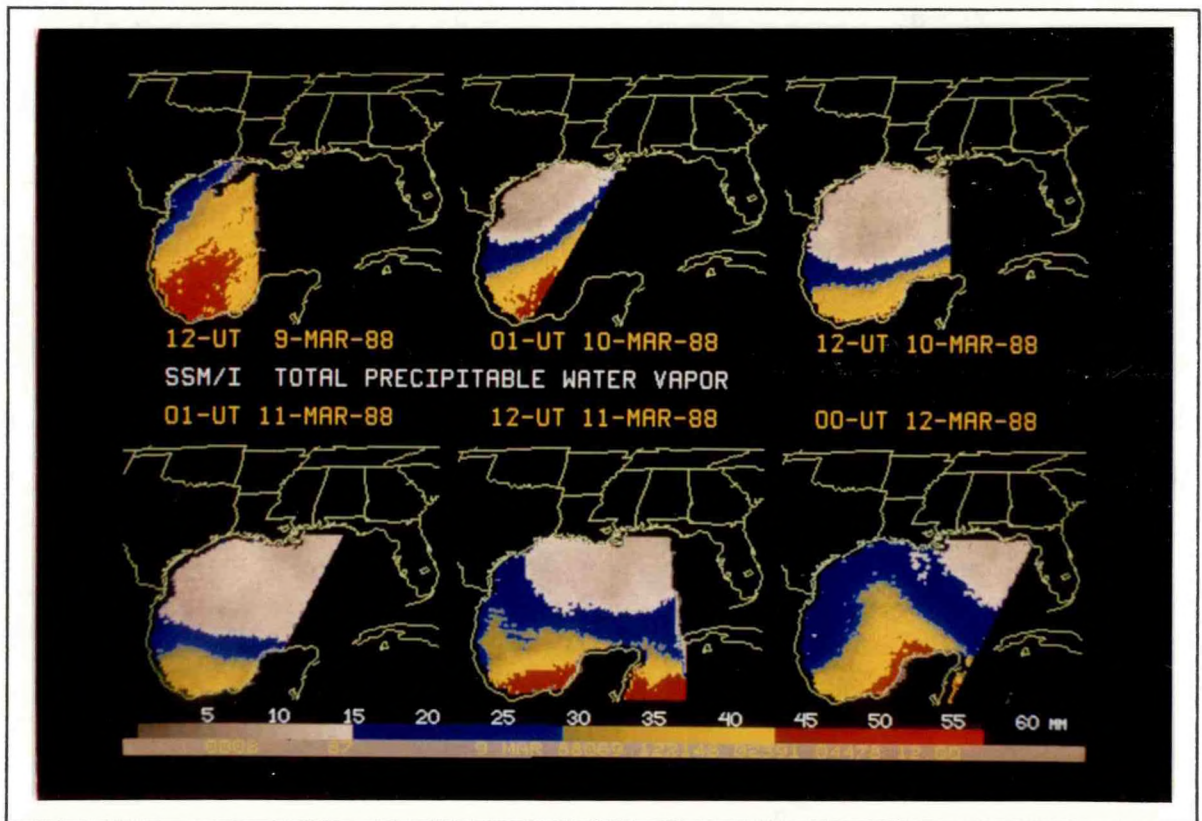


Figure 8. Total precipitable water (in millimeters) determined from microwave satellite (SSM/I) data following an intrusion of polar air over the Gulf of Mexico during 9-12 March 1988.

•The Cooperative Institute for Mesoscale Meteorological Studies (CIMMS) at the University of Oklahoma is studying planetary boundary-layer modeling, and testing of mixed-layer modeling concepts over the Loop Current under cold-air outflow conditions; the Naval Environmental Prediction Research Facility in Monterey, California, is studying trajectories with the Navy Operational Regional Analysis and Prediction System (NORAPS) model to identify airmasses involved in two return-flow episodes; and the University of California at Davis is studying cloud formations associated with return-flow events.

Quasi-Geostrophic Theory and Applications

An examination of the contribution to model-forecast vertical motion from quasi-geostrophic (QG) processes is nearing completion. The implied Q-vector divergence, which is derived from model-forecast height fields, is compared to the model's own independent forecast of vertical motion (for both the LFM and NGM models). Results of the comparison (Fig. 9) suggest that QG diagnostics provide a reasonable guide to model performance in that when the model-forecast vertical motion is consistent with the pattern of vertical motion implied by the forecast Q-vector divergence, the model forecast tends to be a good one. QG diagnostic routines, then, would be helpful in evaluating gridded model-forecast fields in operational forecast offices of the future. When this work is completed, it will provide information about how often discrepancies between these two fields arise and under what circumstances such differences develop.

Satellite Climatologies

NSSL, in collaboration with the Program for Regional Observing and Forecasting Services (PROFS) of the Forecast Systems Laboratory (FSL), has gathered a 5-year

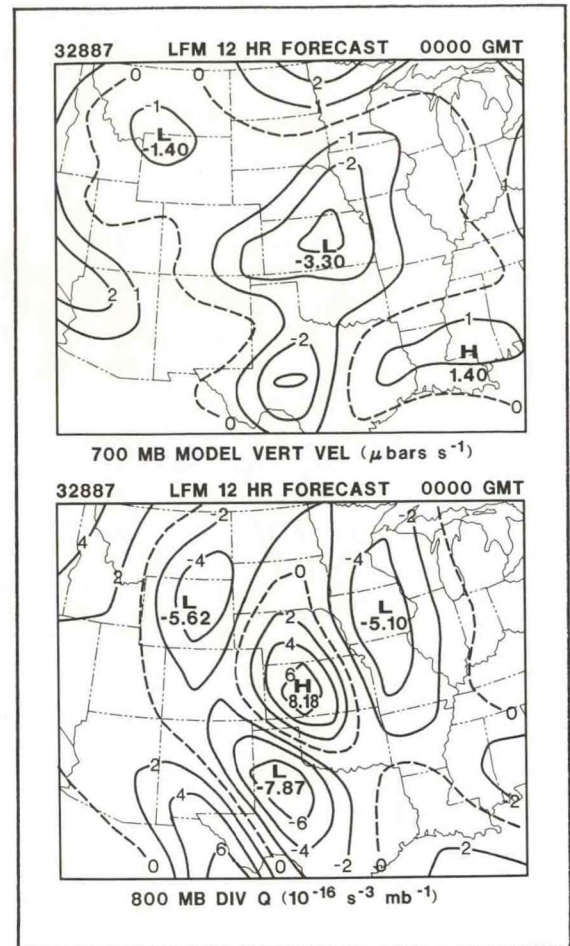


Figure 9. Comparison between (top) 12-h LFM forecast vertical motion and (bottom) Q-vector divergence fields derived from the 12-h LFM forecast heights. In this case, the patterns are noticeably quite different.

archive of hourly digital Geostationary Operational Environmental Satellite (GOES) infrared (IR) data covering most of North America. These data are being processed so they can be used for diagnosing the role of convective storms and systems in defining regional climate for periods as short as 5 to 10 days, and as long as entire seasons. Thunderstorm days were estimated by satellite using occurrence of an IR temperature colder than -32°C for at least one hour to define the necessary condition for a thunderstorm. All hours were examined for the entire month; computations were made for

7 km by 7 km data pixels. These data have been used to construct simple estimates of thunderstorm-day frequency over the western United States and northern Mexico (Fig. 10). Preliminary results show that thunderstorms

over these regions occur considerably more frequently than conventional climatologies indicate. Examination of the warm end of the IR temperature scale reveals that the GOES data capture remarkable detail and mean

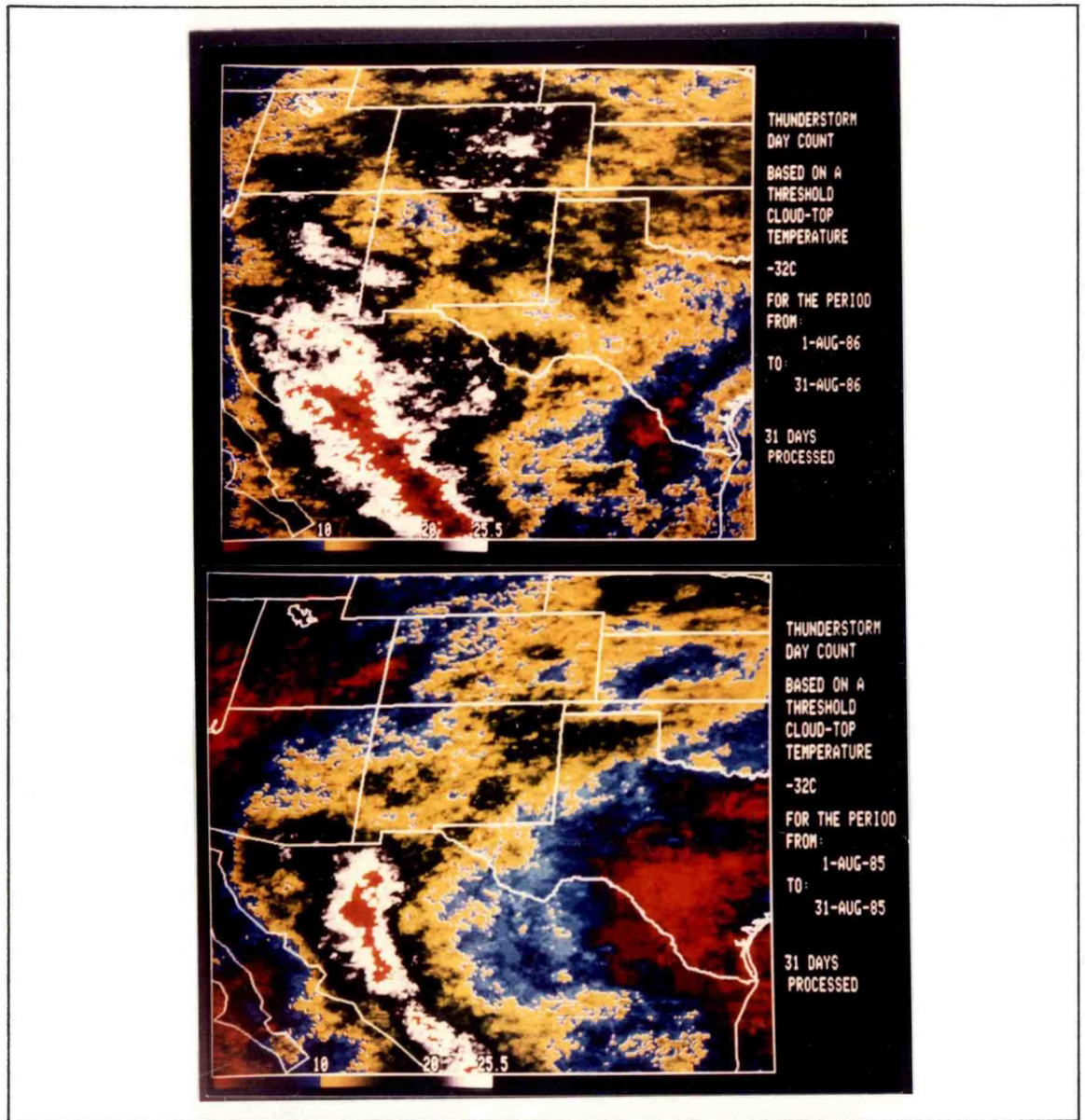


Figure 10. Top: August 1986 thunderstorm days. Scale for number of thunderstorm days across bottom; red areas over Mexican mountains are above 25.5 days. Storms occurred almost every day over the Sierra Madre Occidental of western Mexico, Mogollon Rim of Arizona, and Colorado Rockies. Bottom: August 1985 thunderstorm days. Monsoon flow of moisture into the West was more constrained in the horizontal during 1985 than 1986. Storms occurred much less frequently over Arizona, Utah, New Mexico, and Colorado in 1985; however, the Sierra Madre Occidental remained extremely active during both years.

structures of features such as the Gulf Stream (Fig. 11). These data will be exploited during the next several years to study the role of convective storms in the southwestern U. S. monsoon, and in understanding intermonthly and interannual variability of convective rainfall over the United States.

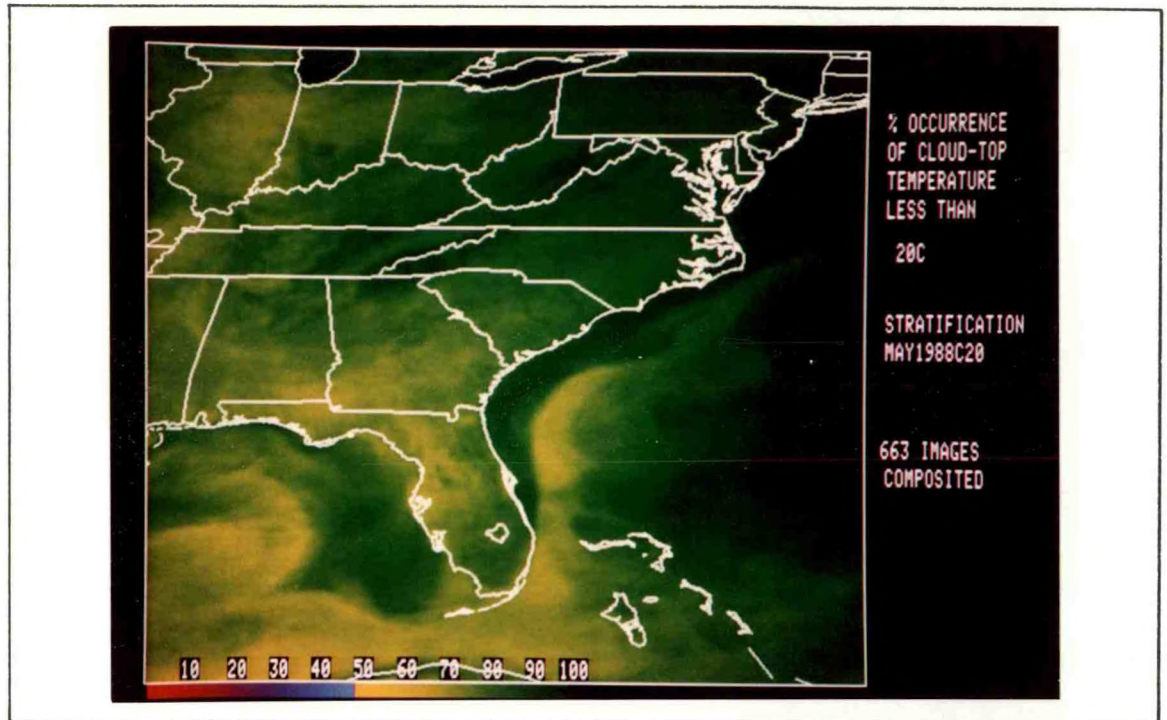


Figure 11. Hourly frequency of occurrence of IR temperatures cooler than 20°C for May 1988. The warm waters of the Gulf Stream are clearly captured as a region of low frequency of cool temperatures. Note the gyre of warm surface waters that was apparently over the northern Gulf during May.

30-Year Upper-Air Dataset

NSSL has obtained an archive of 40 years of upper-air sounding data for North America to furnish a basis for historical case studies. The data were compiled by the FSL, and are stored on magnetic tapes. In the last few years, a 30-year climatological average of these data was compiled by NSSL and FSL for each day of the year, and for the 0000 and

1200 UTC sounding times. The first 10 years of this data base were not used in this analysis because the sounding times differ from those of the last 30 years. An example of one application of these data is given in Fig. 12, showing the interaction of three lines of research: North American climatology, objective analysis studies, and North American monsoon studies that are to be pursued in the Southwest Area Monsoon Project (SWAMP) during the summer of 1990.

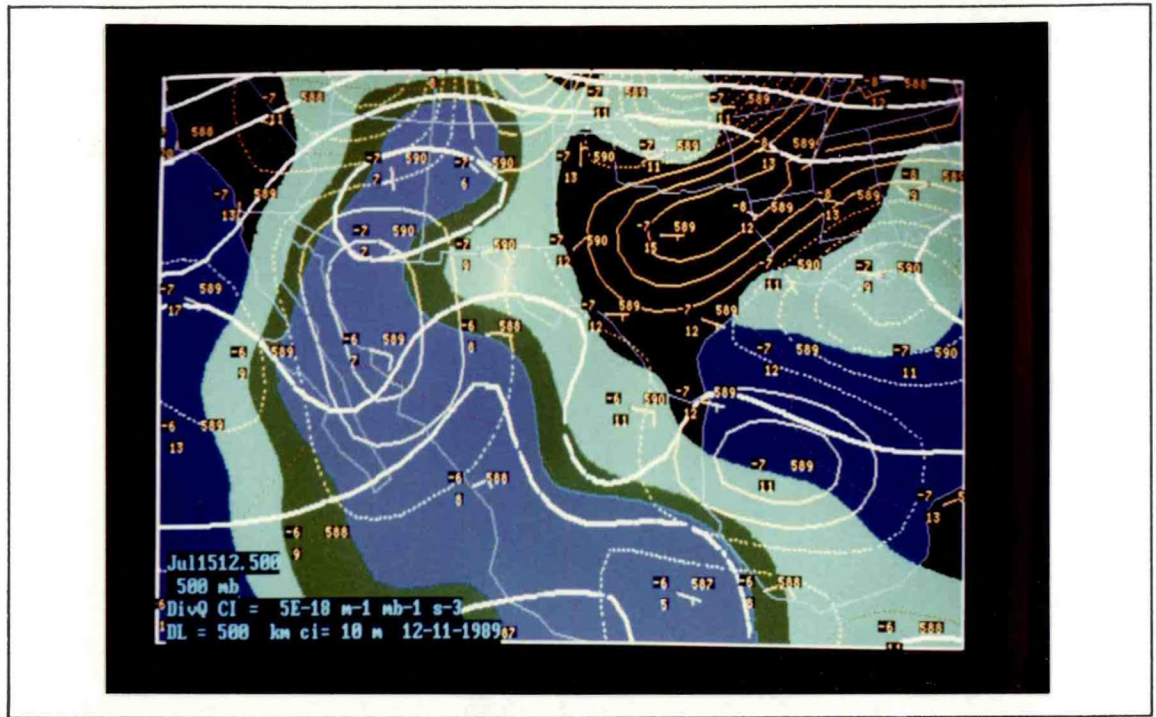


Figure 12. The 500-mb analysis on 15 July at 1200 UTC over Mexico and the southwestern United States. Average height is shown in thick white contours, moisture in green and blue shadings, and temperature in red contours. Divergence of Q-vector field (yellow contours) is solid for positive, dotted for negative, and dashed for zero.

ERBE

The goal of the Earth Radiation Budget Experiment (ERBE) is to assess the feedback of clouds and earth surface characteristics on the earth/atmosphere radiation budget from regional satellite observations. Cloud feedback is an important factor in anticipating the effect of increasing atmospheric CO₂ on climate. In collaboration with the Cooperative Institute for Meteorological Satellite Studies (CIMSS) at the University of Wisconsin, Madison, initial efforts examined the impact of deep convective clouds on the radiative energy

absorbed by the atmosphere over North America during a warm season (Fig. 13). The greenhouse (warming) effect of cold cloud tops at night approximately offsets their cooling effect during daylight hours when the observed nocturnal maximum of such cloud cover is considered. If a diurnal maximum did not exist, a net loss of radiative energy would result. Hence, the diurnal cycle of clouds must be accurately measured or simulated to assess the feedback of clouds. Future research will incorporate additional geostationary satellite data for this purpose. Moreover, effects of landscape variability and tropopause height on the radiation budget will also be considered.

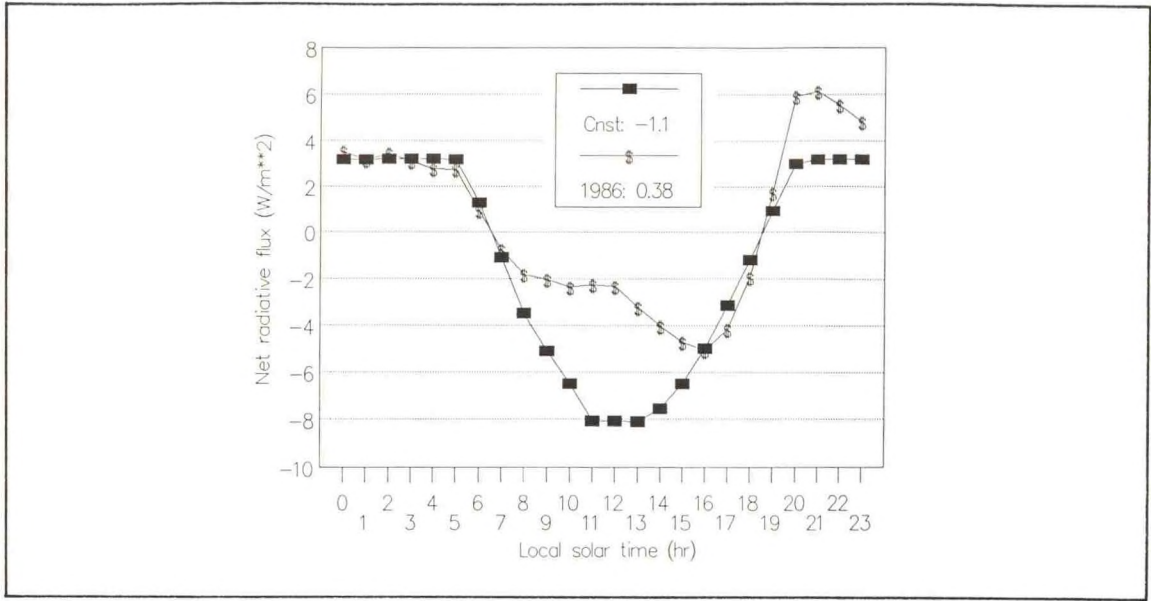


Figure 13. Average hourly change in net radiative flux entering top of atmosphere over a 2000 km by 2000 km area by adding a typical distribution of deep convection over the central United States to a clear atmosphere (\$). Curve marked with squares shows effects of the same amount of convection without diurnal trend. Numbers on right are average daily changes in net radiative flux.

Mesoscale Retrievals

Doppler radar data can be used to deduce the four-dimensional airflow in a weather system. Results can then be used to deduce the pressure and buoyancy forces that were present. Several researchers have performed this type of analysis; two new techniques are being developed along these lines that are particularly relevant to studying the evolution of weather systems. First, from the same wind data, the pressure and buoyancy tendency fields can also be deduced, allowing a view of how the force fields are changing instantaneously. Second, the pressure and buoyancy forces themselves can be decomposed into the parts necessary to maintain a translating weather system at steady state as well as the additional parts that are associated with its evolution. It was found that from two-thirds to three-quarters of the magnitude of the forces present is needed merely to maintain mesoscale weather systems at steady state. Therefore, eliminating this component of the force fields allows the dynamics of system evolution to be better observed. The resulting evolutionary parts of the forces are interpretable physically when related to the life cycles of the systems in which this analysis was performed. It is hoped that with additional research, key changes in the evolutionary parts of the forces, or in the force tendencies, will be related to corresponding changes in the intensity, size, motion, and shape of a weather system, thereby enabling an understanding of how important transitions in weather systems take place.

Fields of perturbation pressure and buoyancy were calculated from dual-Doppler-derived wind fields to quantitatively evaluate the kinematic structure of the Oklahoma-Kansas Preliminary Regional Experiment for STORM-Central (PRE-STORM) 3-4 June 1985 non-squall-line MCS. The methodology is

similar to that used in severe convective storm studies; however, in this case, the domain contains the mesoscale region of the important convective and stratiform rain (80 km by 80 km). To evaluate the effects of time evolution on the calculated perturbation pressure fields, three separate time periods were analyzed. The time derivatives were found to be critical to proper interpretation of the calculated perturbation pressure fields. The perturbation field is primarily the result of two effects: a "kinematic pressure" effect resulting from the interactions of updrafts with the environmental shear, and a "buoyancy" effect resulting from vertical gradients of perturbation temperature. For an idealized updraft embedded in strong shear, the kinematic effect would lead to a relative high-pressure maximum that is upshear of the updraft and a relative minimum on the downshear side (i.e., the shear is trying to push the updraft over). If the updraft is tilted appreciably, then a relative low-pressure zone would be created because of hydrostatic lowering of pressure from the warm air aloft. Both effects can be seen in the example shown in Fig. 14. Near 10 km, on the upshear side of the principal updraft at D:30.5 km, a strong high perturbation existed, and relative low pressure was on the downshear side of the updraft. This couplet of pressure is probably the result of dynamic effects. The mesoscale region of low pressure at D:41 km is probably a reflection of hydrostatic lowering of pressure from the detrainment of updraft air aloft. There was also a broad zone of low pressure at low levels to the northwest of the line that is probably the result of hydrostatic lowering of pressure caused by relatively warm air aloft. The interpretation of the pressure regions is complicated, however, by the mesoscale variations in the wind fields (and associated shear) and the three-dimensionality of the flow. This type of analysis could be compared to numerical simulations of the convective band structure to evaluate the physics of the simulation model.

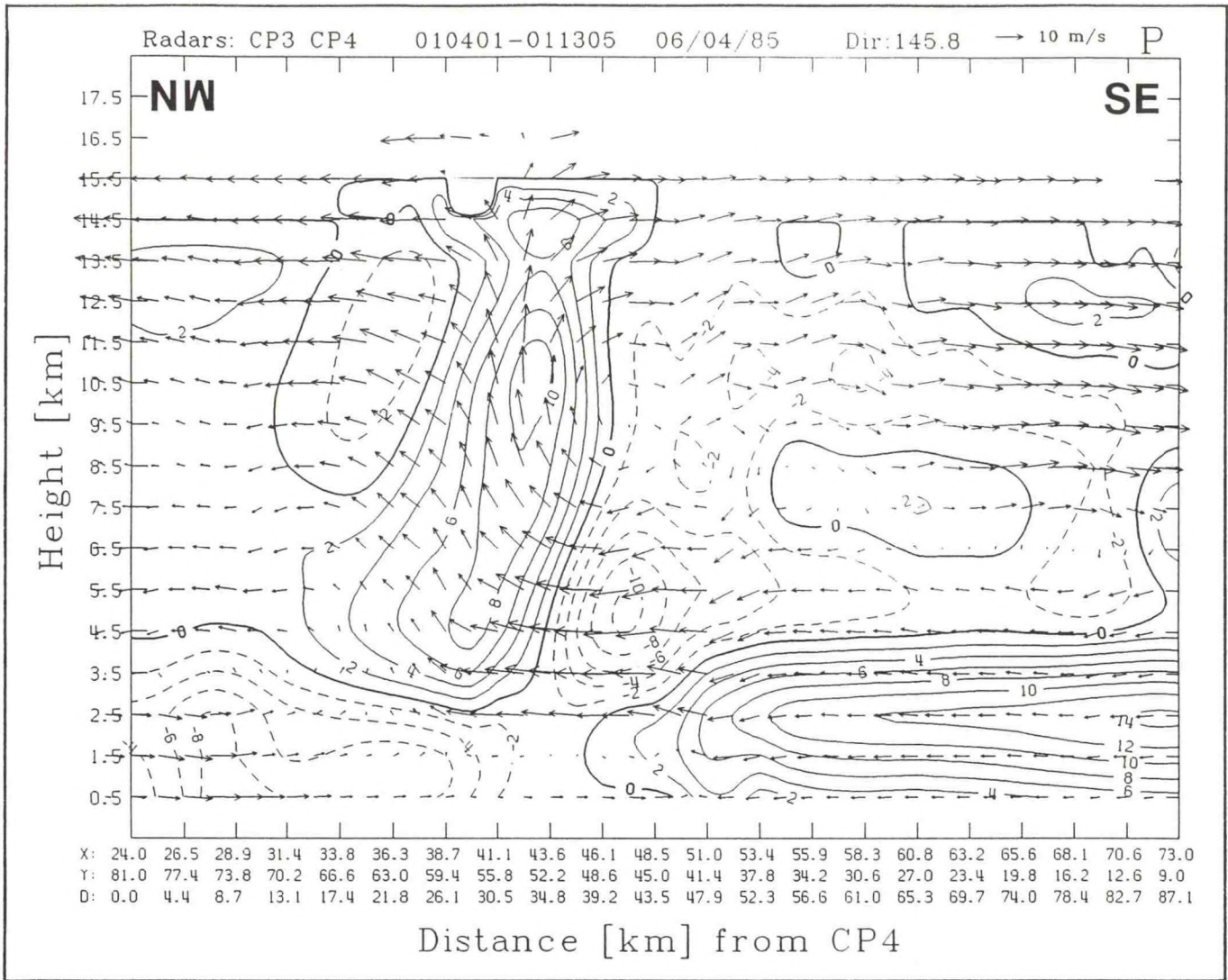


Figure 14. Vertical cross section of relative airflow and perturbation pressure (mb x 10) from southeast to northwest (along approximate inflow direction) through the primary updraft near apex of two intersecting bands on 3-4 June 1985. Negative pressure contours are dashed; zero contour is heavy solid line.

MCS Studies

Doppler radar data were used to derive the four-dimensional wind field in the stratiform region of a squall line observed during PRE-STORM on 11 June 1985. At the time of analysis, the convection in the squall line was 2 hours past its time of maximum intensity and the trailing stratiform precipitation was nearly at its time of maximum intensity. From the wind field, the

pressure and buoyancy forces, as well as the pressure and buoyancy fields, were obtained. The pressure and buoyancy fields were further decomposed into the parts necessary to maintain a translating, steady-state system and the additional parts that were associated with the evolution. At middle levels, air was flowing into the system from the rear (Fig. 15). This air was being accelerated along a pressure gradient that was stronger than that needed to maintain a steady state. This result confirms previous

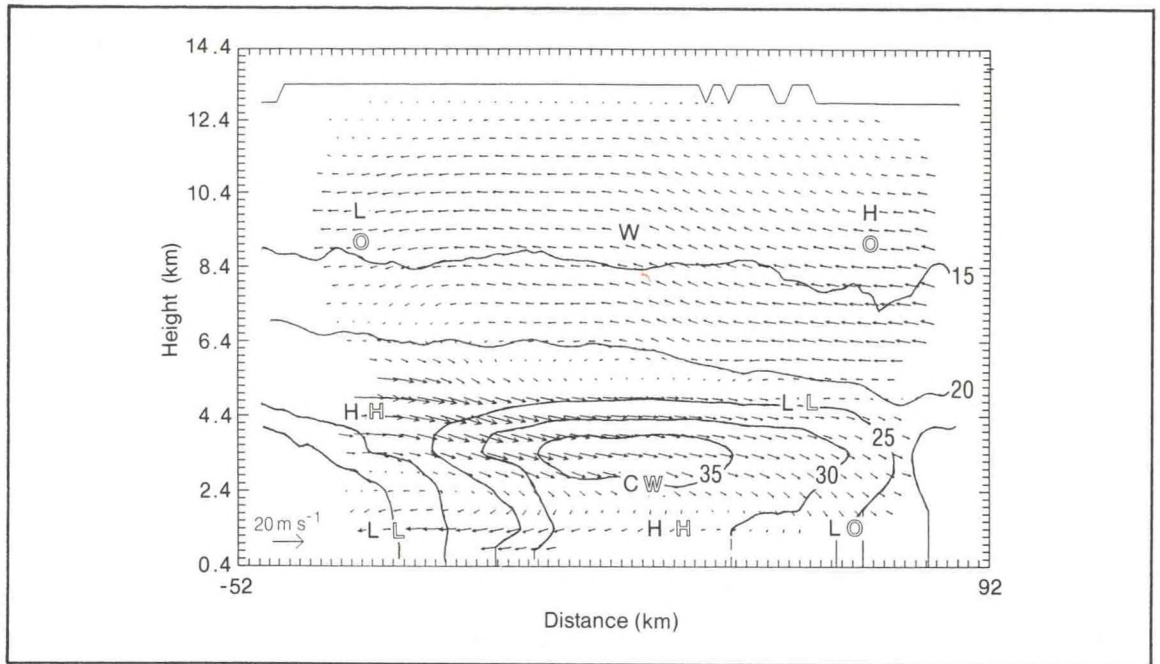


Figure 15. Vertical cross section perpendicular to squall line showing the airflow, radar reflectivity factor, pressure, and temperature in the trailing stratiform region of squall line observed during PRE-STORM on 11 June 1985. Results were derived from Doppler radar data. The leading convective line is off the frame to right; the squall line was moving from left to right. Arrows represent along-line means of the airflow relative to squall line. Length of an arrow corresponds to the displacement of the air in 5 minutes. Contours show along-line means of radar reflectivity factor. Solid letters H, O, and L represent regions of high, near-zero, and low perturbation pressure; W and C represent regions of high and low perturbation temperature. Open letters represent evolutionary components of pressure and temperature fields.

speculations that the rear inflow at middle levels is a characteristic of squall lines later in their lives. At low levels, air was descending and diverging. This air was cold relative to the environment, but not cold enough to maintain this branch of the circulation at a steady state. Apparently, cooling of this air by evaporation and melting of precipitation was being offset by warming caused by compression, once the subsidence and divergence were accelerated sufficiently, preventing further acceleration and actually causing a braking of this branch of the flow. Middle-level pressure gradients were also found to be in the process of weakening; these changes were caused by the collapsing and expanding of the atmosphere below by differential cooling and heating.

The horizontal vorticity dynamics of the 10-11 June 1985 squall line in PRE-STORM were studied to determine if a counterbalance existed between horizontal vorticity advected into the squall line from the environment and horizontal vorticity produced by horizontal buoyancy gradients in the convective region. The inviscid, two-dimensional Boussinesq, horizontal vorticity equation was integrated using kinematic and retrieved thermodynamic fields from a dual-Doppler analysis (Fig. 16). A horizontal-vorticity generation balance was observed when the integration was carried to 50 km behind the gust front, indicating that system-scale dynamics, rather than forces in the immediate vicinity of the gust front, dictated the squall line's evolution.

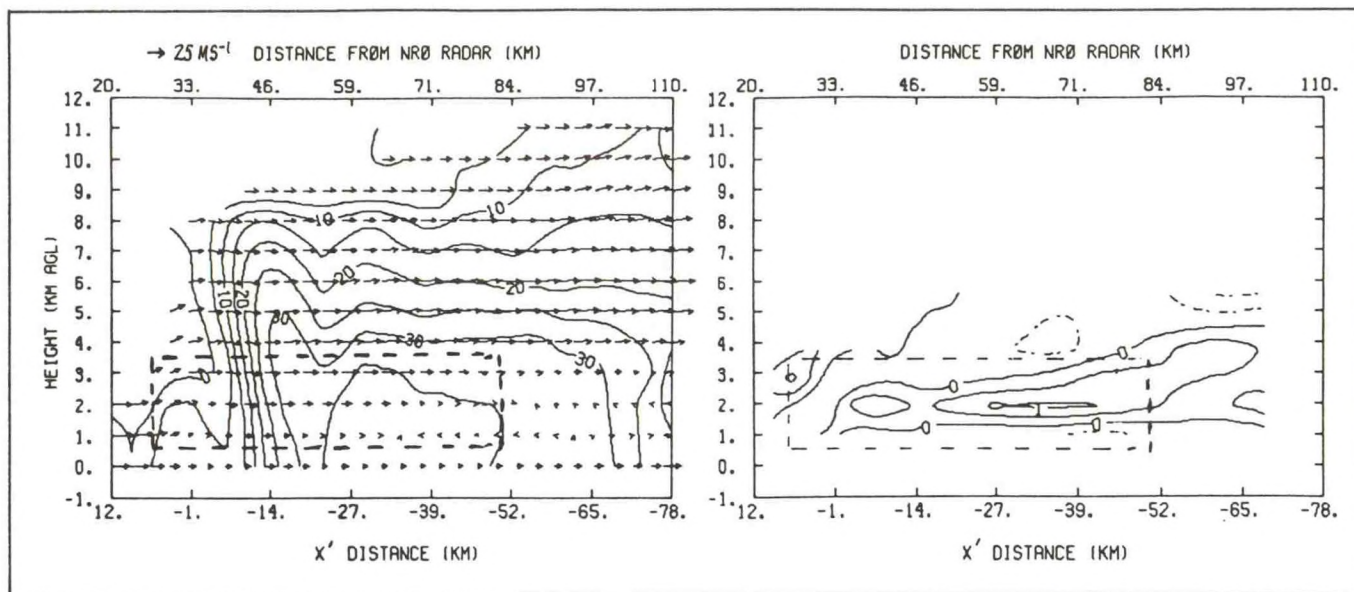


Figure 16. Along-line average of 20 vertical cross sections normal to 10-11 June 1985 squall-line gust front from a dual-Doppler analysis at 0426 UTC. (Left) Squall-line relative airflow and radar reflectivity (dBZ); (right) horizontal buoyancy gradients ($^{\circ}\text{C km}^{-1}$). Dashed line indicates integration area for vorticity equation. X' distance is with respect to gust front.

The momentum budget of a squall line, including the transport of momentum by the vertical air motions, was calculated for several times from Doppler radar data during its existence on 17 July 1981 during the Cooperative CONvective Precipitation Experiment (CCOPE) in Montana. The line was weakening and becoming more two-dimensional during the period of analysis, and the momentum budgets were interpreted in light of this evolution. Despite the fact that updrafts were weakening, the upward transport of front-to-rear momentum remained constant during the period because the updrafts were becoming progressively more tilted. This occurred because the updraft air was being increasingly accelerated rearward within the squall line by a pressure gradient force. Previous work suggested that such a pressure gradient is specifically associated with the more two-dimensional systems. This study shows the increasing importance of this effect as the system evolved to a more two-dimensional shape.

A study was completed of the environmental conditions associated with mesoscale convectively-generated vortices (MCVs) that become apparent in visible satellite imagery after the demise of an MCS's cold cloud shield. The locations and tracks of 24 MCVs are shown in Fig. 17. The majority of MCVs that were observed occurred south of 40°N . Most MCVs emerge from systems similar to mesoscale convective complexes (MCCs), that is, circular upper-level cloud shields. However, in only half of the cases did the MCVs originate in systems that met the stringent size, duration, and cold cloud-top MCC criteria. The result suggests that both the scale and duration of latent heating and the character of the background synoptic or mesoscale setting in which the convective system develops are critical factors controlling whether an MCV is generated. The typical MCV synoptic setting is very weak. The predominant feature at 500 mb was a long-wave ridge. Nearly one-third of the MCV cases were associated with a variation of the ridge pattern where a cut-off

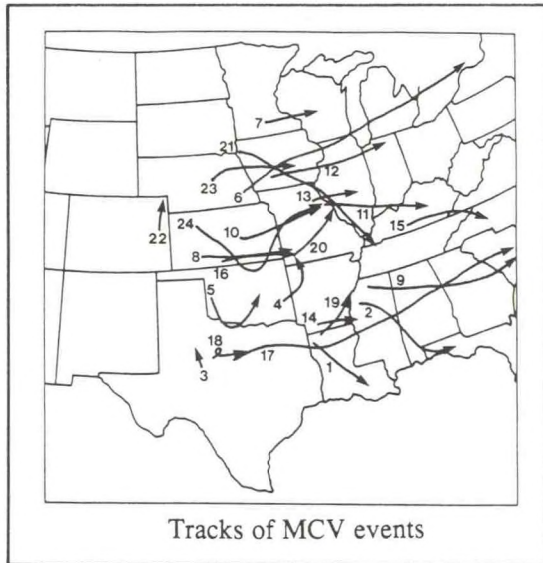


Figure 17. Tracks and locations of 24 MCVs over the central United States from 1981 to 1988.

low is blocked by a higher latitude ridge. Regardless of the pattern, both the environmental winds and the wind shear are weak and decrease with evolving MCV life-cycle stage. For the majority of the cases, the large-scale relative vorticity is negative before the MCV, and gradually increases. Since windspeeds and shears are decreasing, the increase in vorticity reflects the increase of cyclonic circulation in the MCV and its vicinity. Two case studies are under way in collaboration with FSL, using special data sets to illustrate the spectrum of apparent MCV characteristics that may be related to differences in the synoptic-scale setting. One developing MCV that was sampled by the NOAA P-3 on 24 June 1985 during PRE-STORM can be contrasted with another MCV observed by wind profilers on 9 June 1988. The 9 June case was in a quasi-steady state and had a 200-km-diameter circulation that was vertically stacked through a large depth of the troposphere, from 3 to 9 km. In contrast, the 24 June case developed in a much stronger synoptic setting that apparently contributed to a less vertically coherent circulation. Nevertheless, the aircraft data did show that MCVs have a warm core at middle levels.

Observations obtained during PRE-STORM are being used in a continuing study of a vortex that formed within the MCS of 6-7 May 1985. Such vortices have an inherent stability that often allows related convection to redevelop on succeeding days as the storm moves eastward. Analyses show that mesovortices may be the dominant organizational feature within MCSs. For example, the presence of a vortex focuses the middle-level rear inflow into a jet that passes to the south of the vortex center. The intruding flow is dry and potentially cold, and becomes negatively buoyant when chilled by evaporating precipitation. The descending inflow erodes the precipitation and updraft fields, and creates the comma-like shape that characterizes such storms. The 6-7 May case constitutes the most complete collection of rawinsonde observations for an MCS with an embedded vortex. Consequently, an analysis package is being developed to examine this unique data set (Fig. 18). To improve the understanding of MCSs, a vorticity budget study has been initiated to identify those mechanisms

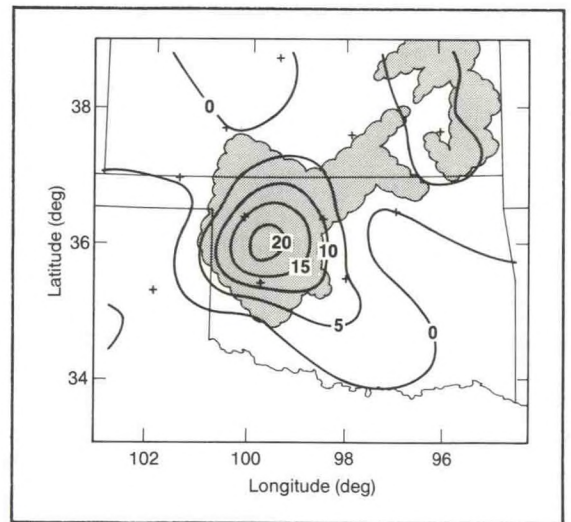


Figure 18. Objective analysis using cubic spline interpolation of relative vertical vorticity at 3 km above mean sea level at 0900 UTC in the 6-7 May 1985 MCS. Contour interval is $5 \times 10^{-5} \text{ s}^{-1}$. Plus sign denotes observation sites located within grid and used in analysis. Low-elevation precipitation pattern is shaded.

whereby vertical vorticity amplifies. Observations suggest that the appropriate vertical vorticity equation must include terms involving the earth spin vorticity (f), which are important on the mesoscale, and that the direct generation of vertical vorticity by horizontal solenoids is negligible.

A multiscale analysis of the 3-4 June 1985 MCS observed during PRE-STORM was completed. This nonsquall MCS exhibited very complex structure and evolution compared to squall-type systems, which have been emphasized in previous studies. Special upper-air soundings, wind profiler measurements, and ground-based dual-Doppler radar scans describe the precipitation structure, airflow, and thermodynamic conditions within the storm

and its supporting environment (Fig. 19). PRE-STORM upper-air observations are blended with synoptic data using a novel "gridless" objective analysis technique. A primary result is the documentation of contrasting structure and mechanisms exhibited by two intersecting convective rainbands within the mature storm. This structure is compared to that of more familiar squall-type systems. NSSL researchers also collaborated with their counterparts at CSU to complete a detailed study of a "wake low" in the surface pressure field. Vertical motions derived from Doppler radar reveal surprisingly strong subsidence at the back edge of the storm's stratiform region adjacent to the wake low, which evidently contributed to the corresponding rapid drop in hydrostatic surface pressure.

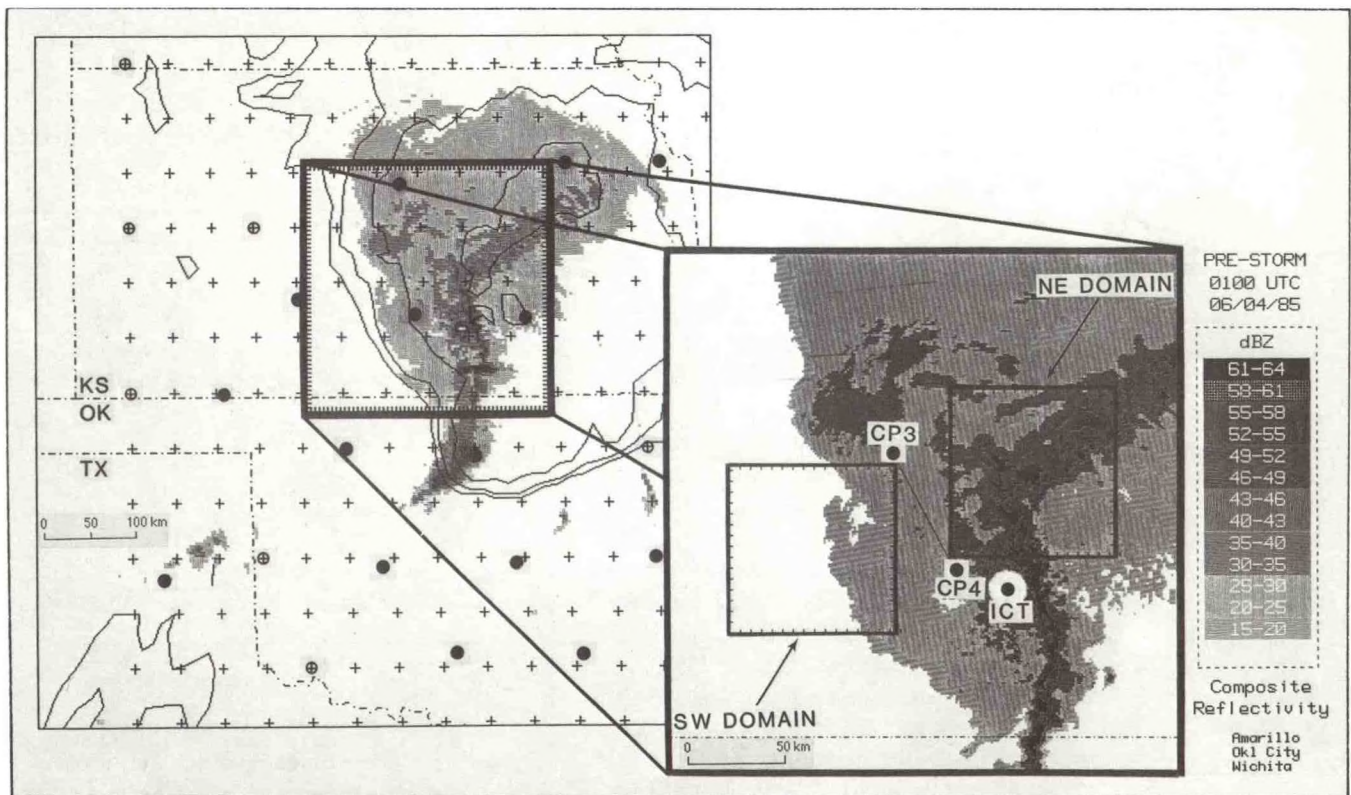


Figure 19. Domains involved in multiscale analysis of 3-4 June 1985 PRE-STORM MCS. Large area at left depicts upper-air network with superimposed low-level radar echo pattern and IR satellite temperature contours describing upper-level cloud shield. Expanded view at right shows locations of Wichita WSR-57 surveillance radar (ICT), CP-3, and CP-4 Doppler radars, and dual-Doppler analysis domains encompassing two contrasting regimes within the storm.

The summertime weather of much of the western United States is dominated by convective precipitation associated with the moist, subtropical flow regime called the southwestern U. S. monsoon. NSSL has been employing satellite and conventional sounding data to study the conditions associated with organized convective precipitations systems embedded in the monsoon flow. Available convective energy for thunderstorms over western Mexico during July and August was found to be extremely large, similar to the strongest of severe storm environments in the central plains. The storms triggered along the slopes of the Sierra Madre within this airmass are extremely intense and grow to great heights with very cold cloud shields (thunderstorms almost daily with top temperatures often colder than -70°C). Organized MCSs occur over the eastern coastal plains of Mexico in late spring and early summer when the average flow at 700 mb is from the west (Fig. 20a). In July and August, the 700-mb flow is from the east, and the active storm region shifts abruptly to the west coast (Fig. 20b). In

both situations, the midlevel flow advects warm, dry air from the plateau over the warm, moist boundary layer air, increasing the convective instability and providing a lid that suppresses convection except in regions of pronounced mesoscale forcing (i.e., flow up the mountain slopes). About twice a week in July and August, highly organized MCSs move slowly westward off the Sierra Madre toward the Gulf of California. Special field data and conventional sounding archives will be used to examine the specific conditions that lead to the propagating MCSs over northwestern Mexico.

Annual tabulations of MCCs for 1986 and 1987 for the United States were completed, as was an analysis of the differences between those years. In 1986, MCCs numbered 58, one short of the previous year's record; the 1987 total of 44 was closer to normal. Although both seasons were convectively active, both years experienced extended periods of deficient MCC occurrence during most of June—a period when MCC activity should be maximizing, as well as translating

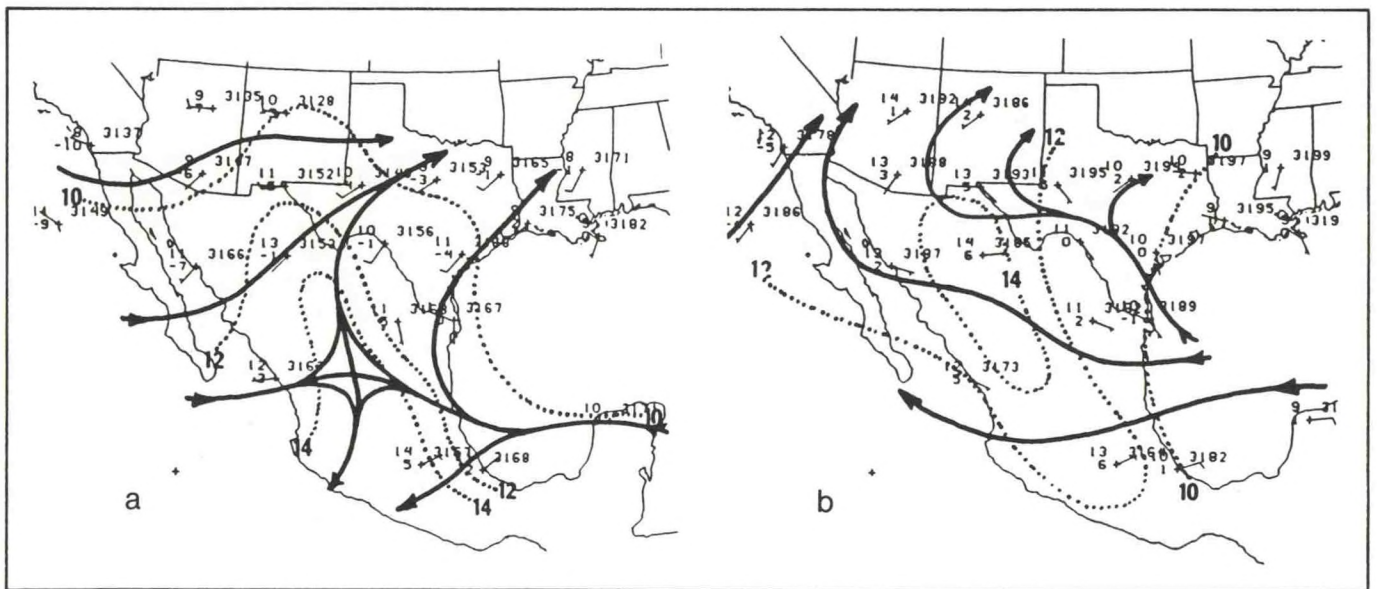


Figure 20. (a) Average 700-mb chart for 12 MCS events over northeastern Mexico. Heavy lines with arrows are streamlines, and dotted lines are isotherms in $^{\circ}\text{C}$. (b) Average 700-mb chart for 25 MCS events over northwest Mexico.

northward (Fig. 21). This time of the year is also when summer crops benefit most from MCC precipitation. The periods of reduced MCC occurrence in June of both years were associated with positive height anomalies in the lower troposphere; as these relaxed, the westerlies descended into the central plains. Destabilizing short waves and resultant enhanced moisture advection from the Gulf of Mexico returned, and a full latitudinal distribution of MCCs followed.

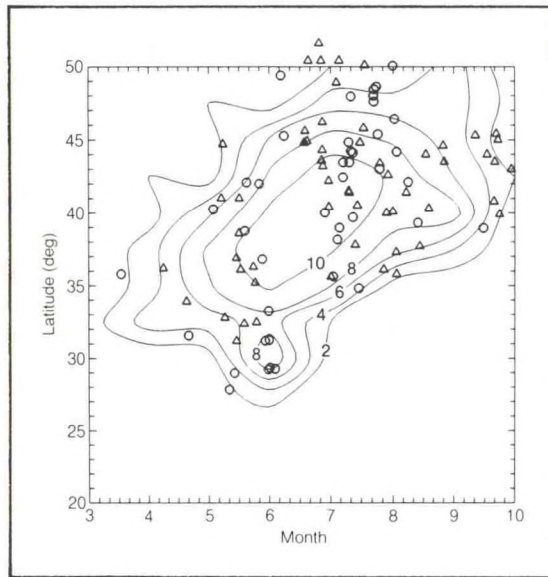


Figure 21. Contours depict latitudinal and seasonal climatological distribution (smoothed) of all MCCs between 1978 and 1985. Triangles represent MCC centroid locations at maximum extent by month and latitude for 1986; open circles are for 1987.

Dynamic retrieval methods were applied to dual-Doppler fields constructed from airborne Doppler observations of an oceanic mesoscale convective band that was observed near the southeastern coast of Taiwan during the Taiwan Area Mesoscale Experiment (TAMEX). This investigation is unique because the retrieved pressures can be compared to in-situ observations when the P-3 penetrated the convective band at several heights. Figure 22 shows a vertical cross section taken normal to the band's orientation. The updraft first tilted westward with height below about 5 km and eastward about 5 km. The strongest mesolow (~ 0.3 mb) was to the east of the high reflectivity zone underneath the eastward sloping updraft above 5 km. The low-level mesolow that should be evident under the westward sloping updraft at low levels is not apparent. The magnitudes of perturbation pressures are about a factor of three lower than those calculated from the 3-4 June PRE-STORM system, corresponding to the weaker vertical motions in this oceanic system. In-situ observations of D-value (middle right figure of Fig. 23 show the mesolow above 4 km at nearly the same location as the retrieval results. The magnitude of the mesolow is also comparable to the retrieved values. However, the aircraft saw a low at low levels near the center of the band, which was not seen in the retrievals. This discrepancy is believed to be due to inadequate resolution of the low-level flow by the airborne Doppler radar. Beam spreading in the high-shear regime at very low levels apparently masked the wind changes at low levels through the band that reflect the presence of the low. These results have important implications for future studies of weak convective lines (e.g., oceanic systems). To adequately resolve the boundary layer inflowing winds, it may be necessary to supplement the airborne Doppler observations with a penetrating aircraft.

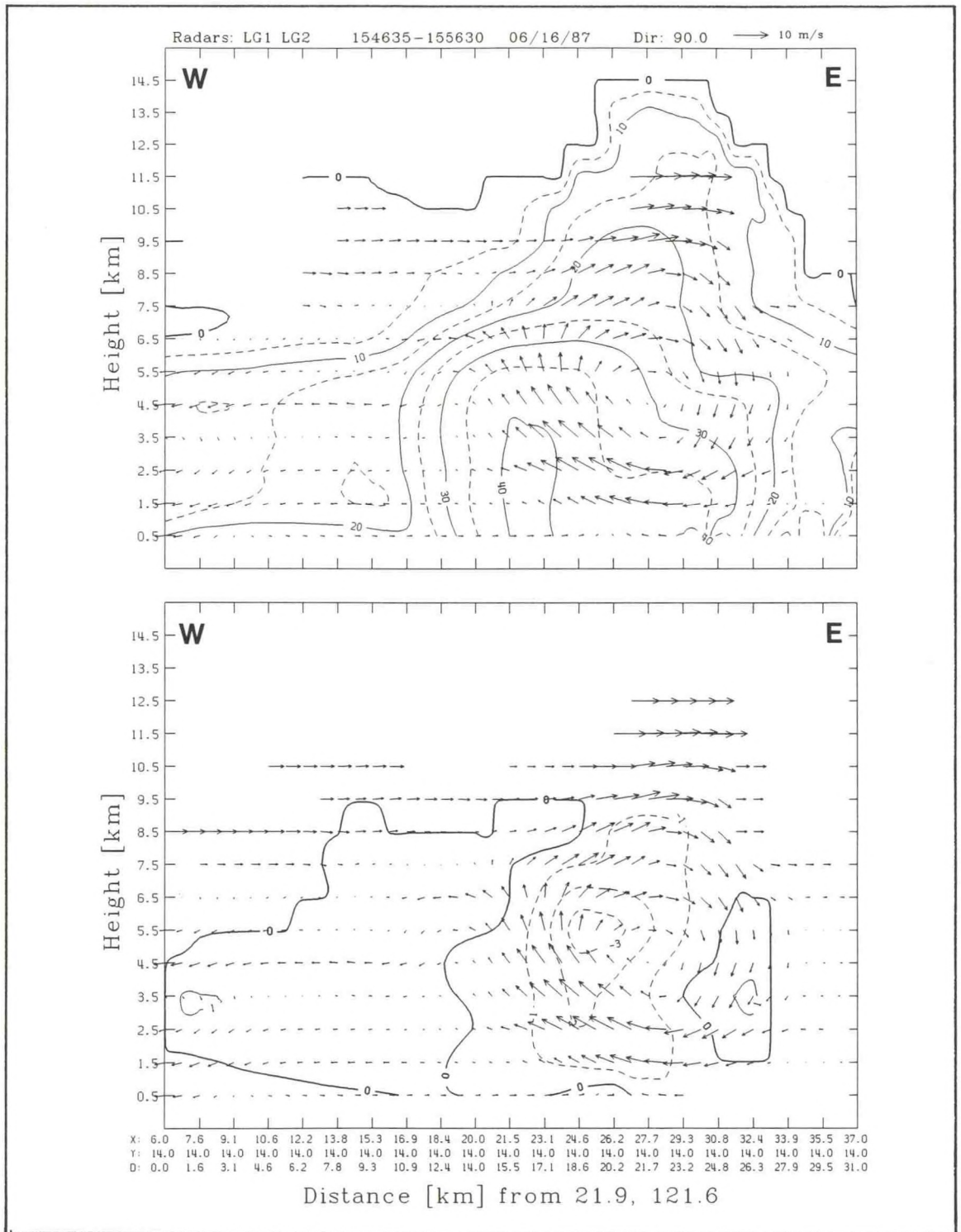


Figure 22. East-west vertical cross sections of relative windflow and radar reflectivity (top) and perturbation pressure (bottom) through the TAMEX convective band on 16 June 1987. Contours of radar reflectivity alternate between solid and dashed for each 5 dBZ contour interval. Contour interval of perturbation pressure is 0.1 mb and contour labels are multiplied by 10; contours of negative perturbation pressure are dashed.

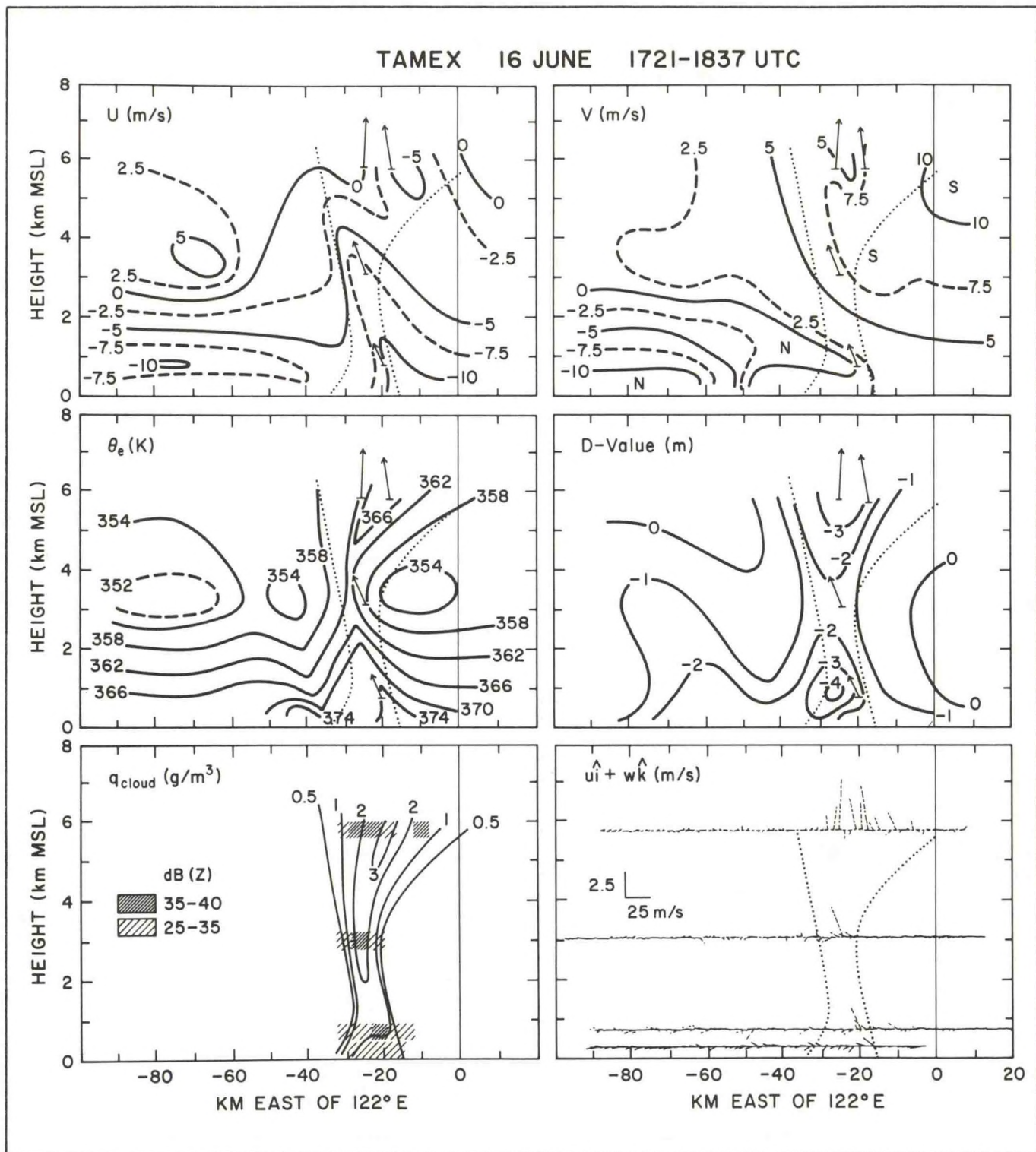


Figure 23. Vertical cross sections of u , v , equivalent potential temperature (θ_e), D-value, cloud water content, and radar reflectivity, and wind vector in the east-west plane for TAMEX case of 16 June 1988. Cross sections were constructed from four east-west passes through the convective band over about 1 hour. Vertical exaggeration (aspect ratio) is about 10:1. Dotted lines bound the region of cloud water content $> 0.5 \text{ g m}^{-3}$.

Lightning in MCSs

Research on lightning strikes in MCSs during PRE-STORM included a comparison of lightning strike locations and rates with satellite IR data, to study how lightning strikes are related to the evolution of MCSs. This study was delayed by difficulties in transferring digital satellite images from the Man-computer Interactive Access System (MCIDAS) to other computers, so satellite data that were recorded from the PROFS satellite link during PRE-STORM are being used. Much of the work on MCSs has been collaborative studies with scientists at CSU. In a recently completed collaborative study, the polarity and location of ground strikes were compared with radar reflectivity patterns for storms during PRE-STORM. The pattern of positive ground flash activity was found to depend on the degree of organization and the extent of the stratiform region. In cases with large, well-organized stratiform regions, most positive ground flashes occurred there, sometimes more than 100 km from the convective line. A small number of negative ground flashes sometimes also occurred in stratiform regions. When the stratiform region was less organized or did not reach as large a horizontal extent, positive ground flashes were closer to the deep convection and appeared more mixed with negative ground flashes. In two cases, strong cells on the southern end of a line had positive ground flashes near and inside the reflectivity core. As a partial evaluation of the mechanisms responsible for positive ground flashes more than 100 km from deep convection, a CSU model was run to examine in situ charge generation. The model showed that, in conditions such as probably existed in the storms we studied, a significant amount of charge could be generated in the stratiform region. The relative contributions by in situ charging and by advection from deep convection, which had been examined briefly in an earlier study, remain to be evaluated. Collaboration has also begun with scientists at the University of Oklahoma to study cloud-to-ground lightning in a storm system from another year. Lightning location, polarity, and rates are being compared with

the occurrence of severe weather and storm evolution from radar data.

A new generation of balloon-borne electric field meters was developed to accompany a LORAN sonde. In 1987, it was found that in the transition zone of an MCS the electric field was generally dominated by the vertical component, suggesting large horizontal stratification of charge. Fields were high, with a maximum of more than 110 kV m⁻¹. Five different charge layers were found, and our measurements in this one case support the CSU model of stratiform charging. Subsequent flights were made into MCSs as part of COPS-89; an analysis is under way. Preliminary results show good agreement in the vertical profile of the electric field in two different MCSs, suggesting it may be possible to define a typical electrical structure to use in modeling studies.

An important case study from COPS-89 was an electric field profile obtained on 7 June 1989 from the trailing stratiform region of an MCS (Fig. 24). Radar, satellite, lightning location, and upper-air data were collected to assemble a cohesive picture of the meteorological situation during this balloon sounding. There were seven electric field profiles collected during COPS-89; both the profiles themselves and the accompanying meteorological environments show great variations. Nevertheless, the 3-4 June and 7 June profiles were characterized by the most extensive stratiform rain areas, and correspondingly had very similar vertical electric fields. Just above cloud base, the two profiles nearly overlaid each other when plotted with respect to height. When plotted versus temperature, the agreement was not as good, except in the suspected microphysical charging regions between -5° and -20°C. Another striking feature common to both soundings was the presence of a 3-km-thick layer in the upper regions of cloud that had very little charge. Yet the differences between the profiles pose major positive charge layers near cloud base, indicative of errors in base estimates (lack of thermodynamic data caused us to resort to

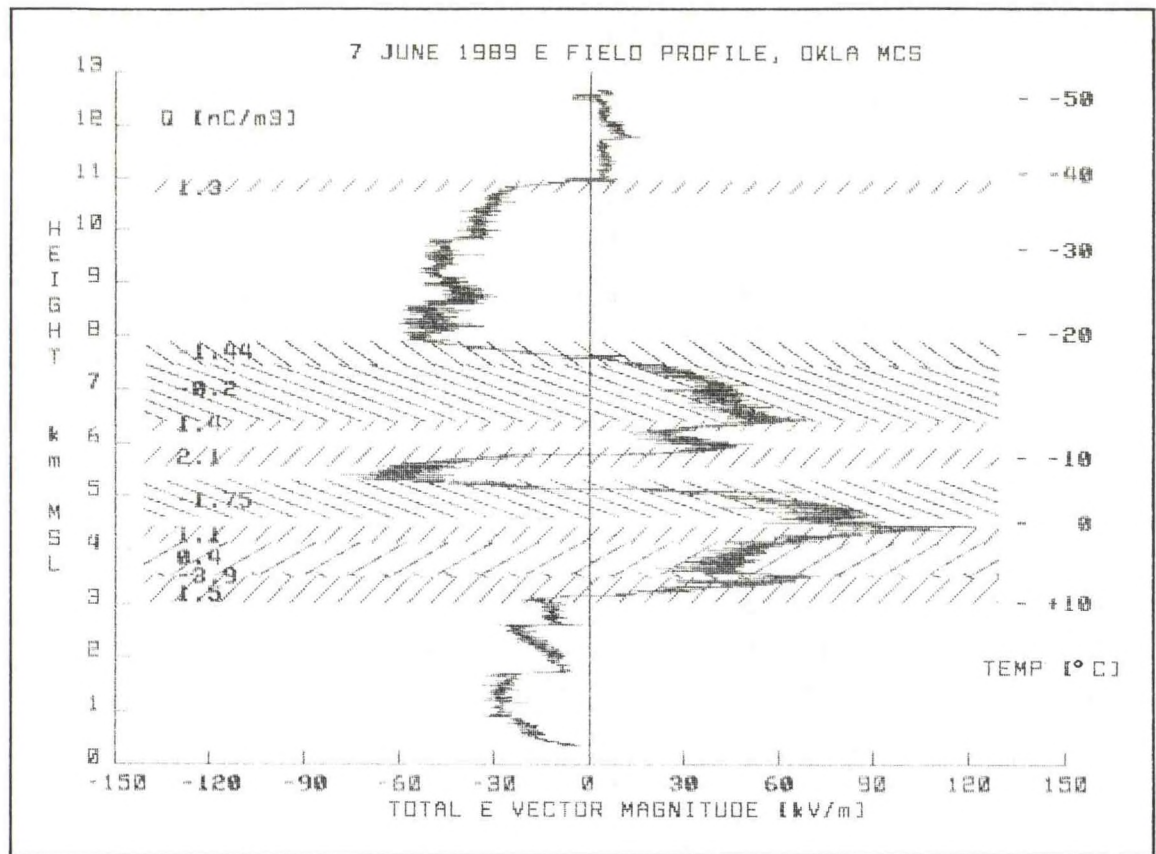


Figure 24. Electric field vertical profile collected on 7 June 1989 in an Oklahoma MCS during COPS-89.

other means of estimation), or showing real differences in space charge generation. What caused the 7 June case to have much larger horizontal field components will be investigated by comparing the cases for ratios of intracloud to cloud-to-ground discharge to see if the horizontal component differentials affected them. More case studies from COPS-89 will be considered, and particle data from the P-3 aircraft will be analyzed. From the latter, it is hoped to examine the possible microphysical charging mechanisms within the trailing stratiform regions, aided by the charging models at NSSL and CSU.

Utilizing data collected during DOPLIGHT 87, the kinematic and electrical structures were investigated for an MCS that passed through central Oklahoma on 18 June 1987. The MCS exhibited a precipitation and

kinematic structure similar to that observed in previous midlatitude systems, consisting of a leading convective line, a trailing region of enhanced stratiform precipitation, and an intervening weak reflectivity transition zone region. Two primary mesoscale airflows were identified: a rear inflow that entered the system's stratiform region and sloped downward towards the convective line, and a midlevel, front-to-rear flow that appeared to accelerate as it penetrated the convective line. A balloon-borne electric field meter was launched from NSSL's mobile laboratory that had been deployed to a location approximately 15 km behind the convective line. From the derived charge structure (Fig. 25), hypotheses were formed on the electrification of the stratiform cloud, concluding that plausible charging mechanisms were 1) screening layer formation

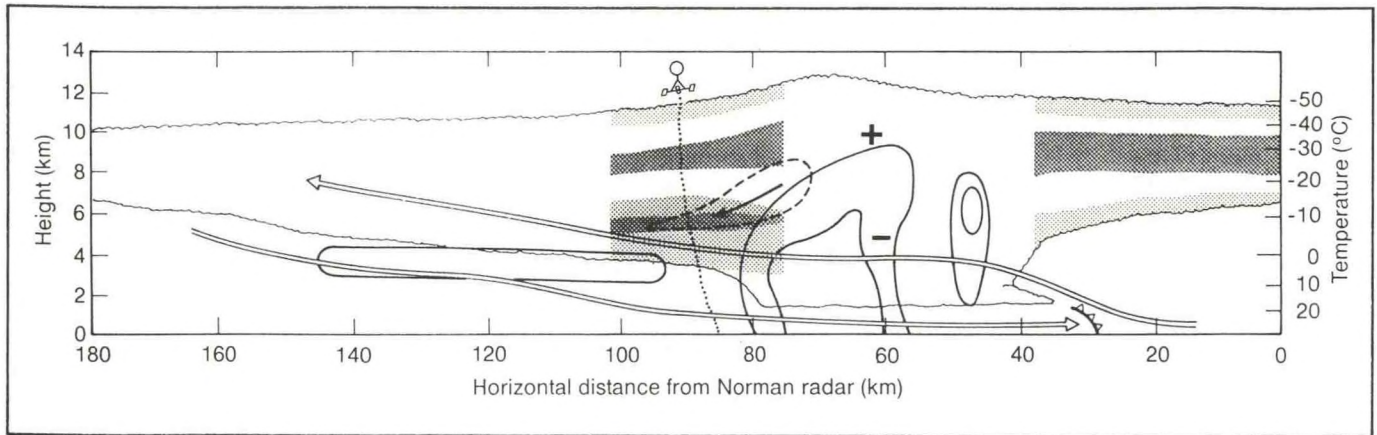


Figure 25. Storm structure and charge distribution of the 18 June 1987 squall system. Heavy lines enclose higher reflectivity regions (>35 dBZ), and streamlines depict the two primary components of the mesoscale airflow. The instrumented balloon's path through the transition zone is delineated by the dotted line. Light shading indicates regions of negative charge, and dark shading represents positive charge.

at the cloud boundaries, 2) advection of charge from the convective core, and 3) local microphysical charging resulting from graupel/ice crystal collisions. A bipolar cloud-to-ground (CG) pattern, with positive CGs in the stratiform region and negative CGs in the convective, developed as the squall system evolved. Advection of positive charge from the upper portions of the convective core was believed to significantly affect both the CG and intracloud flash rates of the convective and stratiform regions. Future work will focus on collecting more data within mesoscale systems, including in situ microphysical measurements, which will be used to ascertain microphysical interactions within the stratiform cloud. An emphasis will be placed on developing a conceptual model that will relate MCS kinematics, microphysics, and electrical structure.

Low-Level Jet Studies

A brief field project was conducted at NSSL during July 1988 to assess the potential for NEXRAD, radars, 403-MHz radar wind profilers, and digital sounding systems to monitor the evolution of the low-level wind for extended periods. The low-level jet was chosen as the phenomenon of interest because

it is neither well-sampled nor resolved by the current upper-air network, yet it is a common feature of the MCS and severe thunderstorm environments. Data from four low-level jet events suggest that the areal-averaged horizontal winds calculated from Doppler radar data using the VAD technique are comparable with the winds observed using a digital sounding system except under weak wind situations, and can capture the detailed vertical structure of boundary-layer phenomena such as the low-level jet (Fig. 26). The maximum speeds for all the observed jets were found between 268 and 471 m above ground level; speeds fell to 50% of their maximum by 1000 to 1500 m. The height of the maximum wind speed of the low-level jet on all days studied was below the planned lowest observation range gate of the NOAA 403-MHz radar wind profiler, indicating that a combination of NEXRAD and profiler data might be needed to sample the important wind field structure of the lower atmosphere. The current NWS data processing software affects the vertical resolution of the low-level wind field in operational, and therefore archived, upper-air soundings. The procedure used to calculate NWS 1000-ft winds actually damps the windspeed profile and artificially increases the height of the level of maximum

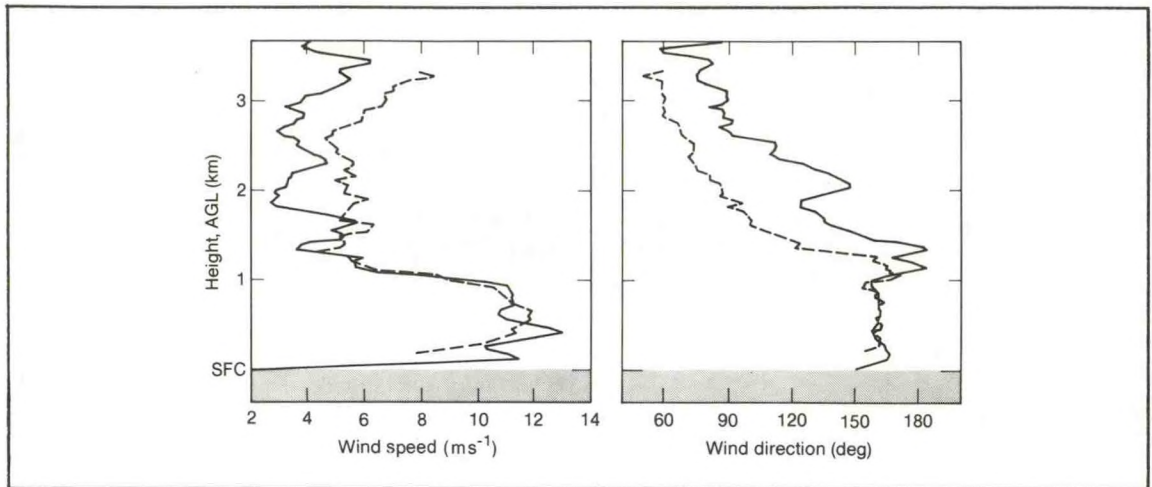


Figure 26. Profiles of M-CLASS (solid) and VAD (dashed) derived wind speed and direction versus height above ground level for 0830 UTC on 7 July 1988.

windspeed associated with the low-level jet. The appropriateness of these highly smoothed 100-ft winds for input into detailed mesoscale models should be carefully considered.

Denver Cyclone Composite Study

The Denver Convergence and Vorticity Zone (DCVZ) was identified from surface mesonetwork observations in northeastern Colorado. It is identified by northerly flow along the foothills west of Denver and southeasterly flow east of the city, and is often associated with severe weather in the Denver area. It has been the subject of many case and modeling studies; there is general agreement that the feature is terrain induced and almost always associated with south or southeast flow at the surface, but the physical mechanism(s) responsible for its formation is uncertain. A compositing approach was used to determine the relative importance of various proposed parameters and mechanism for DCVZ formation. Data were stratified by various flow regimes, DCVZ strength, and other considerations. Figure 27 shows a comparison suggesting that although southeast flow is necessary for

DCVZ formation, it is not the only requirement. A crude stability analysis for each of these categories shows that DCVZ days exhibit a shallow stable layer between 9,000 and 10,000 ft, whereas the southeast-flow/no-DCVZ vertical profile shows well-mixed conditions aloft. More refined analyses will be made using NWS radiosonde data to define further the roles of stability and upper-air forcing.

Mesoscale Dynamics

The finite-element diagnostic model of the extended Sawyer-Eliassen equation was further developed into a prognostic model in combination with the tendency equations for momentum, potential temperature, and water vapor. This model is used to study the formation of frontal rainbands and evolution of potential vorticity (PV) anomalies generated by latent heating and boundary fluxes.

Numerical results show that initial mesoscale anomalies of potential vorticity or temperature may (may not) cause a formation of mesoscale multiple rainbands before the moist PV becomes negative if initial

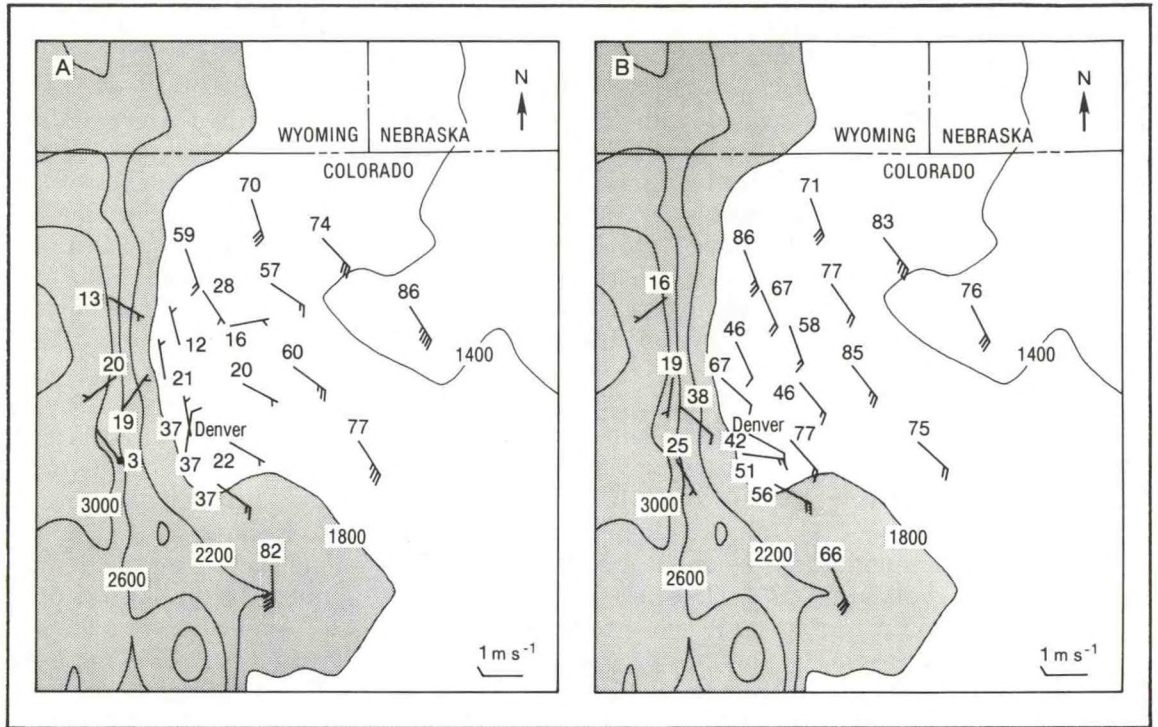


Figure 27. (A) Mean wind and persistence of the mean wind at 2200 UTC for 128 days that a DCVZ was identified. Persistence varies from 0 to 100; low (high) values represent high (little) directional variation within the sample. Contours represents terrain elevation in meters; shaded area is >1800 m. (B) Same as A, but for 20 days identified by southeasterly flow, but no DCVZ.

mesoscale anomalies of moisture also exist (do not exist) in association with (independent of) the temperature anomalies. These bands, formed by moisture anomalies under the condition of positive moist PV, are seen as weak cores of upward motion surrounded by the large-scale moist ascent (rather than separated by mesoscale dry subsidences as for negative moist PV). When the moisture anomalies are lifted above the lifting condensation level and become saturated, the evolution of the bands is largely controlled by the Lagrangian advection of moisture anomalies. As the geostrophic confluence squeezes (stretches) the bands toward (along) the front, the fine structures of moisture anomalies are smoothed by eddy viscosity and multiple bands gradually "merge" into a larger single band. However, when moist PV becomes negative in

the cloud region (but the flow is still stable to viscous symmetric instability), banded substructures can be either intensified or generated internally by the positive feedback between the moist ageostrophic circulation and geostrophic forcing in association with the generation of mesoscale PV anomalies.

Rainbands produce not only horizontal-mean positive (negative) PV anomalies in the lower (upper) levels, but also significant mesoscale PV anomalies in the horizontal. Boundary-layer processes can produce either positive or negative PV flux, depending on the boundary conditions, especially the sensible heat flux. In general, unless very close to an intense surface front, positive (negative) PV flux is produced when warm (cold) air moves onto a cold (warm) surface.

The complex and yet somewhat subtle nature of PV flux near an intense surface front, and its impact on the evolution of vertical motions associated with fronts and frontal rainbands, were studied with a three-dimensional, semigeostrophic diagnostic model. This model is also incorporated in the previously developed semi-Lagrangian and semigeostrophic finite-element (SSF) model, and used to study moist frontogenesis and cyclogenesis. In addition to earlier theoretical results showing that warm (cold) frontogenesis is favorably supported by moist processes (upper-level jet), the new results show that warm-frontal moist ascent is relatively shallow and not supported by upper-level forcing, but the cold-frontal circulation can be enhanced by precipitation cooling. Plans are to continue to develop the SSF model to study moist frontogenesis and cyclogenesis, and compare the results with observational and model-generated data in collaborative work with NSSL and NCAR staff.

FROPEX

In the fall of 1987, dual-Doppler observations were collected during the passage of three "dry" cold fronts during the FRONtal EXperiment (FROPEX) in Oklahoma. Single-Doppler radar VAD analyses and dual-Doppler radar analyses, based essentially on "clear air" returns, depict important details of boundary-layer frontal circulations. Features that were detected include prefrontal low-level jets, prefrontal wind-shift lines, regions of prefrontal downdrafts, fronts, and postfrontal downdrafts. A single-radar analysis of the mean horizontal wind assuming a linear wind field is shown in Fig. 28. Although smoothed significantly, the data show a low-level jet (prior to 1000 CST), a wind shift at about 1000 CST, a nearly constant veering wind between 1000 and 1300 CST, and a surge in windspeed with the passage of the cold front (after 1400 CST). Note that the wind backs with height when the cold air arrives. Of particular interest are the derivatives of the wind field needed to compute vertical velocity and frontogenetical functions. Although the Norman data lags the Yukon data by about one hour, significant features are reproduced in the data.

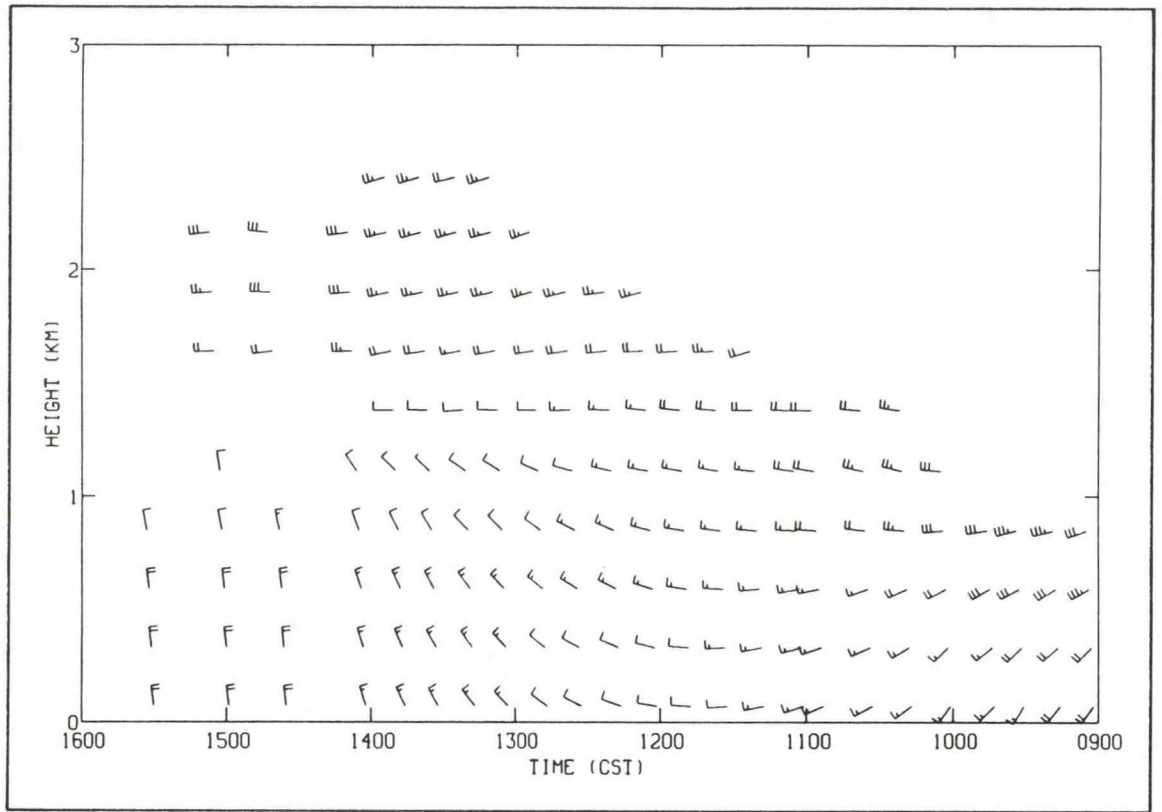


Figure 28. Mean horizontal wind determined from single-radar measurements during the passage of a dry cold front on 16 October 1987. Full wind barb is 5 m s^{-1} . A linearly varying wind field is assumed.

STORM-SCALE STUDIES

Tornadic Storms

The storm-relative helicity of the 0-3-km layer is being developed as a parameter for forecasting mesocyclones from a sounding and from observed storm motion. Like the correlation coefficient, this parameter is a measure of the strength and veering of the low-level, storm-relative winds. Helicity is a linear function of storm motion, is easily computed as an area on a hodograph diagram such as Fig. 29, and is insensitive to the smoothness of the hodograph curve. Thus,

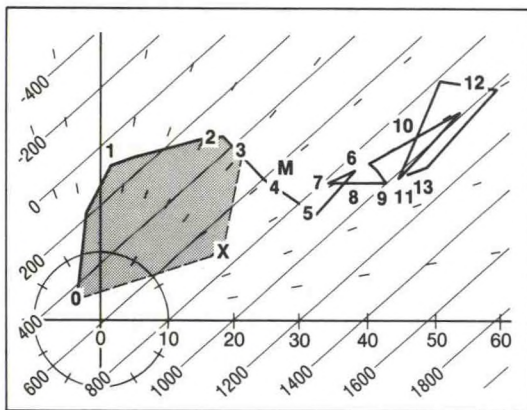


Figure 29. Hodograph for tornado environment on 28 November 1988 at Raleigh, North Carolina. Speed circles are every 10 m s^{-1} , and plus signs are shown on speed circles at 10° increments. Numbers along hodograph curve denote height in kilometers. Large M denotes mean wind between surface and 200 mb, and large X denotes observed storm motion. The storm-relative helicity in the lowest 3 km is twice the area swept out by the storm-relative wind vector between 0 and 3 km; i.e., the shaded area defined by 0123X0. Diagonal straight lines are contours of helicity for this hodograph as a function of storm motion; i.e., the location of X. For observed storm motion of 240° at 20 m s^{-1} , the helicity is $720 \text{ m}^2 \text{ s}^{-2}$. This is a large value compared to the rough threshold of $150 \text{ m}^2 \text{ s}^{-2}$ for mesocyclone development in thunderstorms.

meaningful "updated" values of helicity can be computed after amending the hodograph crudely on the basis of a forecaster's insights and later partial data from surface stations, remote sensors, and numerical forecasts.

Lightning and Storm Structure

Preliminary results from NSSL studies of vertical profiles of electric fields through several storms over the Great Plains show both polarities of electric field in excess of 100 kV m^{-1} . These results were compared to work done in the 1930s, which is still accepted as the "classical" picture. Contrary to the classical picture, storms have more than three charge layers. For example, the early work did not mention the existence of "screening layers" now shown to be a common feature of the boundary region of clouds.

A study was completed of lightning strike locations in the Edmond, Oklahoma, tornadic storm of 1986. As the storm became tornadic, lightning ground flashes occurred more frequently and ground strike points became concentrated near the reflectivity core north of the mesocyclone. As the tornadic stage of the storm ended and the storm became weaker, lightning ground flashes occurred less often and strike points became more scattered. Positive ground flashes were first detected shortly before the tornado began.

The positive ground flash rate reached a peak during the tornadic stage of the storm and decreased slowly as the storm weakened. Most positive strikes were around the periphery of lightning strike activity, outside of reflectivity cores. The behavior of negative ground flashes in the Edmond storm contrasted with the behavior in the Binger storm studied earlier. In the Binger storm, rates of ground strikes near the mesocyclone were low when mesocyclones were strong and increased as mesocyclones dissipated. It was suggested that the small number of ground

strikes near the mesocyclone of the Binger tornado probably was caused by the very strong updraft in a classically organized supercell storm. The hypothesis is that the strong, well-organized updraft lifted negative charge too high and too close to the positive charge above it for negative cloud-to-ground lightning to occur there. The Edmond storm had a shallower mesocyclone and appeared to have a weaker or less organized updraft aloft, so that negative cloud-to-ground lightning was not inhibited as in the Binger storm. A modeling study of the Binger storm has begun to test some of these ideas. Another tornadic storm that occurred in 1981 is also being examined in collaboration with scientists at the University of Oklahoma. Single-Doppler radar data were analyzed from periods throughout the lifetime of the storm, as it progressed from a small, isolated storm to a

supercell storm and finally a multicell storm. When the storm was a supercell, lightning ground flash rates were low, and strikes occurred completely outside 10-dBZ reflectivity contours at low altitudes, underneath overhanging anvils on the southern and western flanks of the storm. As the storm evolved further, ground strikes began occurring within low-altitude reflectivity contours, and eventually most strikes occurred there. Ground flash rates reached a maximum during the multicell stage of the storm.

Simultaneous cloud-to-ground lightning locations (from a three-direction-finder network) and base-scan radar reflectivities were recorded in northeastern Colorado in the summer of 1985. For 12 cloud systems that formed in the area, the location and timing of both positive and negative flashes were

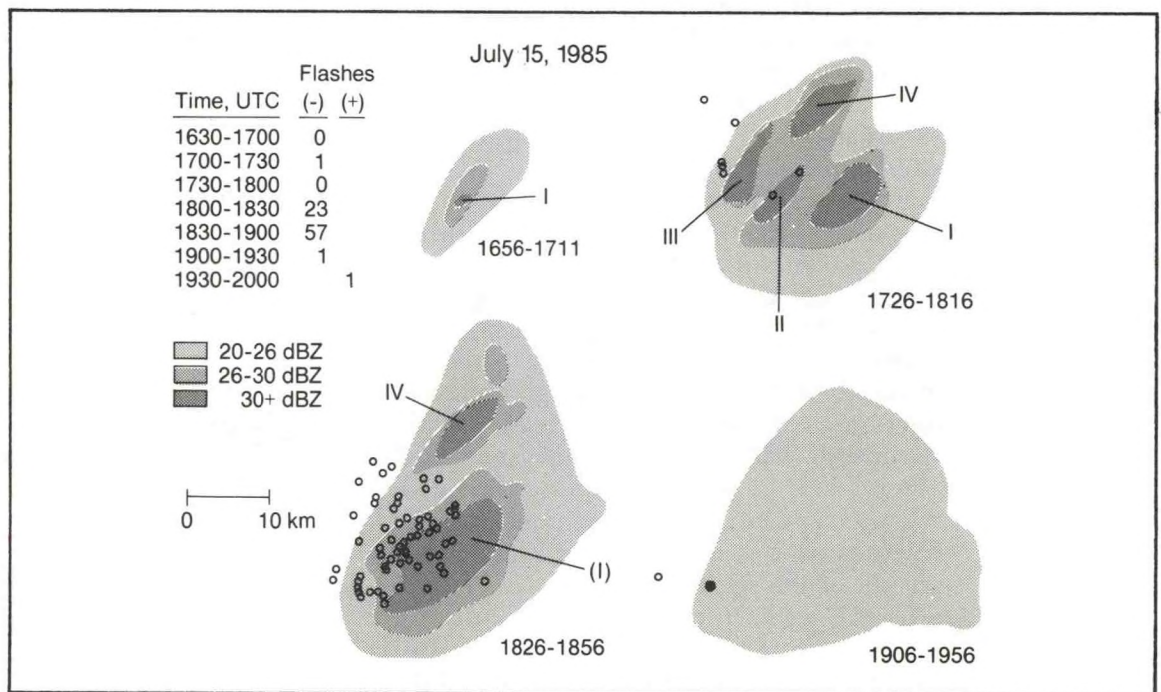


Figure 30. Composite relationship of lightning to radar echoes during the life cycle of a small thunderstorm on 15 July 1985 in northeastern Colorado. Each panel represents a time composite, relative to the storm position for the indicated period. There were 82 negative flashes and 1 positive flash during this storm. Shading shows area covered by echoes at the three reflectivity ranges at some time during the compositing interval. Roman numerals indicate the main cells that developed during the lifetime of the system. Open and solid circles show negative and positive CG flashes, respectively. Inset table shows frequency of flashes every 30 minutes.

correlated with their corresponding reflectivities. Negative flashes were found slightly outside the echoes or in the region of low values but of the highest gradients of reflectivity (Fig. 30). Positives occurred in areas of weak and uniform radar reflectivity away from the intense convective centers, or in the dissipating stages of the storms. Clouds with a moderate radar-detected precipitation rate near the ground produced many negative flashes but few positives; clouds with a high precipitation rate produced few negatives but many positive flashes. (Similar observations have been made for Florida thunderstorms; see next section.) Further research will increase the number of cases and explore the lightning-radar relationships for different degrees of convective organization, especially when thunderstorm clusters develop over northeastern Colorado and lead to the more organized MCSs. Such a study could provide important insights into the charge separation and charge distribution mechanisms of convective systems.

Analysis of lightning strikes triggered by aircraft provided strong evidence that the bidirectional leader process is a major physical mechanism of lightning development during the junction stage of the flash. This mechanism was shown to be pivotal for interpreting high-speed visual observations of air discharges, rocket-triggered lightning flashes to ground, and interferometric data of intracloud flashes. Although additional analyses and observations of different types are needed, the concept of the bidirectional leader emerges as a key physical process in all phases of the lightning discharge. Future efforts will focus on determining characteristics of the bidirectional leader process to be used in a physical model of the lightning discharge.

Storm-Scale Retrievals

Analysis of a severe hailstorm that occurred during the CCOPE Project in Montana in 1982 showed good correspondence between dynamically retrieved and aircraft-measured pressure gradients across the cloudbase updraft. The wind-shear vector in the storm environment changed very little through a large depth in the lower part of the storm, resulting in vertically stacked dynamic pressure perturbations near the updraft, and a consequent small effect on the production of new updrafts and storm motion (Fig. 31). This situation contrasts with the case of a supercell storm where the environmental shear vector and pressure gradients veer with height, resulting in significant vertical pressure gradients and a consequent tendency toward rightward propagation of the storm. The utility of the retrieval method to calculate storm motion based on minimization of pressure solution errors produced by false local velocity changes was also demonstrated.

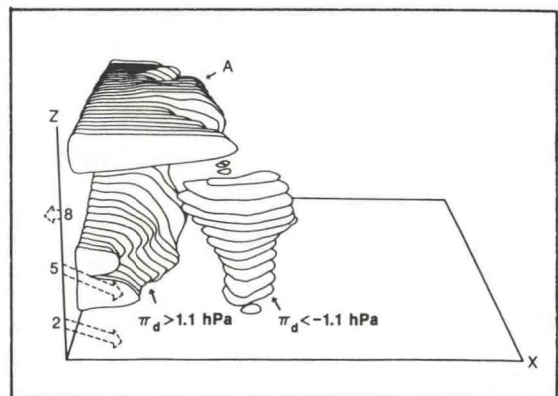


Figure 31. Three-dimensional surfaces of volumes containing deviation pressure greater than 1.1 hPa (at left) and less than -1.1 hPa (at right) in a Montana hailstorm during CCOPE. Vertical axis is 13 km, and horizontal axes are 40 km. Dashed arrows on vertical axis indicate orientation and relative magnitude of environmental shear vector at various altitudes. Excess pressure region at updraft top is marked by A.

Polarization Studies

During the COPS-89 field experiment, a modest amount of data were collected with the NSSL polarimetric radar. The data are in time series, where the reflectivity factor, differential reflectivity, differential propagation constant, and correlation between horizontally and vertically polarized echoes can be obtained. These parameters offer promise for better quantification of rain, as well as discrimination among various types of hydrometeors. A few cases are available for study in heavy rain with possible small hail, including a sample from a stratiform region of an MCC that was collected simultaneously with in-situ measurements by the NOAA P-3 aircraft. Outside collaborators on this project are from the University of Alabama at Huntsville, CSU, and Pennsylvania State University.

Power loss caused by depolarization by rain along propagation paths was quantified in the main channel of a circularly polarized radar (wavelength 10 cm). Heavy precipitation ($>50 \text{ mm h}^{-1}$) caused loss of more than 3 dB along a 30-km path length, and that increased to more than 10 dB when the path length was 50 km. These findings, backed by differential phase measurements with the NSSL radar, affect NEXRAD design.

Quantitative relationships between hydrometeors and their polarimetric signatures continue to be investigated. A multiparameter decision rule is sought that will partition the parameter space of polarimetric measurables so that each partition corresponds to a distinct hydrometeor population. A small step has been made in that direction, with the following main results. Pure rain produces a correlation coefficient between horizontally and vertically polarized echoes of 0.98. The correlation is a measure of shape variations or irregularities in the radar resolution volume, therefore it decreases when diverse particles are present. This measured value is consistent with theoretical predictions.

Similar results are observed in other precipitation that contains hydrometeors of one type. The values that were observed from echoes with good signal-to-noise ratios were not lower than 0.9, which is in full agreement with model results that have been obtained at NSSL for a variety of rain and hail scenarios. Lower numbers were measured from noisy data, suggesting that the correlation could also be used for data quality control. In one storm with large hail, differential reflectivity was negative throughout the core. The values were about -0.5 dB above the melting layer and about -1.0 dB below the layer (Fig. 32). Hailstones modeled as oblate spheroids with their minor axis randomly oriented in the horizontal plane, and axis ratios between 0.6 and 0.8, reproduce all essential features of these measurements. Other investigators have noticed negative differential reflectivity in storms with large hail. Therefore, it is tempting to attribute such observations to similar circumstances.

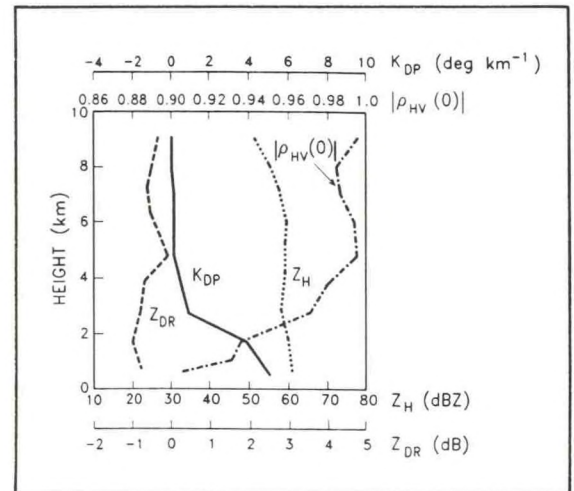


Figure 32. Vertical profiles of reflectivity factor Z , differential reflectivity Z_{DR} , differential propagation constant K_{DP} , and correlation coefficient $\rho_{HV}(0)$ at 1159 UTC on 3 June 1985. Range is 82.5 km, azimuth is 242° ; data averaged over 2.1 km in range.

Kennedy Space Center Studies

A principal emphasis of Kennedy Space Center (KSC) meteorological studies by NSSL scientists has been to provide U. S. Air Force (USAF) forecasters with improved techniques to predict convective development and cloud-to-ground lightning by monitoring the surface wind field. Several other studies have also used the KSC meteorological data to improve understanding of the conditions when lightning occurs in convective storms.

A compositing technique was developed that keys on the maximum base-scan reflectivity of the convective cells. Composites of radar, lightning, and surface winds were constructed during the development, mature, and dissipation stages of cells having their life cycles in the KSC

network. Figure 33 shows the mature stage of a convective line that passed through the KSC network. These composite cases have shown that principal cloud-to-ground lightning activity is on the upshear side of the storm in the reflectivity gradient (similar to the Colorado results) where upward motion resides between the convergent gust front and the reflectivity center.

Recent studies indicate that cloud-to-ground lightning avoids regions of maximum base-scan reflectivity. Figure 34 reinforces the relationship between coincident radar and ground strikes on 21 days in 1987. Hypotheses for this observation include cleansing the water droplet of charge or a lack of space charge density; the stage of the life cycle of the storm most likely plays an important role in the explanations.

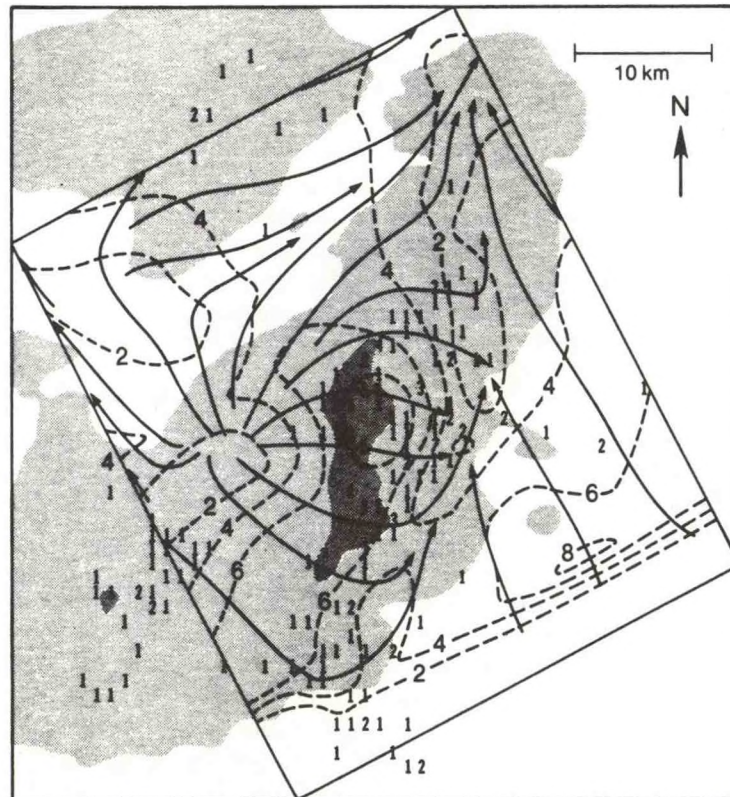


Figure 33. Composite mature stage from 2220 to 2305 UTC on 26 June 1987 in the KSC mesonet network. Reflectivity is shown by shading at thresholds of 20 and 45 dBZ. The number of flashes is shown by small numbers on a 1-x-1 km grid square. Also shown are surface wind streamlines and isotachs in large numbers ($m s^{-1}$).

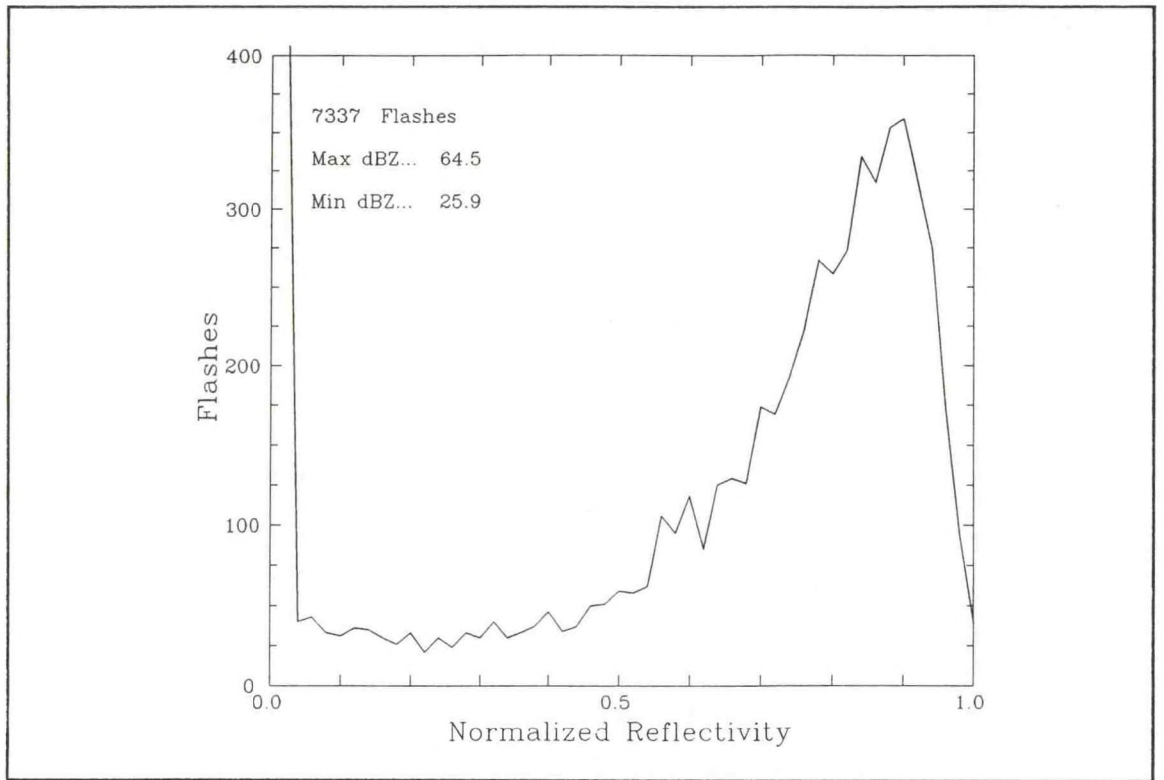


Figure 34. The distribution of flashes versus reflectivity (dBZ) for 21 days in the KSC mesonetwork during the summer of 1987. Because of variations in maximum reflectivity from one scan to the next, reflectivity values were normalized between 0 and 1.

CAPS

In FY 1988, a proposal was submitted by the Norman atmospheric science community to the National Science Foundation (NSF) to establish a Science and Technology Center (STC) at the University of Oklahoma for conducting long-term research on real-time numerical prediction of severe storms. This effort was led by CIMMS and drew on the ideas of the community, which includes NSSL scientists. In December 1988, the University of Oklahoma was announced as 1 center of 11 in the Nation to be funded out of approximately 325 proposals. The University of Oklahoma's Center for the Analysis and Prediction of Storms (CAPS) is initially funded under the STC system for 5 years, with a possible extension to 11 years.

The work will focus on three primary areas of research during the first few years:

- Developing a state-of-the-art numerical prediction model capable of using data from the new observing systems to be deployed in the central United States during the next decade.
- Evaluating the accuracy and sensitivity of model predictions to the quality and quantity of initial and boundary conditions and to other factors.
- Designing assimilation techniques to produce optimal initialization of numerical simulations.

A number of scientists from NSSL are working with CAPS investigators to plan research projects in detail and, in some cases, are contributing to formal proposals to use CAPS funding for graduate students, computer personnel, and other resources. A proposal was submitted to CAPS to provide CPU time on the Illinois CRAY-2 and other support for retrieval and observing system simulation experiments using Doppler radar data with the Klemm-Wilhelmson three-dimensional

nonhydrostatic cloud model. The goal of this study is to use retrieval methods to initialize cloud model simulations and to determine the optimal amount and type of data required for reliable cloud-scale forecasts. At selected points in the model run, simulations will be stopped and restarted using various combinations of "observed" data, retrieved data, and interpolated information; the restarted simulations will be compared with the control run to ascertain the sensitivity of the results to missing or erroneous data.

Four-Dimensional Data Assimilation

Data assimilation studies at NSSL are undertaken in cooperation with CIMMS and CAPS in the Norman meteorological community, as well as the global community. The primary direction that has been chosen for four-dimensional data assimilation development is the variational method within the framework of adjoint methods. The efforts in this area are relatively new, and foundations of the work in applied mathematics and optimal control theory dictate that the work be performed in unison with researchers elsewhere. Primary goals are to determine the best strategy for incorporating the new suite of mesoscale observations, such as those from wind profilers, Doppler radars, and weather satellites into both hydrostatic and nonhydrostatic prediction models.

A nonhydrostatic model using the "backward" (adjoint) code developed by a CIMMS scientist in Hamburg, Germany, was moved to the NSF CRAY in Pittsburgh, Pennsylvania, because of a successful proposal to NSF for computing time. This model is being applied to the dryline situation to simulate the data available from wind profilers in the near future, and to determine their impact on finding the initial state of the atmosphere. Following the simulation studies, data from the dryline case in COPS-

89 will be used to test the initialization schemes.

The difficulty of determining the three-dimensional wind field from single Doppler observations in the unstable boundary layer is now identified as the Wolfsburg/Lilly problem after it was first identified at the University of Oklahoma. Interest has been generated in this challenging issue, which has widespread serious computational problems; there are also concerns about the uniqueness of the solution and other esoteric applied mathematical aspects. The adjoint model was used to revisit this problem, and a successful effort reduced the severe computational overhead associated with finding the wind field from one observed component. The research continues with various combinations of observables in the experiment such as wind components and temperature, and eventually Doppler data, which would affect the use of data from NEXRAD.

A theoretical study has begun on the uniqueness of solutions obtained from adjoint methods applied to fluid dynamical equations in a joint effort between CAPS and the University of Oklahoma. The issue is to determine what is the minimum set of observations in time and space that is essential to guarantee that the initial state can be reconstructed. The effort to date has concentrated on simpler models, but the intention is to add complexity in a stagewise fashion.

Once the computer code has been formulated for a model, the corresponding adjoint code can be written in a straightforward, if somewhat laborious manner. It has been suggested from parallel experience with oceanographic data at the Atlantic Oceanographic and Meteorological Laboratory (AOML) that these adjoint models could be constructed automatically by using computer science methodology inherent in compilers. A pilot project supported by CAPS involves a researcher at Florida International University in Miami. The research has obvious potential to permit modelers to test assimilation methods

without the severe time commitments to coding that are currently required.

The tremendous overhead in computing time necessary to run these adjoint codes makes it imperative to streamline the machine computations as much as possible. This problem is being considered by a CAPS member who specializes in parallel processing and vectorization of machine codes, as well as applied mathematics in variational methods. The adjoint method is being programmed in this parallel mode on the University of Oklahoma Alliant computer, and it will ultimately be installed on the Pittsburgh CRAY. Benchmarks will be established for various components of the forward and backward codes, and new strategies for solving the optimization problem, such as augmented Lagrangian methods, will be tested.

Adjoint assimilation for a barotropic tropical model is being addressed by researchers at NSSL, CAPS, AOML, and the University of Wisconsin CIMSS. Despite its simplicity, this barotropic model in the tropical atmosphere has been used to predict the environment in the vicinity of hurricanes, and it successfully forecasted hurricane tracks. NSSL staff are interested in assimilating satellite-derived winds into the simple model to improve knowledge of the initial state, and thus improve the forecast of storm motion. To determine the utility of these adjoint methods in the operational setting, a pilot study was undertaken to use the barotropic model and various data from the tropics (mostly satellite-derived products) to study assimilation in the presence of a hurricane. The goal is to determine the limitations for this simple model and make a prognosis concerning the suitability of this strategy to other models used in operations. Close collaboration with the NWS National Hurricane Center will take place as the preliminary experiments are finished and the operational performance is examined.

Storm Modeling

In an ongoing study seeking improved understanding of electrification processes in thunderstorms, the formulation and testing of a three-dimensional, time-dependent model of kinematic storm electrification was completed. The model distributes space charge among five liquid and ice hydrometeor categories from the combined effects of both inductive and noninductive collision charge separation mechanisms and charge screening layers. The model assisted in identifying the noninductive graupel-ice charging mechanism as primarily responsible for the initial electrification of a mountain thunderstorm. This conclusion is supported by the first direct comparison of in-situ aircraft measurements and model output at specified locations of observations to be attempted in a cloud modeling study (Fig. 35). The modeled space charge and field distributions are

additionally most consistent with observations if a charging sign reversal temperature of between -10° and -21°C is assumed in calculations. A future project will model the causal relationships between observed lightning activity and electrification processes in the tornadic Binger, Oklahoma, storm. The working hypothesis is that intense convective circulations in the Binger storm carried charged cloud and precipitation particles to high levels of the atmosphere, where resulting electrification was more conducive to intracloud discharges than to ground.

A study of the 7 May 1985 PRE-STORM MCS was initiated to determine the influence of diabatic processes on mesovortex formation. A three-dimensional, time-dependent, mesoscale kinematic model, which accepts time-dependent input airflow analyses and lateral boundary conditions on

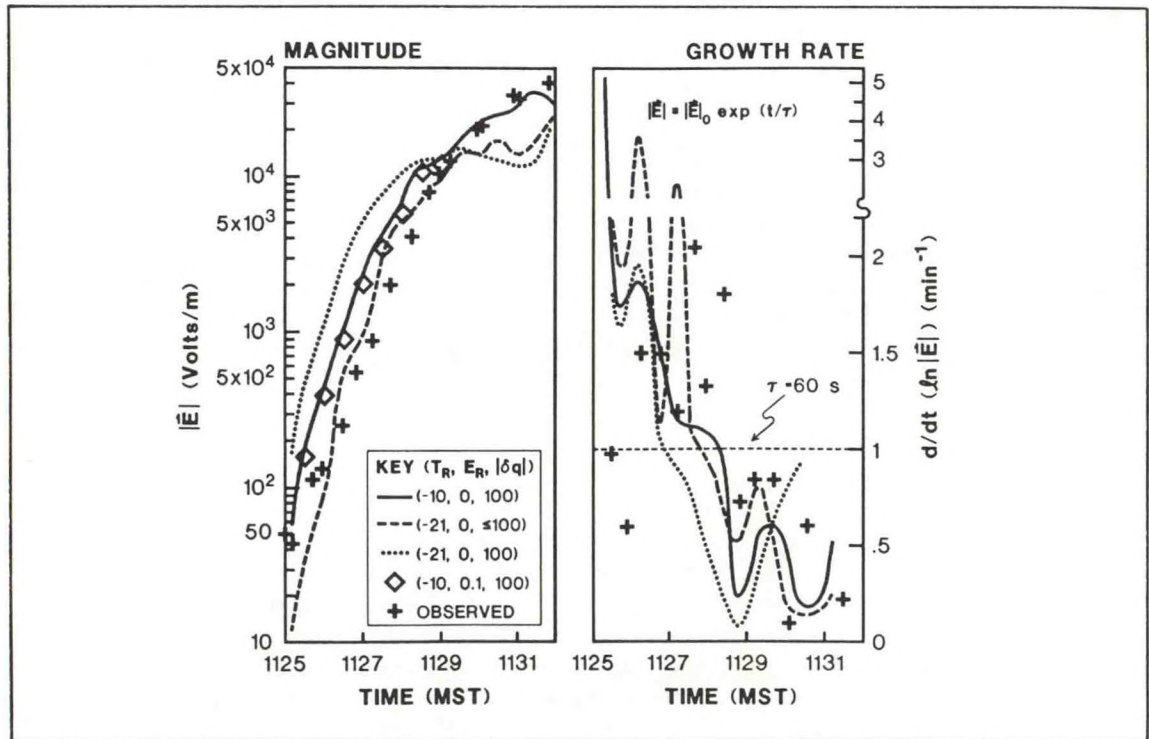


Figure 35. Electric field and its changes in the 31 July 1984 New Mexico mountain storm. Model data are interpolated from gridpoints to known NCAR-NOAA sailplane location. Left: total electric field magnitude. Right: total electric field growth rate following the sailplane motion.

heat and water substance, was developed to generate proxy data on the mesoscale environment for input to a diagnostic dynamic model. A mesoscale objective analysis routine, which can accept both radiosonde and wind profiler data, was developed to provide input airflow analyses for the kinematic model as well as diagnoses of hydrostatic pressure, temperature, and water vapor content. Input of gridded analysis information to the model facilitated a 12-h forecast of temperature and water substance fields (Fig. 36). Resolvable-scale vertical motion lifts moisture and generates a thick cloud layer in the stratiform precipitation region of the MCS. Future efforts will evaluate the reliability and impact of a convective parameterization scheme in the 7 May case by directly inserting output of a one-dimensional model into the kinematic mesoscale model at known locations of deep convection, and verifying model predictions with supplemental radiosonde observations.

A comparison has begun of the warm-cloud microphysics parameterization from

the NSSL cloud model with a detailed warm-cloud microphysics model developed at CIMMS. The goals are to verify and improve existing parameterization methods for possible future inclusion in the CAPS forecast model. The parameterized microphysics module was converted to the VAX and is being interfaced with the same three-dimensional, nonhydrostatic cloud model that drives the detailed microphysical module. Future efforts will concentrate on comparative cloud simulations with both detailed and parameterized microphysics.

Dryline Modeling

Participation in COPS-89 emphasized the planning strategy and collection of data in the environment of an Oklahoma dryline by the NOAA P-3 aircraft, and additionally included responsibility for recording microphysics data on all MCS flights. A major goal of COPS was to obtain data to define the mesoscale environment of an Oklahoma dryline, which will serve as input for future diagnostic and modeling studies of the forces responsible for dryline morphology, evolution, and thunderstorm initiation. A preliminary subjective analysis of data has been initiated to diagnose the mesoscale environment of the dryline of 24 May 1989. In collaboration with researchers at CSU, NSSL staff have also begun to define relationships between land use and dryline morphology. Future research will use two- and three-dimensional simulations of this case using the nonhydrostatic version of the CSU-RAMS mesoscale model.

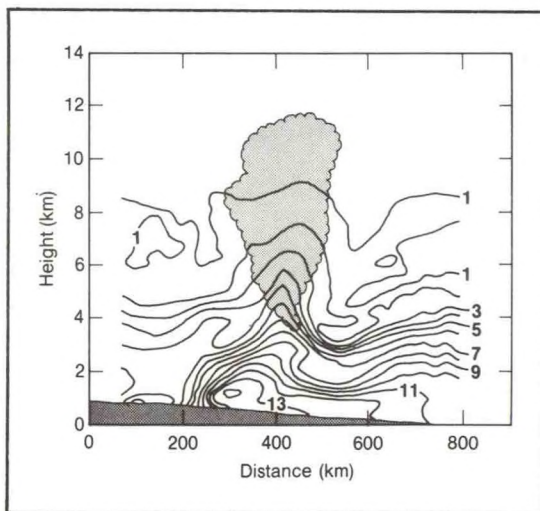


Figure 36. Water vapor and cloud fields in a west-northwest to east-southeast vertical cross section through the stratiform region at 1000 UTC on 7 May 1985 from output of a 12-h forecast. Contours are mixing ratio in grams per kilogram of water vapor. Scalloped curve encloses stratiform cloud region.

Ice Sublimation and Mesoscale Downdrafts

Rear inflow, the intrusion of environmental air into an MCS across the trailing precipitation boundary, is a common feature of many MCSs. The rear inflow observed during an MCS in PRE-STORM on 23-24 June 1985 was examined with regard to the region of origin and the initiating mechanisms. While rear inflow is usually defined relative to the mean propagation speed of the convective line, for 23-24 June the stratiform rain region propagated at half the speed of the convective line, suggesting that a refined definition of rear inflow may be necessary. Observations indicated the inflow origination at the rear of the stratiform rain region, but most likely underneath the anvil cloud shield produced by the convective system. A one-dimensional model with explicit microphysics was used to explore the effects of a precipitating anvil cloud on the atmosphere below. The model-simulated temperature, moisture, and wind fields closely resemble actual observations, and they indicate that a sublimation-initiated mesoscale downdraft below anvil base transported air with high horizontal momentum downward into the middle levels, which were characterized by weak winds. This momentum transport led to unbalanced flow when the mesoscale downdraft weakened, because of decreased snow within the anvil as MCS convective elements decayed and propagated southward relative to the anvil precipitation region. The midlevel winds then veered markedly in response to unbalanced Coriolis accelerations. These results emphasize the importance of ice microphysics to mesoscale circulations that develop within convective systems.

Computing Facilities

NSSL continued to improve its computing capabilities in FY 1989 by adding a VAX 6310, a MicroVax III with a 4660 Ramtek display, and a Concurrent 3280 to replace the PE-3242 at Norman. Many PCs were added at both the Norman and Boulder facilities, and a Ramtek was added at Boulder. A SUN workstation was also bought for use in the FAA program. A 9600-baud link was installed between the Norman and Boulder facilities to allow the Boulder group to use the Norman facilities, and vice versa. A T1 link was installed between the University of Oklahoma and the Norman Laboratory, allowing NSSL to tie into the university network. Most PCs are networked, along with several laser printers; with the addition of a terminal server to the network, modems and the MICOM switch can now be accessed from the network (Fig. 37). The computing facilities will continue to be expanded by adding an additional VAX computer in Boulder, along with a 6250 tape drive and disk subsystem to the Concurrent 3280. TCP/IP will be added to the Concurrent 3280, allowing it to connect to the network. The PC network will continue to expand, and a new high-resolution color camera will be added to the graphics computer. In addition, an uninterruptible power supply system will be added to support the computer facility in Norman.

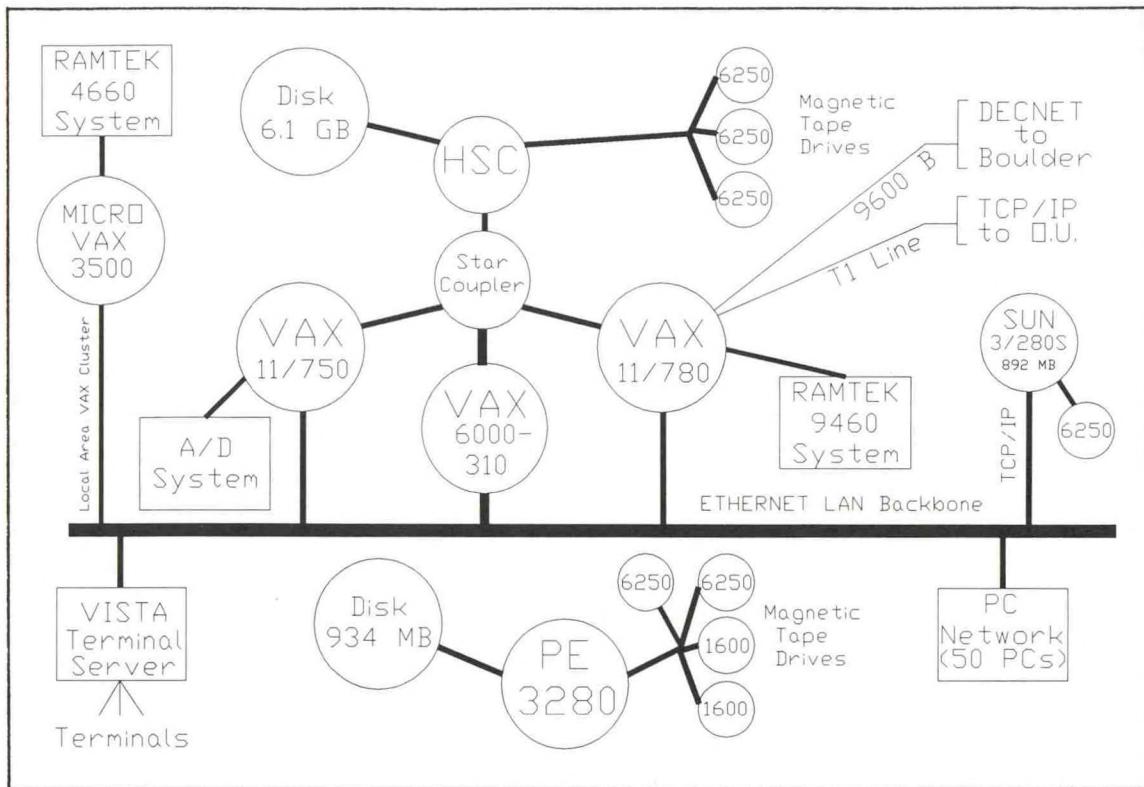


Figure 37. Configuration of NSSL computing facilities in Norman.

Microburst Handbook

Microbursts: A Handbook for Visual Identification was published in color this past year. Photographs and accompanying text describe the theoretical and observational evidence for a thunderstorm-induced vortex circulation that impinges on the ground. Such circulations were responsible for several fatal crashes of commercial aircraft in the United States during the last decade. The large initial printing was exhausted shortly after publication, a second printing was made to fulfill the extensive demand, and a third is planned for the large number of requests that have been received by the Government Printing Office. Distribution was made to every NWS station, to all major FAA, military, university, NCAR, and National Aeronautics and Space Administration (NASA) facilities involved in research and applications related to microbursts, and recently to commercial aviation interests in the United States and other countries. In the coming year, a poster version of essentially the same material will be produced.

Forecasting Convection in KSC Region

NSSL scientists worked with several agencies with forecasting responsibilities in the central Florida region. This area will receive the second NEXRAD radar (after Norman); a new NWS station was commissioned in 1988 at Melbourne where the NEXRAD will be located.

The lightning hazard at KSC continues to be a unique and critical issue for NASA and the USAF in this region. Lightning hazards at KSC were studied to help make better forecasts for the preparation and launch of space vehicles. Further study was made of the surface-convergence method of short-term forecasting of cloud-to-ground lightning in

summer months using the average divergence over the entire mesonet network; this method is often effective in anticipating flashes by tens of minutes. Additional research isolated the signal of individual thunderstorms in the wind field to reduce the time and space scales of the lightning threat given by the full-network approach. Other studies concentrated on the complex relationships between lightning, radar reflectivity, and surface winds, and on the accuracy of the lightning-detection network at KSC. The results of these studies were given to NASA staff and USAF forecasters at KSC, and are now part of their operational forecasting procedures. With the opening of the Melbourne NWS station, NSSL began to help bring NWS and NASA/USAF interests together. When the NEXRAD arrives, NSSL will help to bridge the gap further through a variety of research and operational activities.

Training

Three remote training modules on thunderstorm characteristics and severe storm structure were prepared for NWS Headquarters. Preparation of text and case examples for two additional modules on Doppler radar principles and characteristics was begun. Considerable support was given to NWS NEXRAD efforts. A training unit was established in Norman in a building adjacent to NSSL, and the Laboratory has agreed to act as scientific advisor to this unit. Initial training documents prepared by the NWS and by the NEXRAD contractor (UNISYS Corporation) were reviewed. Seminars and workshops on mesoscale and radar meteorology were presented at several NWS offices and other locations.

A Guide for Interpreting Doppler Velocity Patterns, which was prepared early in FY 1988, was printed by the NEXRAD Joint System Program Office in FY 1989. This color training guide presents simulated Doppler

velocity patterns for a variety of environmental flow features, as well as flow features found within severe thunderstorms. The first training document of its kind, it has been enthusiastically received by potential users of the NEXRAD system and is being used by universities and government agencies for Doppler radar training.

Tropical cyclone structure was studied, and an analytical simulation program was developed in conjunction with AOML. The program can be used to derive radar samples of reflectivity and radial velocity (Fig. 38). The simulated radar fields can be produced for any chosen range and elevation angle to the storm, and contain differing effects of

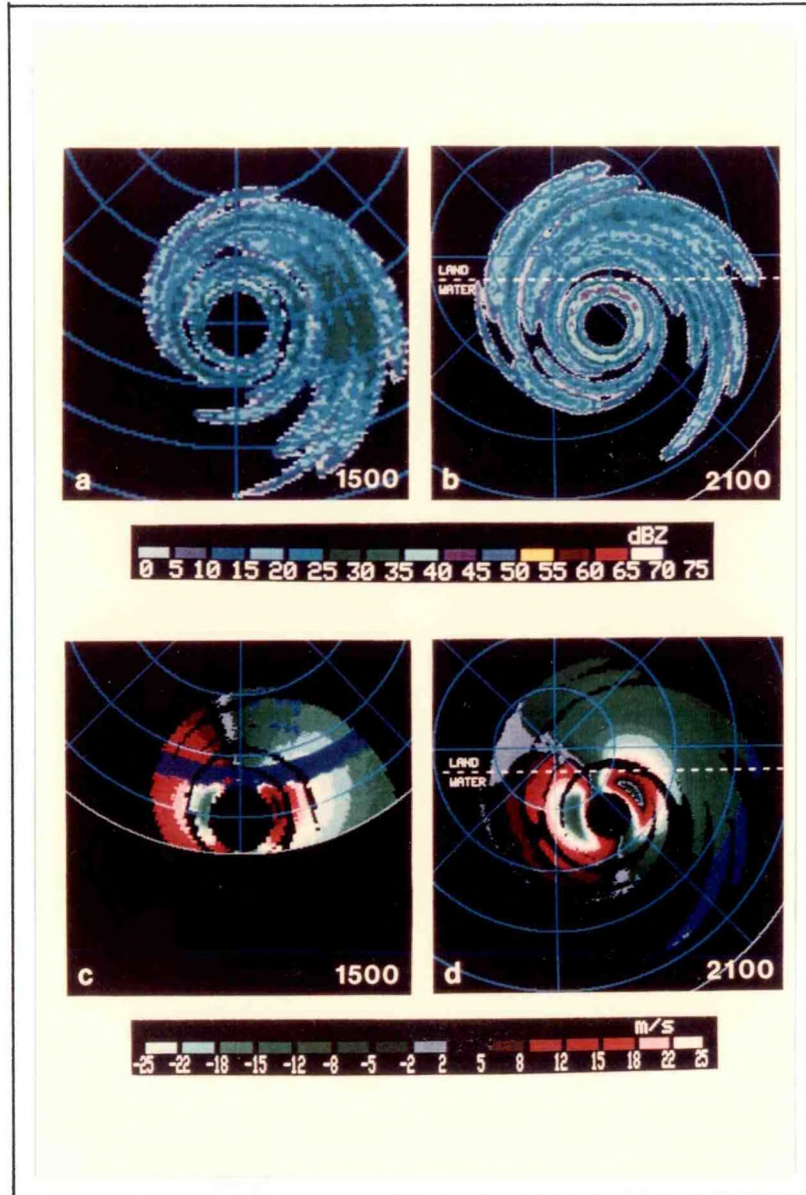


Figure 38. (a, b) Simulated Doppler radar reflectivity and (c, d) radial velocity for a land-falling hurricane for 6 hours of movement from 1500 to 2100 UTC. Purple color in (c) and (d) indicates region where radial velocity estimates are unavailable because of radar sampling constraints.

water and land surfaces. The simulated data can be used for training and education and for verification of radar-based tropical cyclone algorithms.

As a component of a program to develop training materials for the NWS on severe storm structure and classification, a special class of supercell storms has been proposed. Such storms often are associated with heavy precipitation, and so have been called high precipitation (HP) supercells (in contrast with low precipitation [LP] supercells). Examples of these storms are being studied (Fig. 39) to determine if they have a unique connection to the environments in which they form. Early work suggests that in some cases, the character of these storms depends critically on horizontal inhomogeneities in their environment. If this finding is validated in future work, it has important implications for the dynamics of rotating storms and how such storms interact with their surroundings. The training development

emphasizes the transfer of knowledge from the research community to operational offices. The training development effort is expected to culminate next year in a videotape series on severe storm structure that will also include workbooks and tests to be used in training for NEXRAD.

TDWR

NSSL developed an algorithm to detect gust fronts and other wind shifts using Doppler radial velocity fields in the mid-1980s. Since then, the algorithm has been continually upgraded, so that in its present state it detects approximately 88% of all strong gust fronts and forecasts their location up to 20 minutes in advance. This algorithm was evaluated in real-time testing in the High Plains (Denver) and the Great Plains (Kansas City) during 1989. During these tests, algorithm products were sent to air



Figure 39. HP supercell photographed near Colorado City, Texas, on 2 June 1989; baseball-sized hail and strong wind gusts occurred from this storm. (Photograph © 1989, C.A. Doswell.)

traffic controllers to provide wind-shear hazard warnings and forecasts of frontal passage for planning purposes. The gust front algorithm is one of two main algorithms that will be used with the FAA's TDWR system. Improvements to the algorithm during FY 1989 included a new technique to forecast the location of gust fronts, a new technique to track and predict gust fronts as they pass over the radar, a method to produce smoother representations of the front, and new methods to associate gust fronts in the vertical (between two low-elevation angle scans) and in time. An example of gust front detections overlain on a Doppler velocity field is shown in Fig. 40. A study was also completed on the use of the gust front detection algorithm with the NEXRAD system. It was found that gust fronts should be detected out to about 100 km with the NEXRAD system if some small changes are made to the algorithm. It was also determined that the gust front algorithm

can detect a number of other wind shift lines, such as synoptic fronts or sea-breeze fronts. A goal for 1990 is to add both azimuthal shear and reflectivity thin-line detection to the gust front algorithm so that gust fronts oriented along azimuths can be detected by the algorithm. NSSL scientists also plan to participate in another operational test of the TDWR system during the summer of 1990 near Orlando, Florida.

A Doppler velocity dealiasing algorithm developed at NSSL has undergone further improvements. This algorithm uses only two radials of data to help properly dealias the present radial. Error checks ensure that errors that may occur are either corrected or not allowed to propagate. This algorithm has been run in real time for two years on the TDWR prototype radar, and few errors have been noticed. This algorithm correctly dealiased 99.8% of Doppler velocities in four

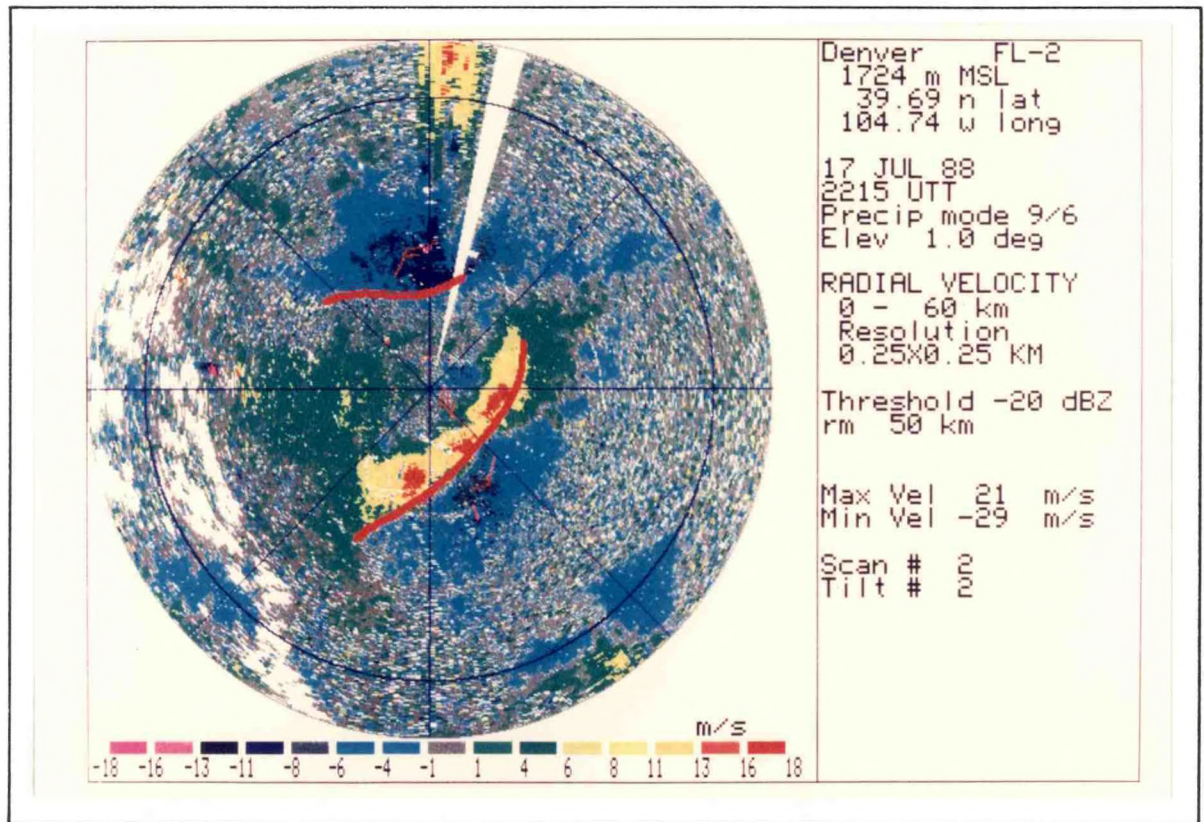


Figure 40. Doppler velocity field with gust front algorithm detections overlaid on it. Positive velocities are away from radar, negative toward radar. Data were collected with the MIT/Lincoln Laboratory prototype radar on 17 July 1989 near Denver.

cases with extreme aliasing problems. An example of the algorithm's performance on one of these cases is shown in Fig. 41. This algorithm takes only 1.8 seconds to dealias a 360° by 200-gate array of velocity data on the

NEXRAD computer system. Because of this algorithm's speed and effectiveness, it has been selected for use with the NEXRAD and terminal NEXRAD systems.

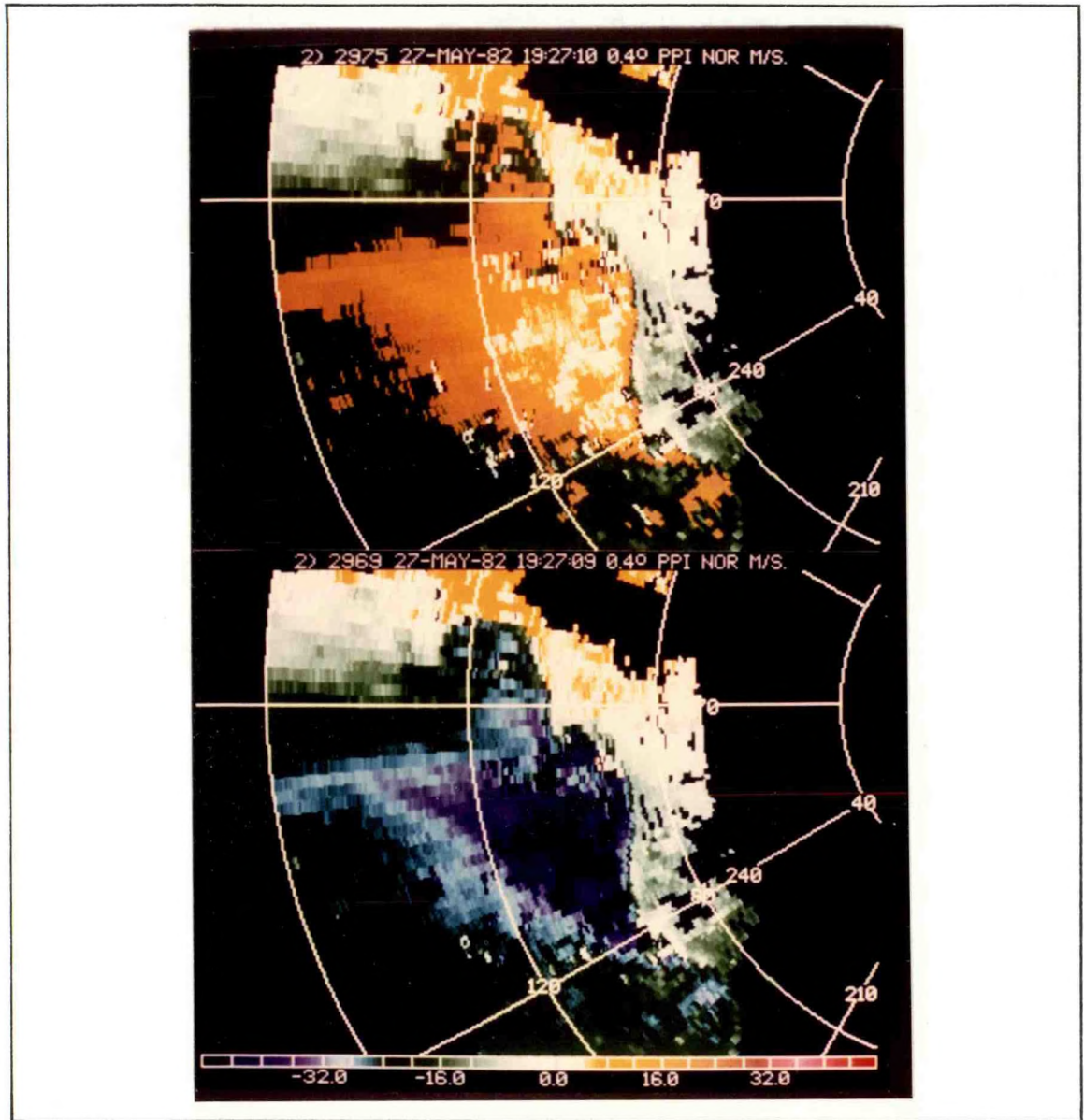


Figure 41. Example of performance of velocity dealiasing algorithm on an extreme aliasing case. Data were collected on a severe gust front southwest of radar; positive velocities are away from radar, negative toward radar. Nyquist velocity is 22.5 m s^{-1} . (Top) Velocity field before dealiasing, where velocities behind discontinuity are all positive (aliased). (Bottom) Velocity field after dealiasing with NSSL algorithm, resulting in sharp discontinuity along leading edge. Velocities as high as 50 m s^{-1} were measured behind the front, and gate-to-gate (220-m gate spacing) radial velocity differences were as much as 45 m s^{-1} .

NEXRAD Research and Development

The NEXRAD mesocyclone detection algorithm was improved. The Similarity Index (SI) was developed to enhance mesocyclone detection and input to warning forecasters. The index quantitatively determines how closely the observed data fit the model mesocyclone initialized with algorithm output parameters (Fig. 42).

The relationship between divergent outflow magnitude at upper storm levels and hailstorm intensity was investigated by analyzing single-Doppler radar data for 49 severe hailstorms. Two different techniques were developed for use with single-Doppler radar data to estimate the magnitude of divergent outflows. The techniques show considerable accuracy in predicting the maximum hailstone size that a thunderstorm will produce, with correlation coefficients between the predictors and maximum hailstone size as high as 0.89 (Fig. 43). The data also show that predictions of maximum hailstone size have an 80% chance of being accurate to within ± 1.4 cm.

The hail core aloft algorithm (HCAA) is part of a new hail algorithm being developed at NSSL. It is a reflectivity-based algorithm, and it is based on the

demonstrated success of the RADAP-II vertically integrated liquid (VIL) algorithm and techniques used during several hail suppression experiments. To satisfy the different needs of the NWS, USAF, and FAA, the HCAA has separate components for indicating any size hail and only severe hail. To determine the presence of hail of any size, the height of the 45 dBZ echo above the freezing level is used. To determine the presence of severe hail, a temperature-weighted vertical integration of the radar-derived hailfall kinetic energy is used. The HCAA was tested using Doppler radar data collected by NSSL on 12 storm days in 1987 and 1988. Up to this point, only the HCAA's severe hail prediction capability has been evaluated. Initial test results are very encouraging, with a probability of detection as high as 97%, a false alarm ratio as low as 16%, and a critical success index as high as 82%.

An initial version of a TVS algorithm was implemented and run in real time during the 1989 TDWR demonstration in Kansas City. The purpose of the algorithm is detection and short-term prediction of tornadoes using data from a single Doppler radar. The algorithm detected the only TVS that occurred during the demonstration. There were no false alarms. In addition, the algorithm was tested with TDWR-format

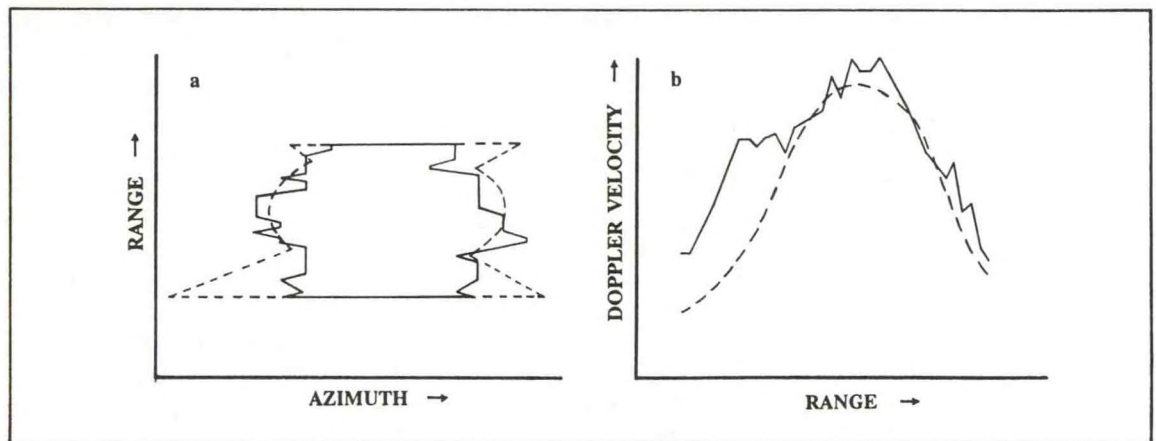


Figure 42. (a) Observed (solid lines) and modeled (dashed lines) pattern vector envelopes. (b) Observed (solid lines) and modeled (dashed lines) Doppler velocity difference profiles along the pattern vector envelopes.

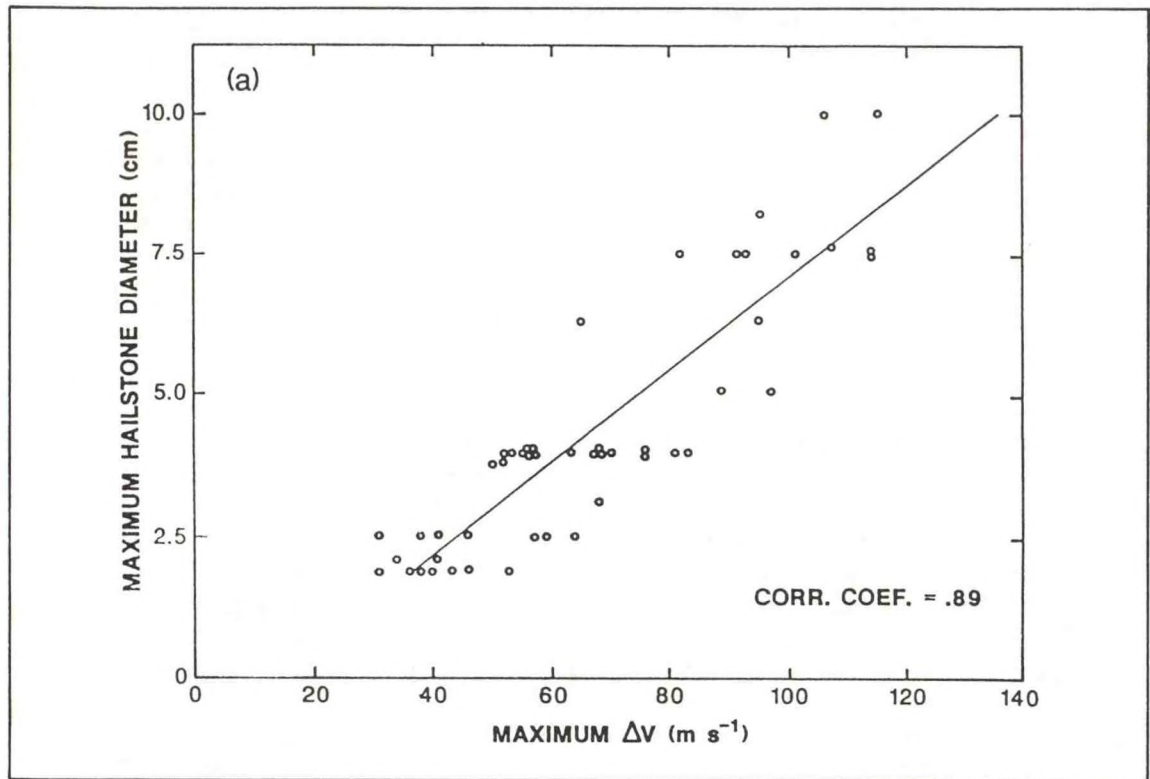


Figure 43. Maximum hailstone diameter versus values of change in V for 49 storm cases. Values of change in V are determined by taking maximum radial velocity difference within the divergent outflow region.

data from 15 June 1988, when four tornadoes occurred in and around Denver. All four tornadoes were detected, with no false alarms. The average warning lead time for all five tornadoes was 5.5 minutes.

Experimental Forecasting and Verification

As part of a continuing commitment to involvement in support of operational forecasting, several forecasting experiments were conducted in the springs of 1987, 1988, and 1989 in cooperation with the Norman WSFO. These experiments were aimed primarily at determining baseline skill levels in forecasting important aspects of convective storms; e.g., mesocyclones, severe convective weather events, and the convective mode. Although verification of

these forecasts is not yet complete, these exercises are valuable learning experiences for possible applications of new science and technology in operational weather offices. It is anticipated that another experiment in this series will be conducted during the spring of 1990, with a special emphasis on quantitative precipitation forecasting.

In collaboration with NSSFC in Kansas City, NSSL performed comprehensive verification of the severe thunderstorm and tornado watches issued by NSSFC. Some new approaches for evaluation of forecasts were developed to emphasize relative skill levels as a function of geographical location, time of day, time of year, and so on. This effort is well on its way to completion, with the results likely to have important implications about how forecasting of severe convective weather is to be done in the future. Plans for extension of this work include an effort to

combine the forecast verification with information about the large-scale meteorological setting in order to assess quantitatively the extent to which severe convective weather forecasting success depends on the large-scale meteorological structure. The verification effort will be extended to include heavy precipitation associated events.

Results of collaborative research with the Techniques Development Laboratory of NWS provided a good correspondence between lightning frequency, radar echo intensity, low-level moisture flux, and circulation. Contrary to the literature, freezing-level height and wind shear were not as important as the boundary layer fields in determining thunderstorm formation and subsequent positive ground flash activity. A significant correlation was also found between the occurrence of severe local storms

and elevated rates of 30 or more positive flashes to ground per hour.

IOT&E

The NEXRAD Interim Operational Test and Evaluation (IOT&E) was conducted from March to September 1989. NSSL provided the following services to IOT&E: forecasting for data collection, storm intercept and damage survey on 43 days to verify severe weather occurrence (Fig. 44), algorithm evaluation, and operation of a system loader. The loader simulated network conditions with communication and data requests from multiple radar sites and several national centers. Input was provided to the final report on the NEXRAD test, which was prepared by the USAF Operational Test and Evaluation Center.

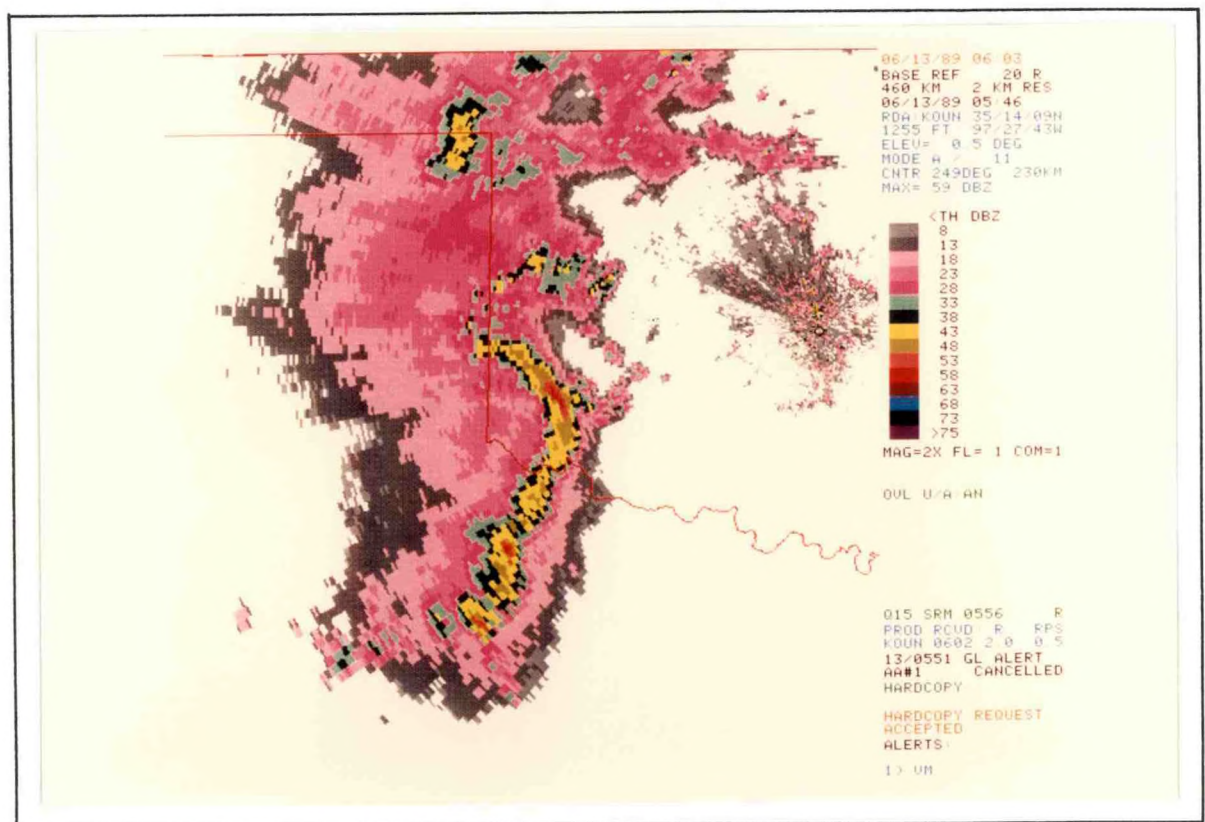


Figure 44. NEXRAD base reflectivity for 0546 UTC on 13 June 1989 at elevation angle of 0.5°. A bowed squall-line segment is in southwestern Oklahoma. NSSL intercept teams verified hail and significant damaging winds from this storm.

GUFMEX Workshops

Eight scientists (research meteorologists, operational forecasters, and NWS program directors) involved in the field phase of GUFMEX visited NWS Southern Region Forecast Offices in San Antonio and Alvin, Texas, and Slidell, Louisiana. These visits were designed to review the field program and give preliminary results on the research. Also, since many of the forecasters at these stations were involved in the project, their opinions and ideas on various aspects of the project were solicited.

The workshops were organized so that a series of brief overviews of the project was

presented in the morning. The topics were related to synoptic overviews, satellite and special upper-air data that were collected, and flight data collected from the NOAA P-3 aircraft. The afternoon was set aside for interaction and further discussion between the forecasters and the visiting scientists.

As a result of the workshop, forecasters at San Antonio and Slidell are contributing to the research phase of GUFMEX. Projects are being identified that have potential to aid forecasting during these cool-season return flows and satisfy the project goals. Furthermore, a questionnaire designed by forecasters is being used to track these events during the coming season.

NSSL STAFF FY 1989

Office of the Director

Robert A. Maddox	Director
Doviak, Richard J.	Electrical Engineer
Meacham, Mary E.	Librarian
Walton, Joy L.	Secretary
Winston, Karen	Meteorological Aid

Administration

Loyce M. Tillman	Administrative Officer
Gregory, Patricia R.	Purchasing Agent
Kelly, Stephanie K.	Administrative Aid

Doppler Radar and Remote Sensing Group

Dusan S. Zrnic	Manager
Brandes, Edward A.	Meteorologist
Brown, Rodger A.	Meteorologist
Davies-Jones, Robert P.	Meteorologist
Doswell, Charles A. III	Meteorologist
Gold, David	Meteorological Aid
Lynn, Kelly S.	Clerk Typist
Spaeth, Daniel	Meteorological Aid

Forecast Applications Research Group

Donald W. Burgess	Manager
Eilts, Michael D.	Meteorologist
McPherson, Sandra D.	Secretary
Mitchell, Dewayne	Physical Science Aid
Morris, Dale	Physical Science Aid
Oakland, Susan	Physical Science Aid
Prentice, Robert A.	Met'l Technician
Vasiloff, Steven V.	Meteorologist
Witt, Arthur	Meteorologist
Wood, Vincent T.	Meteorologist

Mesoscale Research Division (Boulder)

David P. Jorgensen	Manager (Acting)
Augustine, John A.	Meteorologist
Bartels, Diana L.	Meteorologist
Blanchard, David O.	Meteorologist
Caracena, Fernando	Physicist
Chandler, Sandra J.	Special Assistant
Daugherty, John R.	Physical Scientist
Holle, Ronald L.	Meteorologist
Howard, Kenneth W.	Meteorologist
Hueftle, Robert A.	Computer Programmer
López, Raúl E.	Meteorologist
Meitín, José G., Jr.	Meteorologist
Ortiz, Robert	Meteorologist
Smull, Bradley F.	Meteorologist
Watson, Andrew I.	Meteorologist

Meteorological Research Group

John M. Lewis	Manager
Hane, Carl E.	Meteorologist
McPherson, Sandy	Secretary
Rabin, Robert M.	Meteorologist
Stensrud, David J.	Meteorologist
Ziegler, Conrad L.	Meteorologist

Scientific Support Division

Douglas E. Forsyth	Manager
Devericks, Lawrence S.	Clerk-Typist
Doctor, Jo Retta	Secretary
Fredrickson, Sherman E.	Meteorologist

Computing and Data Management

Jain, Michael H.	Meteorologist
Ross, Catherine L.	Computer Assistant
Skaggs, Gary A.	Meteorological Technician
Wardius, Gerald J.	Electronics Technician

Engineering

Carter, John K.	Electronics Engineer
Zahrai, F. Allen	Electronics Engineer

Technical Support

Anderson, Glen H., Jr.	Lead Technician
Griffin, Lawrence P.	Electronics Technician
McGowen, James W.	Electronics Technician
Nealson, Dennis E.	Electronics Technician
Schmidt, J. Michael	Electronics Technician
Wahkinney, Richard	Electronics Technician Student Trainee

Field Support

Crisp, Charlie A.	Met'l Technician
Curran, Edward B.	Field Support Meteorologist

George, Charlie, Jr.	Meteorological Aid
Porter, Christopher	Physical Science Aid
Showell, Lester C.	Met'l Technician
Wheeler, Douglas R.	Meteorological Aid

National Weather Service COOP Program

Boyd, Brian	Meteorology Student Trainee
Davis, Jeffery	Meteorology Student Trainee

Storm Electricity and Cloud Physics Group

David W. Rust	Manager
Crider, Donna	Meteorological Aid
MacGorman, Donald R.	Physicist
Mazur, Vladislav	Physicist
McCourry, Stanton A.	Engineering Aid
Rhoden, Gene	Meteorological Aid
Shepherd, Tommy R.	Physical Science Aid
Younkins, Mary L.	Secretary

FY 1989 PUBLICATION LIST

- Balakrishnan, N., and D.S. Zrnic', 1989: Correction of propagation effects at attenuating wavelengths in polarimetric radars. Preprints, 24th Conference on Radar Meteorology, March 27-31, Tallahassee, FL, Amer. Meteor. Soc., Boston, 287-291.
- Balakrishnan, N., and D.S. Zrnic', 1989: Suggested use of cross-correlation between orthogonally polarized echoes to infer hail size. Preprints, 24th Conference on Radar Meteorology, March 27-31, Tallahassee, FL, Amer. Meteor. Soc., Boston, 292-296.
- Balakrishnan N., D.S. Zrnic', J. Goldhirsh, and J. Rowland, 1989: Comparison of simulated rain rates from disdrometer data employing polarimetric radar algorithms. *J. Atmos. Oceanic Tech.*, 6, 476-486.
- Bartels, D.L., 1989: Mid-level cyclonic vortices generated by mesoscale convective systems. M. S. Thesis, University of Oklahoma, Norman, OK, 131 pp.
- Brandes, E.A., and R.M. Rabin, 1989: Cold front structure as seen by Doppler radar and tall instrumented tower. Preprints, 24th Conference on Radar Meteorology, March 27-31, Tallahassee, FL, Amer. Meteor. Soc., Boston, 459-462.
- Brown, R.A., 1989: Initiation and propagation of thunderstorm mesocyclones. Ph.D. Dissertation, University of Oklahoma, Norman, OK, 321 pp.
- Brown, R.A., 1989: On the initiation of updraft rotation within the Agawam, Oklahoma, supercell storm. Preprints, 24th Conference on Radar Meteorology, March 27-31, Tallahassee, FL, Amer. Meteor. Soc., Boston, 66-69.
- Brown, R.A., and V.T. Wood, 1989: A guide for interpreting Doppler velocity patterns. Report No. R400-DV-101, The NEXRAD Joint System Program Office, Silver Spring, MD, 51 pp.
- Burgess, D.W., and J. Marwitz, 1989: The observed inflow structure of a thunderstorm with a mesocyclone. Preprints, 24th Conference on Radar Meteorology, March 27-31, Tallahassee, FL, Amer. Meteor. Soc., Boston, 70-72.
- Caracena, F., R.L. Holle, and C.A. Doswell III, 1989: Microbursts: A handbook for visual identification. NOAA/ERL, National Severe Storms Laboratory, Norman, OK (Available from U.S. Superintendent of Documents, Washington DC 20402, Req. No. 9.01701), 35 pp.
- Christian, H.J., V. Mazur, B.D. Fisher, L.H. Ruhnke, K. Crouch, and R.P. Perala, 1989: The Atlas/Centaur lightning strike incident. *J. Geophys. Res.*, 94, 13,169-13,177.
- Davies-Jones, R.P., 1989: A generalized Q vector and its interpretation. IAMAP 89 Brief Review Papers and Abstracts, Vol. 1, Fifth Scientific Assembly of the International Association of Meteorology and Atmospheric Physics, July 31-August 12, University of Reading, United Kingdom, 1, MF33.
- Doswell, C.A. III, 1988: On the use of hodographs--vertical wind profile information in severe storms forecasting. NOAA/NWS/SRH, Scientific Services Division, Fort Worth, Texas, and NOAA/ERL, National Severe Storms Laboratory, Norman, OK, 19 pp.

- Doswell, C.A. III, 1989: Fundamental concepts of operational mesoscale analysis and forecasting for severe convective storms (Part I). WMO Programme on Short- and Medium-Range Weather Prediction Research, PSMP Report Series No. 30, 81-99.
- Doswell, C.A. III, 1989: Fundamental concepts of operational mesoscale analysis and forecasting for severe convective storms (Part II). WMO Programme on Short- and Medium-Range Weather Prediction Research, PSMP Report Series No. 30, 101-117.
- Doswell, C.A. III, 1989: Recent research findings on the role of vertical wind shear: Applications to forecasting. WMO Programme on Short- and Medium-Range Weather Prediction Research, PSMP Report Series No. 30, 141-155.
- Doswell, C.A. III, and J.A. Flueck, 1989: Forecasting and verifying in a field research project: DOPLIGHT '87. *Wea. Forecasting*, 4, 97-109.
- Doviak, R.J., and D.R. Christie, 1989: Thunderstorm-generated solitary waves: A wind shear hazard. *J. Aircraft*, 26, 423-431.
- Doviak, R.J., and K.W. Thomas, 1988: The wavefront shape and position of a great solitary wave of translation. Proceedings, International Geoscience and Remote Sensing Symposium, September 13-16, Edinburgh, Scotland, 1833-1837.
- Eilts, M.D., 1989: Estimation of microburst asymmetry with a single Doppler radar. Preprints, 3rd International Conference on the Aviation Weather System, January 30-February 3, Anaheim, CA, Amer. Meteor. Soc., Boston, 57-61.
- Eilts, M.D., and S.K. Oakland, 1989: Convergence aloft as a precursor to microbursts. Preprints, 24th Conference on Radar Meteorology, March 27-31, Tallahassee, FL, Amer. Meteor. Soc., Boston, 190-193.
- Eilts, M.D., and S.D. Smith, 1989: Efficient dealiasing of Doppler velocities using local environment constraints. Final Report DOT/FAA/SA-89/1, Federal Aviation Administration, Washington, DC, 37 pp.
- Eilts, M.D., and S.D. Smith, 1989: Real-time Doppler velocity dealiasing. Preprints, 24th Conference on Radar Meteorology, March 27-31, Tallahassee, FL, Amer. Meteor. Soc., Boston, 194-197.
- Forsyth, D.E., D.W. Burgess, M.H. Jain, and L.E. Mooney, 1989: DOPLIGHT '87: Application of Doppler radar technology in a National Weather Service office. Preprints, 24th Conference on Radar Meteorology, March 27-31, Tallahassee, FL, Amer. Meteor. Soc., Boston, 198-202.
- Goodman, S.J., H.J. Christian, and W.D. Rust, 1989: A comparison of the optical pulse characteristics of intracloud and cloud-to-ground lightning as observed above clouds. *J. Appl. Meteor.*, 27, 1369-1381.
- Goodman, S.J., D.E. Buechler, P.D. Wright, and W.D. Rust, 1988: Lightning and precipitation history of a microburst-producing storm. *Geophys. Res. Lett.*, 15, 1185-1188.
- Goodman, S.J., D.E. Buechler, P.D. Wright, W.D. Rust, and K.E. Nielsen, 1989: Polarization radar and electrical observations of two microburst producing storms. Preprints, 24th Conference on Radar Meteorology, March 27-31, Tallahassee, FL, Amer. Meteor. Soc., Boston, 109-116.
- Grice, G.K., K.W. Howard, S.L. Barnes, and C.A. Doswell (editors), 1988: A guide for operational meteorological research. National Weather Service, Fort Worth, TX, 84 pp. and appendices A-D.

- Hane, C.E., and M.A. LeMone, 1989: Retrieval of pressure and buoyancy from Doppler-derived winds in a High Plains hailstorm. Preprints, 24th Conference on Radar Meteorology, March 27-31, Tallahassee, FL, Amer. Meteor. Soc., Boston, 38-41.
- Houze, R.A., S.A. Rutledge, M.I. Biggerstaff, and B.F. Smull, 1989: Interpretation of Doppler weather radar displays of midlatitude mesoscale convective systems. *Bull. Amer. Meteor. Soc.*, 70, 608-619.
- Howard, K.W., and R.A. Maddox, 1988: A satellite-based climatology of warm season thunderstorms over Mexico. Preprints, III InterAmerican Congress of Meteorology and III Mexican Congress on Meteorology, November 14-18, Mexico City, Mexican Meteorological Organization, Mexico City, 414-417.
- Howard, K.W., and R.A. Maddox, 1988: Mexican mesoscale convective systems--A satellite perspective. Preprints, III InterAmerican Congress on Meteorology and III Mexican Congress on Meteorology, November 14-18, Mexico City, Mexican Meteorological Organization, Mexico City, 404-408.
- Jorgensen, D.P., and M.A. LeMone, 1989: Characteristics of convective vertical velocity events observed by P-3 aircraft during TAMEX. Proceedings, Workshop on TAMEX Preliminary Scientific Results, June 22-30, Taipei, Republic of China, National Science Council, Taipei, and National Science Foundation, Washington, DC, 203-213.
- Jorgensen, D.P., and M.A. LeMone, 1989: Precipitation and kinematic structure of the TAMEX 16 June mesoscale convective system. Part II: Pressure and buoyancy perturbations derived from airborne Doppler radar data. Proceedings, Workshop on TAMEX Preliminary Scientific Results, June 22-30, Taipei, Republic of China, National Science Council, Taipei, and National Science Foundation, Washington, DC, 103-109.
- Jorgensen, D.P., and M.A. LeMone, 1989: Vertical velocity characteristics of oceanic convection. *J. Atmos. Sci.*, 46, 621-644.
- Jorgensen, D.P., M.A. LeMone, and B. Jou, 1989: Precipitation and kinematic structure of an oceanic mesoscale convective system. Part I: Airborne Doppler radar analysis. Proceedings, 18th Conference on Hurricanes and Tropical Meteorology, May 16-19, San Diego, CA, Amer. Meteor. Soc., Boston, 232-233.
- Jou, B., D.P. Jorgensen, and B.F. Smull, 1989: Precipitation and kinematic structure of the TAMEX 16 June mesoscale convective system. Part I: Airborne Doppler radar analysis. Proceedings, Workshop on TAMEX Preliminary Scientific Results, June 22-30, Taipei, Republic of China, National Science Council, Taipei, and National Science Foundation, Washington, DC, 77-81.
- Klinge-Wilson, D., S.H. Olson, W. Wilson, W.P. Mahoney III, S.D. Smith, A. Witt, and M.D. Eilts, 1989: Gust front detection algorithm for the terminal Doppler weather radar. Part II: Performance Assessment. Preprints, Third International Conference on the Aviation Weather System, January 30-February 3, Anaheim, CA, Amer. Meteor. Soc., Boston, 398-402.
- Lang, S.L., P.S. Ray, and C.L. Ziegler, 1989: Retrieval and evolution of microphysical fields in a small mountain thunderstorm. Preprints, 24th Conference on Radar Meteorology, March 27-31, Tallahassee, FL, Amer. Meteor. Soc., Boston, 93-96.
- LeMone, M.A., and D.P. Jorgensen, 1989: Precipitation and kinematic structure of an oceanic mesoscale convective system. Part II: Results from analysis of in-situ data. Proceedings, 18th Conference on Hurricanes and Tropical Meteorology, May 16-19, San Diego, CA, Amer. Meteor. Soc., Boston, 234-235.

- LeMone, M.A., and D.P. Jorgensen, 1989: Precipitation and kinematic structure of the TAMEX 16 June mesoscale convective system. Part III: Analysis of in-situ data. Proceedings, Workshop on TAMEX Preliminary Scientific Results, June 22-30, Taipei, Republic of China, National Science Council, Taipei, and National Science Foundation, Washington, DC, 110-117.
- Lewis, J.M., 1989: GUFMEX: A study of return flow in the Gulf of Mexico. *Bull. Amer. Meteor. Soc.*, 70, 24-29.
- Lewis, J.M., C. Hayden, and J. Derber, 1989: A method for combining radiances and wind shear to define the temperature structure of the atmosphere. *Mon. Wea. Rev.*, 117, 1193-1207.
- Lewis, J.M., and L.C. Showell, 1988: GUFMEX: A study of return flow in the Gulf of Mexico. Preprints, III InterAmerican Mexican Congress of Meteorology and III Mexican Congress on Meteorology, November 14-18, Mexico City, Mexican Meteorological Organization, Mexico City, 106-109.
- López, R.E., D. Atlas, D. Rosenfeld, J.L. Thomas, D.O. Blanchard, and R.L. Holle, 1989: Estimation of areal rainfall using the radar echo area time integral. *J. Appl. Meteor.*, 28, 1162-1175.
- López, R.E., R.L. Holle, W.D. Otto, and R. Ortiz, 1989: Cloud-to-ground lightning in Colorado: Flashes of both polarities related to meteorological conditions, radar echoes, and severe weather. Proceedings, 1989 International Conference on Lightning and Static Electricity, September 26-28, Bath, United Kingdom, Royal Aerospace Establishment, Farnborough, Hampshire, United Kingdom, 1A.2.1-7.
- López, R.E., R.L. Holle, and A.I. Watson, 1989: Meteorological studies with cloud-to-ground lightning data: Samples of recent analyses. Proceedings, 4th WMO Technical Conference on Instruments and Methods of Observation (TECIMO-IV), September 4-8, Brussels, Belgium, WMO/TD No. 303, Geneva, Switzerland, 275-280.
- López, R.E., W.D. Otto, J.R. Daugherty, and R.L. Holle, 1989: The relationship between radar and lightning characteristics of northeastern Colorado storm systems. Preprints, 24th Conference on Radar Meteorology, March 27-31, Tallahassee, FL, Amer. Meteor. Soc., Boston, 85-88.
- MacGorman, D.R., D.W. Burgess, V. Mazur, W.D. Rust, W.L. Taylor, and B.C. Johnson, 1989: Lightning rates relative to tornadic storm evolution on 22 May 1981. *J. Atmos. Sci.*, 46, 221-250.
- MacGorman, D.R., and W.D. Rust, 1989: An evaluation of the LLP and LPATS lightning ground strike mapping systems. Preprints, 5th International Conference on Interactive Information and Processing Systems for Meteorology, Oceanography, and Hydrology, January 30-February 3, Anaheim, CA, Amer. Meteor. Soc., Boston, 249-254.
- MacGorman, D.R., and W.L. Taylor, 1989: Positive cloud-to-ground lightning detection by an LLP direction-finder network. *J. Geophys. Res.*, 94, 13,313-13,318.
- Mach, D.M., and W.D. Rust, 1989: A photoelectric technique for measuring lightning-channel propagation velocities from a mobile laboratory. *J. Atmos. Oceanic Tech.*, 6, 439-445.
- Mach, D.M., and W.D. Rust, 1989: A solid state lightning propagation speed sensor. Preprints, 27th Aerospace Sciences Meeting, January 9-12, Reno, NV, American Institute of Aeronautics and Astronautics, paper AIAA-89-0785.

- Mach, D.M., and W.D. Rust, 1989: Photoelectric return-stroke velocity and peak current estimates in natural and triggered lightning. *J. Geophys. Res.*, 94, 13,327-13,247.
- Maddox, R.A., and K.W. Howard, 1988: Mexican mesoscale convective systems - Two case examples. Preprints, III InterAmerican Congress on Meteorology and III Mexican Congress on Meteorology, November 14-18, Mexico City, Mexican Meteorological Organization, Mexico City, 89-93.
- Maddox, R.A., and K.W. Howard, 1988: Mexican mesoscale convective systems--Large scale environmental conditions. Preprints, III InterAmerican Congress on Meteorology and III Mexican Congress on Meteorology, November 14-18, Mexico City, Mexican Meteorological Organization, Mexico City, 395-399.
- Marshall, T.C., W.D. Rust, W.P. Winn, and K.E. Gilbert, 1989: The electrical structure in two thunderstorm anvil clouds. *J. Geophys. Res.*, 94, 2717-2181.
- Matejka, T., 1989: Pressure and buoyancy forces and tendencies in a squall line and their relation to its evolution. Preprints, 24th Conference on Radar Meteorology, March 27-31, Tallahassee, FL, March 27-31, Amer. Meteor. Soc., Boston, 478-481.
- Mazur, V., 1989: A physical model of lightning initiation on aircraft in thunderstorms. *J. Geophys. Res.*, 94, 3326-3340.
- Mazur, V., 1989: Triggered lightning strikes to aircraft and natural intracloud discharges. *J. Geophys. Res.*, 94, 3311-3325.
- Mazur, V., B.D. Fisher, and P.W. Brown, 1989: Cloud-to-ground strikes to the NASA F-106 airplane. Preprints, 1989 International Conference on Lightning and Static Electricity, September 26-28, Bath, United Kingdom, Royal Aerospace Establishment, Farnborough, Hampshire, United Kingdom, 8A.4.1-3.
- Meitín, J.G., and A.I. Watson, 1989: Comparison of the kinematic structure and precipitation characteristics of squall and non-squall mesoscale convective systems. Preprints, 24th Conference on Radar Meteorology, March 27-31, Tallahassee, FL, Amer. Meteor. Soc., Boston, 486-489.
- Nielsen, K., and D.R. MacGorman, 1989: Lightning ground flash rates relative to mesocyclone evolution on 8 May 1986. Preprints, 24th Radar Conference on Radar Meteorology, March 27-31, Tallahassee, FL, Amer. Meteor. Soc., Boston, 117-120.
- Passarelli, R.E., Jr., and D.S. Zrníc', 1989: An expression for phase noise. Preprints, 24th Conference on Radar Meteorology, March 27-31, Tallahassee, FL, Amer. Meteor. Soc., Boston, 433-435.
- Passi, R.M., and R.E. López, 1989: A parametric estimation of systematic errors in networks of magnetic direction finders. *J. Geophys. Res.*, 94, 13,319-13,328.
- Pitts, F., B. Fisher, V. Mazur, and T. Brown, 1988: Researching lightning strikes to aircraft. *IEEE Spectrum*, 7, 34-38.
- Rabin, R.M., 1989: Diagnosing short-term changes in temperature profiles from single Doppler radar data. *Mon. Wea. Rev.*, 117, 1501-1516.
- Reap, R.M., and D.R. MacGorman, 1989: Cloud-to-ground lightning: Climatological characteristics and relationship to model fields, radar observations and severe local storms. *Mon. Wea. Rev.*, 117, 518-535.

- Rust, W.D., 1989: Lightning. *Science*, 242, 1713-1714.
- Rust, W.D., 1989: Utilization of a mobile laboratory for storm electricity measurements. *J. Geophys. Res.*, 94, D11,13,305-13,311.
- Rust, W.D., and T.C. Marshall, 1989: Mobile, high-wind, balloon-launching apparatus. *J. Atmos. Oceanic Tech.*, 6, 215-217.
- Rutledge, S.A., and D.R. MacGorman, 1989: Observations of positive cloud-to-ground lightning flashes from mesoscale convective systems. Preprints, 24th Conference on Radar Meteorology, March 27-31, Tallahassee, FL, Amer. Meteor. Soc., Boston, 122-125.
- Sachidananda, M., and D.S. Zrníc', 1989: Efficient processing of alternately polarized radar signals. *J. Atmos. Oceanic Tech.*, 6, 173-181.
- Smith, S.D., and R.M. Rabin, 1989: Considerations in estimating horizontal wind gradients from an individual Doppler radar or a network of wind profilers. *J. Atmos. Oceanic Tech.*, 6, 446-458.
- Smith, S.D., and R.M. Rabin, 1989: Estimation of divergence in the prestorm boundary layer. *J. Atmos. Oceanic Tech.*, 6, 459-475.
- Smith, S.D., A. Witt, M. Eilts, L. Hermes, D. Klinge-Wilson, S. Olson, and J. Sanford, 1989: Gust front detection algorithm for the terminal Doppler weather radar, Part I: Current status. Preprints, 3rd International Conference on Aviation Weather Systems, January 30-February 3, Anaheim, CA, Amer. Meteor. Soc., Boston, 31-34.
- Smull, B.F., and J.A. Augustine, 1989: Structure and environment of a non-squall mesoscale convective complex observed during PRE-STORM. Preprints, 24th Conference on Radar Meteorology, March 27-31, Tallahassee, FL, Amer. Meteor. Soc., Boston, 502-505.
- Steinhorn, I., and D.S. Zrníc', 1989: Differential propagation constant and differential reflectivity characterize rain and hail in high reflectivity regions. Preprints, 24th Conference on Radar Meteorology, March 27-31, Tallahassee, FL, Amer. Meteor. Soc., Boston, 367-370.
- Stensrud, D.J., and R.A. Maddox, 1988: Opposing mesoscale circulations: A case study. *Wea. Forecasting*, 3, 189-204.
- Stumpf, G.S., and W.A. Gallus, 1989: An examination of new convective development with a PRE-STORM squall line case. Preprints 24th Conference on Radar Meteorology, March 27-31, Tallahassee, FL, Amer. Meteor. Soc., Boston, 506-509.
- Trier, S.B., D.B. Parsons, and T.J. Matejka, 1989: An observational and numerical study of a subtropical cold front during TAMEX. Preprints, 24th Conference on Radar Meteorology, March 27-31, Tallahassee, FL, Amer. Meteor. Soc., Boston, 561-564.
- Trier, S.B., D.B. Parsons, and T.J. Matejka, 1989: Observations of a cold front during TAMEX. Proceedings, Workshop on TAMEX Preliminary Scientific Results, June 22-30, Taipei, Republic of China, National Science Council, Taipei, and National Science Foundation, Washington, DC, 186-195.
- Uyeda, H., and D.S. Zrníc', 1988: Fine structure of gust fronts obtained from the analysis of single Doppler radar data. *J. Meteor. Soc. Japan*, 66, 869-881.

- Vasiloff, S., 1989: Vorticity dynamics of a squall line: A Doppler radar analysis of the 10-11 June 1985 squall line. M. S. Thesis, University of Oklahoma, Norman, OK, 100 pp.
- Watson, A.I., R.E. López, and R.L. Holle, 1988: Surface convergence techniques and the prediction of lightning at Kennedy Space Center. Addendum, 1988 International Aerospace and Ground Conference on Lightning and Static Electricity, April 19-22, Oklahoma City, OK, NOAA/ERL/National Severe Storms Laboratory, Boulder, CO, 32-39.
- Watson, A.I., R.L. Holle, R.E. López, R. Ortiz, and J.R. Daugherty, 1989: Use of the surface wind field as a predictor of thunderstorms and cloud-to-ground lightning at Kennedy Space Center. Preprints, 1989 International Conference on Lightning and Static Electricity, September 26-28, Bath, United Kingdom, Royal Aerospace Establishment, Farnborough, Hampshire, United Kingdom, 9B.2.1-7.
- Watson, A.I., R.E. López, J.R. Daugherty, R. Ortiz, and R.L. Holle, 1989: A composite study of Florida thunderstorms, using radar, cloud-to-ground lightning, and surface winds. Preprints, 24th Conference on Radar Meteorology, March 27-31, Tallahassee, FL, Amer. Meteor. Soc., Boston, 126-129.
- Watson, A.I., R.E. López, R.L. Holle, J.R. Daugherty, and R. Ortiz, 1989: Short-term forecasting of thunderstorms at Kennedy Space Center, based on the surface wind field. Preprints, 3rd International Conference on the Aviation Weather System, January 30-February 3, Anaheim, CA, Amer. Meteor. Soc., Boston, 222-227.
- Watson, A.I., J.G. Meitín, and J.B. Cuning, 1988: Evolution of the kinematic structure and precipitation characteristics of a mesoscale convective system on 20 May 1979. *Mon. Wea. Rev.*, 116, 1555-1567.
- Williams, E.R., A.I. Watson, L.M. Maier, W. Jafferis, and J. Weems, 1989: A case study of a low lightning rate storm during the Florida winter. Preprints, 3rd International Conference on the Aviation Weather System, January 30-February 3, Anaheim, CA, Amer. Meteor. Soc., Boston, 393-397.
- Zacharias, D., 1989: A case study of the May 10, 1985 tornado outbreak in northern Kansas. M.S. Thesis, University of Oklahoma, Norman, OK, 135 pp.
- Ziegler, C.L., and P.S. Ray, 1989: Doppler radar retrieval of the microphysical and electrical structure of a mountain thunderstorm. Preprints, 24th Conference on Radar Meteorology, March 27-31, Tallahassee, FL, Amer. Meteor. Soc., Boston, 97-99.
- Zrnic', D.S., N. Balakrishnan, and M. Sachidananda, 1989: Polarimetric measurements determine the amounts of rain and hail in a mixture. Preprints, 24th Conference on Radar Meteorology, March 27-31, Tallahassee, FL, Amer. Meteor. Soc., Boston, 396-400.
- Zrnic', D.S., and R.J. Doviak, 1989: Effect of drop oscillations on spectral moments and differential reflectivity measurements. *J. Atmos. Oceanic Tech.*, 6, 532-536.

MAJOR SEMINARS AT NSSL — at Norman (N) and Boulder (B)

- 3 November 1988 Dr. D. Hogg, CIRES, Boulder, CO, presented "Rain, radiometry, and NEXRAD." (N)
- 3 November 1988 Dr. T. Matejka, NCAR, Boulder, CO, presented "Pressure and buoyancy forces in a squall line and their relation to its evolution." (N)
- 4 November 1988 Ms. S. Crocker, MIT Lincoln Laboratory, Lexington, MA, presented "Range obscuration mitigation in TDWR environment." (N)
- 12 November 1988 Dr. P. Hildebrand, NCAR, Boulder, CO, presented "The capabilities and potential of airborne Doppler radar." (N)
- 19 January 1989 Mr. G. Stumpf, Colorado State University, Fort Collins, CO, presented "Surface pressure features associated with a midlatitude mesoscale convective system in O.K. PRE-STORM." (N)
- 25 January 1989 Dr. B. Smull, NSSL, Boulder, CO, presented "Mesoscale organization of springtime rainstorms in Oklahoma." (N)
- 26 January 1989 Dr. S. Kidder, CIRA, Fort Collins, CO, presented "Microwave instruments on next-generation environmental satellites: New opportunities." (N)
- 1 March 1989 Dr. R. Passi, Institute for Naval Oceanography, Stennis Space Center, MS, and Mr. Claude Morel, NCAR, Boulder, CO, presented "CLASS data processing—A theoretical review." (N)
- 2 March 1989 Dr. R. López, NSSL, Boulder, CO, and Dr. R. Passi, Institute for Naval Oceanography, Stennis Space Center, MS, presented "The use of lightning data in meteorological research at the MRD of NSSL in Boulder, CO." (N)
- 7 March 1989 Dr. R. Strauch, Wave Propagation Laboratory, ERL, Boulder, CO, presented "Remote measurement of temperature by R.A.S.S." (N)
- 23 March 1989 Dr. D. Husson, National Laboratory for Study of Atmospheric Flows, Aubiere, France, presented "Research works carried out with the S-band dual polarization radar Anatol: An overview." (N)
- 30 March 1989 Dr. A.E. MacDonald, Forecast Systems Laboratory, ERL, Boulder, CO, presented "A mesoscale research support system." (N)
- 4 April 1989 Dr. F. Caracena, NSSL, Boulder, CO, presented "Adventures in objective analysis." (N)
- 10 April 1989 Mr. W. Martin, NSSL, Norman, presented "Measurement of turbulence within a model of cardiac valve flow using Doppler ultrasound." (N)

- 11 April 1989 Dr. J. Testud, CNET-CNRS, Issy-les-Moulineaux, France, presented "Asterix: A French project for an airborne Doppler radar." (N)
- 13 April 1989 Dr. S. Reyes, CICESE, Ensenada, Mexico, presented "Scientific research in Ensenada, Mexico" and "Proposal of meteorological experiments in Mexico." (N)
- 27 April 1989 Dr. J. Wilczak, Wave Propagation Laboratory, ERL, Boulder, CO, presented "Case study of a Denver cyclone associated tornado observed during CINDE." (N)
- 28 April 1989 Mr. S. Hunter, NSSL, Norman, presented "Lightning near Vandenburg AFB as related to various synoptic patterns." (B)
- 12 May 1989 Mr. D. Baumhefner, NCAR, Boulder, CO, presented "Predictability error growth—What is it and how can it be used?" (B)
- 25 May 1989 Dr. D. Parsons, NCAR, Boulder, CO, presented "Dynamics of a microburst downdraft." (N)
- 25 May 1989 Dr. J. Flueck, CIRES, Boulder, CO, and Dr. J. Marwitz, University of Wyoming, presented "The Greek randomized hail suppression experiment." (N)
- 28 August 1989 Dr. S.-T. Soong, University of California at Davis, presented "Numerical simulations of topographical effects on airflow and precipitation." (N)
- 7 September 1989 Dr. C. Hartsough, Naval Environmental Prediction Research Facility, presented "Frontal interaction with orography: Objective cross-sectional analysis of diabatic circulations and vertical motions using ALPEX data." (N)
- 20 September 1989 Dr. S. Lakshmiarahan, School of Electrical Engineering and Computer Science, University of Oklahoma, presented "Parallel processing: For fun and profit." (N)

MEETINGS HOSTED BY NSSL

- | | |
|-----------------------|---|
| 1 March 1989 | COPS-89 Planning Meeting in Norman. |
| 6-10 March 1989 | STORM Regional Data Assimilation Workshop in Norman. |
| 30 April & 4 May 1989 | GUFMEX Overview Meetings at National Weather Service offices in San Antonio and Houston, Texas, and Slidell, Louisiana. |
| 27 June 1989 | Portion of Summer Scholars Program (Hosted by Department of History of Science, University of Oklahoma). |
| 28 June 1989 | Portion of Summer Institute for Earth Science Teachers (Hosted by School of Meteorology, University of Oklahoma). |
| 24-25 August 1989 | STORM Experimental Forecast Center Workshop in Norman. |

VISITORS TO NSSL — at Norman (N) and Boulder (B)

R. Alberty	NWS Forecast Office, Phoenix, AZ (N)
K. Aydin	Pennsylvania State University, University Park, PA (N)
J. Ball	Office of Atmospheric Research, NOAA, Rockville, MD (B)
R. Balling	Arizona State University, Tempe, AZ (N)
W. Bauman	USAF, Patrick Air Force Base, FL (B)
W. Beasley	National Science Foundation, Washington, DC (B)
D. Beran	Forecast Systems Laboratory, ERL, Boulder, CO (N)
R. Biedinger	NWS Forecast Office, Coral Gables, FL (B)
C. Bhumralkar	Office of Atmospheric Research, NOAA, Rockville, MD (N)
H. Bluestein	University of Oklahoma, Norman, OK (B)
V. Bringi	Colorado State University, Fort Collins, CO (N)
B. Carpenter	<u>U. S. News & World Report</u> , Washington, DC (B, N)
R. Cervany	Arizona State University, Tempe, AZ (N)
V. Chandrasekar	University of Alabama, Tuscaloosa, AL (N)
S. Christian	CBS's "Good Morning America", New York, NY (N)
S. Crocker	MIT Lincoln Laboratory, Lexington, MA (N)
J. Ding	Shanghai Meteorological Center, Shanghai, China (N)
H. Fiala	Bundesamt fur Zivilluftfahrt, Vienna, Austria (N)
J. Fletcher	Director, ERL, Boulder, CO (N)
J. Flueck	CIRES, University of Colorado, Boulder, CO (N)
M. Forsyth	USAF, Scott Air Force Base, IL (B)
D. Frankel	KTAADN Systems, Newton, MA (B)
J. Gamache	Atlantic Oceanographic & Meteorological Lab., Miami, FL (B)
R. Ge	Institute of Mesoscale Meteorology, Beijing, China (B, N)
P. Gigliotti	Bureau of Meteorology, Melbourne, Australia (B, N)

J. Golden	Nat. Weather Service Headquarters, Silver Spring, MD (B)
E. Gorgucci	Instituto Di Fisica Dell'Atmosfera, Rome, Italy (N)
G. Grice	NWS Southern Region, Fort Worth, TX (B, N)
C. Hartsough	Naval Environmental Prediction Res. Fac., Monterey, CA (N)
J. Hastings	Forecast Systems Laboratory, ERL, Boulder, CO (N)
P. Hildebrand	National Center for Atmospheric Research, Boulder, CO (N)
D. Hogg	CIRES, University of Colorado, Boulder, CO (N)
D. Husson	Nat. Lab. for Study of Atmospheric Flows, Aubiere, France (N)
W. Jafferis	NASA, Kennedy Space Center, FL (B)
B. Jou	National Taiwan University, Taipei, Taiwan (B)
G. Kardon	Ofc. of Atmos. Res., Sea Grant Ofc., NOAA, Rockville, MD (B)
S. Kidder	CIRA, Colorado State University, Fort Collins, CO (N)
P. Krider	University of Arizona, Tucson, AZ (B)
F. LeDimet	Université Blaise Pascal, France (N)
S. Liong	Texas Tech. University, Lubbock, TX (N)
C. Lu	Colorado State University, Fort Collins, CO (N)
A. MacDonald	Forecast Systems Laboratory, ERL, Boulder, CO (N)
T. Marshall	University of Mississippi, Oxford, MS (N)
W. Martin	University of California at Berkeley (N)
J. Marwitz	University of Wyoming, Laramie, WY (N)
K. Mielke	NWS Western Region, Salt Lake City, UT (B)
C. Morel	National Center for Atmospheric Research, Boulder, CO (N)
C. Nappo	Air Resources Laboratory, ERL, Oak Ridge, TN (N)
J. Nall	National Transportation Safety Board, Washington, DC (N)
S. Nelson	National Science Foundation, Washington, DC (N)
J. Nicholson	NASA, Kennedy Space Center, FL (B)
G. North	Climate Services Systems Research Program, Lubbock, TX (N)

R. Orville	State University of New York at Albany (B)
D. Parsons	National Center for Atmospheric Research, Boulder, CO (N)
R. Passi	Inst. for Naval Oceanography, Stennis Space Center, MS (B, N)
K. Peppard	National Transportation Safety Board, Washington, DC (N)
M. Peterson	Chief Scientist, NOAA, Washington, DC (N)
D. Phillips	Salt River Project, Phoenix, AZ (N)
E. Rasmussen	Colorado State University, Fort Collins, CO (N)
G. Rao	Saint Louis University, Saint Louis, MO (N)
S. Reyes	CICESC, Ensenada, Mexico (N)
S. Rutledge	Colorado State University, Fort Collins, CO (B, N)
K. Sakurai	Japan Meteorological Agency, Tokyo, Japan (B)
G. Scarchilli	Instituto Di Fisica Dell'Atmosfera, Rome, Italy (N)
R. Strauch	WPL/ERL/NOAA, Boulder, CO (N)
S. Soong	Dept. of Land, Air and Water Res., Univ. of Calif. at Davis (N)
K. Taylor	Dept. of History of Science, Univ. of Okla., Norman, OK (N)
J. Testud	CNET-CNRS, Issy-les-Moulineaux, France (B, N)
A. Thomas	Office of Atmospheric Research, NOAA, Rockville, MD (N)
J. Weaver	NESDIS/NOAA, Fort Collins, CO (B, N)
S. Weiss	NWS Nat. Severe Storms Forecast Ctr., Kansas City, MO (N)
J. Wilczak	Wave Propagation Laboratory, ERL, Boulder, CO (N)
E. Zipser	National Center for Atmospheric Research, Boulder, CO (N)
P. Zumbusch	Lightning Location and Protection, Inc., Tucson, AZ (N)